

University of Alberta

**Co-gasification of Biomass with Coal and Oil Sand Coke
In a Drop Tube Furnace**

by

Chen Gao

A thesis submitted to the Faculty of Graduate Studies and Research
in partial fulfillment of the requirements for the degree of

Master of Science
in
Chemical Engineering

Department of Chemical and Materials Engineering

©Chen Gao
Fall 2010
Edmonton, Alberta

Permission is hereby granted to the University of Alberta Libraries to reproduce single copies of this thesis and to lend or sell such copies for private, scholarly or scientific research purposes only. Where the thesis is converted to, or otherwise made available in digital form, the University of Alberta will advise potential users of the thesis of these terms.

The author reserves all other publication and other rights in association with the copyright in the thesis and, except as herein before provided, neither the thesis nor any substantial portion thereof may be printed or otherwise reproduced in any material form whatsoever without the author's prior written permission.

Examining Committee

Dr. Rajender Gupta, Chemical and Materials Engineering, University of Alberta

Dr. Zhenghe Xu, Chemical and Materials Engineering, University of Alberta

Dr. Amit Kumar, Mechanical Engineering, University of Alberta

ABSTRACT

Chars were obtained from individual fuels and blends with different blend ratios of coal, coke and biomass in Drop Tube Furnace at different temperatures. Based on TGA experimental data, it was shown that the effect of the blending ratio of biomass to other fuels on the reactivity of the co-pyrolyzed chars is more pronounced on the chars prepared at lower temperature, due to the presence of synergetic effects originating from the interaction of the two fuels.

SEM images showed differences in shapes and particle size of char particles from biomass and coal/coke. These also show the agglomeration of coal and coke chars with biomass char particles at high temperatures. The agglomeration may be the reason for the non-additive behaviour of the blends. BET analysis showed increase in the surface area with an increasing temperature for biomass and coal, but the trend for coke was inversely related to the temperature.

ACKNOWLEDGEMENT

This research was made possible through the financial support from Alberta Energy Research Institute and the National Scientific and Engineering Research Council by the strategic project grant “Synergies in Co-gasification of Biomass, Coke & Coal”.

The author would like to thank her research supervisor Dr. Rajender Gupta, a righteous advisor with a considerate heart. His patient instructions always showed the direction and inspiration.

Special thanks are given to Dr. Hassan Katalambula for his great help and encouragements. Additionally, may thanks to Mr. Farshid Vejahati, his contributions on the DTF experiment were indispensable for this work.

The author also wishes to thank Mr. Mike Xia from NINT and Mr. George Braybrook from Department of Earth and Atmospheric Sciences for the support on TGA and SEM analysis, respectively.

TABLE OF CONTENTS

CHAPTER I INTRODUCTION	1
I-A: Coal use status	1
I-B: A clean coal technology and co-gasificaton.....	2
I-C: Objectives of this work.....	7
Reference	9
CHAPTER II LITERATURE REVIEW	10
II-A: Composition of the feedstock	10
II-A-1 Composition of biomass.....	10
II-A-2 Composition of coal	12
II-A-3 Composition of petroleum coke.....	13
II-A-4 Comparison of fuel characteristics.....	14
II-B: Understanding gasification.....	15
II-C: Importance of studying pyrolysis process.....	20
II-D: Review of related work on co-gasification	21
II-E: Co-gasification of biomass and coal	26
II-E-1 Factors influencing the co-gasification	27
II-E-2 Catalyst on coal gasification.....	35
II-E-3 Interaction effect in the co-gasification of biomass/coal/pet- coke mixtures	36
II-F: Gasification power plant: IGCC;	38
II-G: Review of experimental procedures;	41
II-G-1: Drop tube furnace (DTF)	41
II-G-2: Thermogravimetirc analyzer (TGA).....	44
II-G-3: Brunauer-Emmett-Teller measurement (BET)	47
II-G-4: Laser diffraction mastersizer	50
II-G-5: Scanning electron microscope (SEM)	52
Reference	56

CHAPTER III EXPERIMENT DESCRIPTION.....	68
III – A: Experimental apparatus.....	69
III – B: Fuels characterization.....	72
III – C: Char preparation.....	73
III – D: Measurement of char gasification reactivity.....	75
CHAPTER IV RESULTS AND DISCUSSION	76
IV – A: Effect of blending on char surface area.....	76
IV – B: Char reactivity.....	80
IV-B-1 Char reactivity rate with CO ₂ at 1180°C.....	83
IV-B-2 Char reactivity rate with CO ₂ at 800°C.....	85
IV – C: Morphological analysis of pyrolysis char	98
IV – D: Particle size distribution.	102
Reference	107
CHAPTER V CONCLUSION	109
APPENDIX A: PAPER AND CONFERENCE PRESENTATION	112

LIST OF TABLES

Table 1.1 Advantage of co-gasification of biomass with other feedstock ...	6
Table 2.1 Ultimate analyses (wt%) of biomass material and fossil fuel cracking feedstock and their equivalent chemical formula	11
Table 2.2 Composition and heating value tests on several feedstocks	15
Table 2.3 Reactions happened during gasification	18
Table 2.4 Properties of biomass	33
Table 3.1 Proximate and ultimate analyses of fuels	73
Table 3.2 Blending fuels ratio and their abbreviation	74
Table 4.1 Pore structure and BET surface area of Genesee coal/fluid, coke/biomass pure and blended chars at a ratio of 1:1	78
Table 4.2 Assumed GC or FC proportion in blended char	96

LIST OF FIGURES

Figure 2.1 Effect of temperature on gas composition for co-gasification...	28
Figure 2.2 Effect of oxygen flow rate/fuel ratio on gas composition for co-gasification.....	30
Figure 2.3 Effect of oxygen/steam ratio on gas composition for co-gasification	31
Figure 2.4 Decreasing fraction of combustible for several biomass, lignin, and cellulose	34
Figure 2.5 IGCC integration scheme	40
Figure 2.6 Schematic of the PDTF facility	42
Figure 3.1 Schematic of DTF	69
Figure 3.2 Schematic of collector probe.....	71
Figure 3.3 Temperature calibration for DTF	72
Figure 4.1 Effect of pyrolysis temperature on the surface area (SA) for three pure char namely, Genesee coal, fluid coke, and sawdust chars.....	77
Figure 4.2 Scheme of how to calculate K based on TGA result	82
Figure 4.3 TG results for GCS 1-1 chars, gasified isothermally at 1180°C with carbon dioxide.	83
Figure 4.4 DTG curves for rate of gasification vs. Time for GCS 1-1 blended chars, formed at 700,1100,1250,1400°C, respectively.	85
Figure 4.5 TGA results for Genesee coal and sawdust (GCS 1-1) blended char pyrolyzed at 700, 1100, 1250, and 1400°C.....	86
Figure 4.6 TGA results for fluid coke and sawdust (FCS 1-1) blended char pyrolyzed at 700, 1100, 1250, and 1400°C.....	88
Figure 4.7 Effect of the blending ratio and pyrolysis temperature on reactivity of Genesee coal and sawdust blended char	89
Figure 4.8 Effect of the blending ratio and pyrolysis temperature on reactivity of fluid coke and sawdust blended char	94

Figure 4.9 Effect of the assumed blending ratio and pyrolysis temperature on reactivity of coal and sawdust blended char.....	96
Figure 4.10 Effect of the assumed blending ratio and pyrolysis temperature on reactivity of fluid coke and sawdust blended char.....	97
Figure 4.11 SEMs of chars at 100× magnification, showing effect of pyrolysis temperature on particle morphology of Genesee coal and sawdust at 1:1 blending ratio.....	99
Figure 4.12 SEMs of chars at 300× magnification, showing effect of pyrolysis temperature on porosity of char particles.....	101
Figure 4.13 Agglomeration between coal and biomass particles at higher temperature	102
Figure 4.14 Pores development in fluid coke chars	102
Figure 4.15 Temperature effect on the particle size distribution of char.	105

CHAPTER I

INTRODUCTION

I-A: Coal use status;

Coal is usually used as a solid fuel to produce heat through combustion, and is responsible for about 40% of electricity generation in the world. The large abundance of coal makes it a reliable and long-term fuel source for both domestic and export purposes in countries like Canada, Australia and South Africa. Data also shows that the coal reserve to production ratio is almost 10 times bigger than oil and gas corresponding ratios ^[1].

According to National Energy Board ^[1], Canada has 78.8 billion tonnes of proven coal resources. Over 70% of coal resources occur in Alberta and in coal reserves in Alberta are more than double of oil sands reserves. In Alberta, almost 89% of electricity is generated by coal fired power plant. The total coal production in Alberta was estimated at 28 million tonnes in 2003. According to the data published by the World Coal Institute (WCI) on Coal Facts 2007th edition, coal provides 25% of the global primary energy needs and generates 40% of the world's electricity. Compared to petroleum and natural gas, which are in relatively shorter

supply, the amount of coal deposit is abundant. WCI also estimates that proven coal reserves worldwide will last 155 years at the current production levels ^[2].

Coal combustion releases large amounts of pollution to the atmosphere. These pollutants include PM2.5 and PM10 (particles smaller than 2.5, 10 μm in aerodynamic diameter), NO_x and SO_x, lead and mercury, as well as O₃, VOC's (volatile organic compounds) and CO. The combustion of coal is also suspected to produce dioxin ^[3] at low temperature. Advances in combustion technology reduced the absolute amount of pollution emitted from combustion sources by 31% from 1970 to 1997 ^[3], even while energy production has increased by 40%. This great achievement does not, however, include reductions of carbon dioxide (CO₂), a greenhouse gas. The reduction of greenhouse gas has emerged over the last decade as a challenging new problem.

I-B: A clean coal technology and co-gasification;

In recent years, global warming and its immense effects on our ecosystems because of the emission of greenhouse gases, of particular importance, carbon dioxide, have been the center of attention worldwide. Coal-fired power plants have been held responsible as the main anthropogenic source of carbon emission of the environment. In response to

this issue, recently, the acceptance of an integrated gasification combined cycle (IGCC), which is a more efficient and cleaner way of electricity production, has increased internationally. The heart of the IGCC technology is the gasification process, which its cost and reliability are largely influenced by feed quality and operating conditions.

Gasification is a process that converts carbonaceous materials, such as coal, petroleum, biofuel, or biomass, into carbon monoxide and hydrogen by reacting the raw material at high temperature with a controlled amount of oxygen and/or steam ^[4]. The resulting gas mixture is called synthesis gas or syngas and is itself a fuel. Gasification is a method for extracting energy from many different types of organic materials.

Gasification is the front runner among clean technologies for the conversion of carbonaceous solid in the production of electricity, ammonia and liquid fuels, with the possibility of producing methane and hydrogen for fuel cells and has already been adopted as a clean coal technology in many countries. Gasification can be integrated with other technologies for advanced power generation, particularly combustion turbines and eventually solid oxide fuel cells. The resulting systems are highly efficient, squeezing more value from each pound of feedstock. Gasification provides an effective means of capturing and storing or sequestering carbon dioxide,

a greenhouse gas. This is because gasification produces a much higher concentration of carbon dioxide than direct combustion of coal in air, and this helps to make carbon capture and storage more economical than it would be otherwise ^[5]. Another major factor that leads to the interest in gasification is the volatility and high prices of oil and natural gas. However, adoption of this new technology is largely related to the full appreciation of the gasification behaviour of different fuels and blends.

The steady increase of synthetic crude production from oil sand in western Canada has resulted in massive production and accumulate of oil sand coke (>6000 tons/day). This may represent almost 1000 MW of electricity, if all production is utilized as the feedstock in an integrated gasification-combined cycle (IGCC) plant ^[4]. Oil sand coke, one kind of petroleum coke (pet-coke), is a by-product derived from oil sand refinery cracking process, and two types of coke exist depending upon the production process, and these are: fluid and delayed coke. Most of the delayed coke produced by Suncor is combusted on site, whereas all fluid coke produced by Syncrude is stockpiled. The cokes have high carbon content (above 80%) with non-graphitic structure. Oil sand coke is a free (zero-cost) solid waste, and because of its low reactivity, use of this fuel in its pure form is not well-developed. For the sake of clarity, the oil sand coke used in this study is fluid coke, a term that will be used in the text as

well. The advantage of petroleum coke is that it has a high calorific value, however, its high sulphur and vanadium content puts it in a very disadvantageous position from an environmental perspective, as compared to coal. In particular, vanadium oxide (V_2O_5) causes slag of boiler pipes. V_2O_5 can be accumulated in the selective catalytic reduction (SCR) NO_x removal catalyst, and serves as an oxidation catalyst, thereby oxidizing SO₂ into SO₃. SO₃ then forms deposits in the downstream process together with ammonia^[6]. Therefore, a gasification process not emitting SO_x and NO_x and yet capable of generating power and producing new chemical materials is the best process for utilizing oil sand coke.

Biomass, on the other hand, is one of environmentally friendly fuels. It contains less sulphur and ash but more hydrogen than coal. Therefore, biomass is likely to be an attractive clean development mechanism option for reducing green house gas emission. However, only biomass cannot be used for a fuel since its heating value is relatively low. Therefore, Co-gasification of biomass and coal can be considered as a potential fuel-base for gasification and further synthesis gas (syngas: CO+H₂) production and methanol/dimethyl ether (DME) synthesis. Co-gasification of biomass and coal has been proposed as a bridge between energy production based on fossil fuels and energy production based on renewable fuels.

Combined gasification of biomass and coal/pet-coke allows achievement of economy of production, operational stability, decreasing the impact on the environment and optimal thermal efficiency for the process. Comparison between sole biomass gasification and co-gasification is as given in the Table 1.1.

Table 1.1 Advantage of co-gasification of biomass with other feedstock ^[7]	
Disadvantage of sole biomass gasification	Advantage of co-gasification
Small scale	Big scale (economically)
Tar production Low gasification temperature	No tar production Tar converted to gas at high T Bio-ash as catalyst to coal gasification High gas yield
Low heat value High CO ₂ content	High heat value CO ₂ converted to CO at high T
Fluidization quality: Anomalistic shape, Inert bed particle (sand), abrasion	Fluidization quality: Coke as bed particles, Abrasion reduced and power saved

Gasification of solid fuel can be divided in two main stages: pyrolysis or devolatilization and subsequent gasification of the remaining

char, with the second stage being the controlling step of the overall process. Gasification means the partial oxidation and conversion of a carbonaceous solid or liquid substance into a synthesis gas (syngas) in which the major components are carbon monoxide (CO) and hydrogen (H₂), while pyrolysis refers to the thermal decomposition of a carbonaceous material in the absence of oxygen. Knowledge about the reactivity of chars and their structure variation as reaction progress is fundamental for the design of gasification reactors, because char gasification determines the final conversion achieved in the process ^[8].

I-C: Objectives of this work;

The objective of the present work is to investigate the interaction of different fuels and elucidate any advantages that may arise from the binary and co-gasification of coal/biomass/coke. Specific investigations will be as follows:

- (1) The temperature and feedstock in the pyrolysis reaction in Drop Tube Furnace will be varied to investigate their effects on the morphology, porosity, kinetic properties of produced chars;
- (2) Char reactivity data will be acquired for the reaction of carbon dioxide with Genesee coal, Fluid coke and biomass chars, both alone and selected mixtures;

- (3) From the experimental results, any potential synergism will be examined between pairs of single fuel char and blended fuel char from the pyrolysis process in DTF;
- (4) Temperature and blending ratio effect on synergism of blended char will be discussed and explained;
- (5) Factors leading to synergism (e.g. shrinking and agglomeration) of particles will be explained.

References

- [1]. National Energy Board (NEB). Energy Reports - Canada's Energy Future: Scenarios for Supply and Demand to 2025 (revised in 2003). 2007(11/30/2007)
- [2]. World Coal Institute (WCI). Coal Facts 2007th edition. 2007
- [3]. Environmental Protection Agency, National Air Quality and Emissions Trend Report. 1997, Environmental Protection Agency: Washington, D.C.
- [4]. Fitzer. E., Kochling K-H, Boehm H.P., Marsh H. Recommended terminology for the description of carbon as a solid. Pure & Appl. Chem., Vol. 67, No. 3, pp. 473-506, IUPAC 1995
- [5]. Edward Furimsky. Gasification of oil sand coke: Review. Fuel Processing Technology, Vol.56, pp. 263–290, 1998
- [6]. Sang Jun Yoon, Young-Chan Choi, See-Hoon Lee, Jae-Goo Lee. Thermogravimetric study of coal and petroleum coke for co-gasification. Korean J. Chem. Eng., Vol. 24, No. 3, pp. 512-517, 2007
- [7]. Jicheng Bi. Co-gasification of biomass and coal in a fluidized bed. The 2nd Biomass-Asia Workshop, Bangkok, Dec.13-15, 2005
- [8]. Raymond. C. Everson and Hein. W. J. P. Neomagus, Henry Kasaini, Delani Njapha. Reaction kinetics of pulverized coal-chars derived from inertinite-rich coal discards: Gasification with carbon dioxide and steam. Fuel, Vol. 85, pp. 1076-1082, 2006

CHAPTER II

LITERATURE REVIEW

This chapter includes a review on composition of feedstock, gasification and co-gasification and experimental procedures.

II-A: Composition of the feedstock;

Prior to presenting a detailed review, the detailed properties of solid fuels are briefly presented.

II-A-1 Composition of biomass

Biomass materials that have been used as pyrolysis feedstock include cellulosic refuse, wood, crop residues, agricultural processing wastes and sewage sludge. Biomass can be analyzed based on ASTM standard. These tests include ultimate analysis and proximate analysis. Table 2.1 provides a summary of the ultimate analysis of a series of various biomass materials. Some typical fossil fuels are included for the sake of comparison. It is evident that, whilst biomass materials have a higher hydrogen/carbon ratio compared to coals, they have more than twice as much oxygen compared with different types of coal. In comparison with crude petroleum feedstock, the oxygen content of biomass is about fifty times higher. Hydrocarbon fossil fuels such as heavy oil make up for the

lack of oxygen by being comprised of twice as much carbon and hydrogen as a typical biomass material.

Table 2.1 Ultimate analyses (wt%) of biomass and fossil fuel cracking feedstock with their equivalent chemical formula ^[1]						
Material	C	H	O	S	N	Equivalent Formula
Cellulose	43.4	6.4	50.0	0.0	0.0	$C_6H_{10.6}O_{5.2}$
Aspen-Poplar	48.0	6.2	45.6	0.0	0.2	$C_6H_{9.3}O_{4.3}$
Birch-Flour	48.7	6.4	44.4	0.0	0.1	$C_6H_{9.3}O_{4.1}$
Bagasse	49.4	6.4	43.5	0.1	0.6	$C_6H_{9.4}O_4$
Municipal SW	52.3	6.7	39.3	0.1	0.5	$C_6H_{9.2}O_{3.4}$
Cow Manure	54.0	6.5	33.1	0.7	3.9	$C_6H_{9.6}O_{2.9}$
Spent-coffee	57.0	7.6	32.9	0.1	2.1	$C_6H_{9.6}O_{2.6}$
Peat	58.0	6.1	32.9	0.3	2.5	$C_6H_{7.6}O_{2.6}$
Sewage Sludge	57.1	7.9	29.2	0.0	5.8	$C_6H_{10.0}O_{2.3}$
Lignin	62.8	5.9	27.3	2.2	1.5	$C_6H_{6.7}O_2$
Lignite Coal	72.2	5.2	20.3	0.6	1.7	$C_6H_{5.2}O_{1.3}$
Sub-bit. Coal	75.5	5.4	17.0	0.5	1.6	$C_6H_{5.1}O_{1.1}$
Petroleum WV	83.6	12.9	3.6	n.a.	n.a.	$C_6H_{11.1}O_{0.2}$
Cold Lake	83.7	10.4	1.1	4.4	0.4	$C_6H_{8.9}O_{0.06}$

The main constituent of biomass materials is cellulose. Cellulose is the main building block of plant cell walls and is a biopolymer with the

elementary chemical formula $(C_6H_{10}O_5)_n$. Extensive research into the structure of cellulose has identified it as a linear polysaccharide composed of anhydroglucose units linked to each other. Lignin is the other major component of plants and provides the plant tissue with mechanical strength. It may be isolated from plants as it is insoluble during hydrolytic removal of polysaccharides ^[2].

II-A-2 Composition of coal

Coal is a fossil form, produced over millions of years by the effect of temperature and pressure on the remains of plants. The Ultimate (elemental) analysis (C, H, N, S and O contents) of some typical coals is shown in Table 2.1. Coal has a very complex and diverse structure. Coals are composed of a complex mixture of organic materials containing mostly carbon, hydrogen and oxygen. They also contain smaller amounts of sulphur, nitrogen and some trace elements. Different coals have different degrees of maturity depending on their composition and the geological conditions in which they matured over time. This is known as the “rank” of the coal. A high rank coal has higher carbon content and lower oxygen and hydrogen composition, compared to a lower rank coal. Lignite is a typical low rank coal, whilst anthracite is identified as a high rank coal ^[3].

II-A-3 Composition of petroleum coke

Petroleum coke is produced through the thermal decomposition of heavy petroleum process streams and residues. It is a product of extreme temperature and pressure treatments that convert heavy petroleum feedstock into a solid substance composed predominately of carbon.

The three most common feedstock used in coking operations are reduced crude (vacuum residue), thermal tar, and decant oil (catalytically cracked clarified oil). These are heated to thermal cracking temperatures and pressures (485 to 505°C at 400 KPa) that create petroleum liquid and gas product streams. The material remaining from this process is a solid concentrated carbon material, petroleum coke ^[3].

Petroleum coke is composed primarily of elemental carbon organized as a porous polycrystalline carbon matrix. The specific chemical composition of any given batch of petroleum coke is determined by the composition of the feedstock used in the coking process, which in turn are dependent upon the composition of the crude oil and refinery processing from which the feedstock is derived.

II-A-4 Comparison of fuel characteristics

It can be very useful to compare the characteristics of the possible fuels: coal, coke and different types of biomass. As it can be seen from Table 2.2, all biomass types are quite similar and have some differences with the other fuels. Biomass has more moisture and volatiles than coal or coke. Its LHV (lower heating value) is roughly the same as that of the coal and half of that of the coke. The same can be said about carbon content. The difference between biomass and coal is that the first has high oxygen content and the second high ash content. Biomass has about twice the hydrogen content than the other fuels. Lastly, biomass has low sulphur content, especially if compared with coke, as shown in the table 2.2^[4].

Table 2.2 Composition and heating value tests on several feedstocks ^[4]								
	Coal	Coke	W.S	B.S	P.W	O.T	W.T	Cynara
Moisture(wt%)	2	2	12.1	13.8	8	15	15	8
<i>Proximate analysis (wt%, d.b.)</i>								
Volatile matter	22.1	12.4	73.6	75	76.3	78.1	76.6	76.5
Fixed carbon	31.4	87.0	18.5	19.3	18.1	18.9	20.7	17.7
Ash	46.5	0.58	7.9	5.7	5.6	3	2.7	5.8
<i>Ultimate analysis (wt%, d.b.)</i>								
C	40.6	87.7	45.6	45.6	47.2	49.8	49	46.8
H	2.8	3.8	5.7	5.6	5.7	6	5.7	5.8
O	8.4	0.19	40	42.5	39.2	40.4	41.8	40.7
N	0.82	1.5	0.7	0.5	2.2	0.7	0.7	0.7
S	0.88	6.2	0.09	0.09	0.09	0.06	0.05	0.13
Ash	46.5	0.58	7.9	5.7	5.6	3	2.7	5.9
<i>LHV (kJ/kg, w. b.)</i>								
LHV	15.10	33.22	14.47	14.40	16.36	15.78	15.18	16.04
W.S=Wheat Straw, B.S=Barley Straw, P.W=Pine Wood, O.T=Olive Tree, W.T=Wine Tree								

II-B: Understanding gasification

Gasification is a proven manufacturing process that converts hydrocarbons such as coal, petroleum coke (pet-coke) and biomass to a synthesis gas (syngas), which can be further processed to produce chemicals, fertilizers, liquid fuels, hydrogen and electricity. Gasification is not a combustion process. It is a flexible, commercially proven and efficient

technology that produces the building blocks for a range of high-value products from a variety of low-value feedstock.

A hydrocarbon feedstock is injected with oxygen and steam into a high temperature pressurized reactor until the chemical bonds of the feedstock are broken. The resulting reaction produces the syngas. The syngas is then cleansed to remove impurities such as sulphur, mercury, particulates and trace minerals. Carbon dioxide can also be removed at this stage. The clean syngas is then used to make either a single product such as fertilizer or multiple products such as hydrogen, steam and electric power.

In conventional combustion technology, a hydrocarbon feedstock is burned using excess air to ensure complete combustion. In gasification the amount of oxygen is generally one-fifth to one-third the amount theoretically required for complete combustion. Carbon monoxide (CO) and hydrogen (H₂) are the main components of the produced gas, only a fraction of the carbon is combusted.

Gasification of a hydrocarbon feedstock can be divided into two-stage process. The first one is the fast pyrolysis of the feedstock, an essentially thermal effect which consists of a sudden release of volatiles accompanied by drastic changes in the morphology and molecular structure

of the fuel particles and the second one is the chemical reaction between the oxidizing agent, such as steam, carbon dioxide, oxygen or a mixture of these gases and both the gaseous (volatile matters) and the solid (char) products of pyrolysis at a much higher temperature.

This two-stage process can be summarized as ^[5]:

- Pyrolysis (also called mild gasification, thermal decomposition, carbonization or devolatilization)

A hydrocarbon feedstock + heat → char + liquids + gases

- Gasification

Char + gasifying agent → gases + ash (and/or slag)

Much of the oxygen fed to the gasifier, either as pure oxygen or in air, is used up by oxidation reaction (partial combustion or combustion) and thereby provides the heat necessary to dry the coal, to break chemical bonds in the feedstock, to raise the products to reaction temperature and to drive the following gasification reactions. Table 2.3 shows the basic reactions that take place during fuel gasification.

Table 2.3 Reactions happened during gasification ^[5]	
Oxidation	$C + O_2 \rightleftharpoons CO_2$ $C + (1/2)O_2 \rightleftharpoons CO$
Boudouard	$C + CO_2 \rightleftharpoons 2CO$
Water-gas	Primary $C + H_2O \rightleftharpoons CO + H_2$
	Secondary $C + 2H_2O \rightleftharpoons CO_2 + 2H_2$
Methanation	$C + 2H_2 \rightleftharpoons CH_4$
Water-gas shift	$CO + H_2O \rightleftharpoons CO_2 + H_2$
Steam reforming	$CH_4 + H_2O \rightleftharpoons CO + 3H_2$
Dry reforming	$CH_4 + CO_2 \rightleftharpoons 2CO + 2H_2$
Tars reforming	$2C(s) + 2H_2O \rightleftharpoons CO_2 + CH_4$

Like all chemical reactions, these tend to a state of equilibrium. The operating temperature and pressure are important in determining equilibrium concentrations of the gases produced.

Gasification with carbon dioxide (Boudouard reaction) is endothermic and for a given carbon in the absence of a catalyst, takes place at several orders of magnitude slower than the C-O₂ reaction at the same temperature. The reaction proceeds very slowly at temperature below 1000K, and is inhibited by its product.

Gasification with steam (water-gas reaction) is an endothermic reaction which is favoured by elevated temperature and reduced pressure and, in the absence of a catalyst, occurs slowly at temperatures below 1200K. The unanalyzed reaction is inhibited by its product but is generally somewhat faster than the C-CO₂ reaction under the same conditions.

Gasification with hydrogen (Methanation/hydrogasification reaction) is very slow except at high temperatures.

When a coal particle enters a gasifier it is first dried by the hot gases present in the reactor. As the temperature of the coal particle exceeds approximately 673K the pyrolysis reactions occur. During pyrolysis hydrogen-rich volatile matter is evolved and tars, oils, phenols and hydrocarbon gases form. The char residue contains the remaining mineral matter and carbon.

When the temperature of the remaining char exceeds approximately 973K the gasification reaction proceed. The char reacts with O₂, steam (H₂O), CO₂, H₂ and the gases react among themselves to approach equilibrium and produce the final gas mixture.

The water-gas shift reaction has influence on the CO/H₂ ratio, which can be important if the gas is for use in synthesis.

II-C: Importance of studying pyrolysis process.

Naturally, pyrolysis is the initial stage in any gasification process, which divides the feedstock into a hydrogen-rich fraction, consisting of gases and tar (volatile matter), and a carbon-rich solid residue (char), because whenever a solid fuel is subjected to high temperature devolatilisation occurs. Volatile matter is a mixture of low molecular weight compounds (hydrogen, oxides of carbon, methane, etc) and higher molecular weight hydrocarbons, such as light oils and tars. The solid residue is a composite of the non-volatile or “fixed” carbon mixed with the inorganic mineral matter which will form ash upon oxidation.

In the pyrolytic stage the solid fuel is converted into char as an intermediate product which is subsequently or simultaneously gasified. The treatment condition in pyrolysis strongly affects the yield and the reactivity of the char, and consequently influences the subsequent process. In gasification, the temperatures and product distributions are strongly influenced by pyrolysis. Maximization of the rate of evolution and yield of volatiles reduces reliance on relatively slower heterogeneous gas-solid reactions ^[6]. In addition, the pyrolysis process controls swelling, particle

agglomeration, char reactivity and char physical structure ^[7]. Therefore among the different aspects of investigation, the kinetics of char gasification plays a very important role since it provides valuable data for better design of gasifier.

Moreover, if the heating of the feedstock particles is carried out under an oxygen-free atmosphere, the solid product obtained can be readily isolated and recovered for its full characterization. The importance of this relies in the fact that the isolated material is the final product of the pyrolysis stage and at the same time, the starting point of the subsequent gasification stage. A full knowledge of this material can simplify the study of overall gasification stage ^[8].

II-D: Review of related work on co-gasification;

Previous investigations on the co-gasification of biomass/coal blends have mostly concentrated on the mechanism of production of gas and liquid phase species ^[9-13]. Additionally, there are also few studies that have focused on the interaction effect (also known as the catalytic or synergetic effect) between coal, biomass and other fuels, such as petroleum coke and plastics ^[10-16].

Zhang et al. ^[14] studied co-pyrolysis of legume straw and Dayan lignite in a free-fall reactor under atmospheric pressure in nitrogen environment, over a temperature range of 500-700°C. The results showed that the compositions of the gaseous products from the blended samples are not all in accordance with those of their parent fuels. Moreover, under the higher blending ratio conditions, the char yields were lower than the theoretical values calculated on pyrolysis of each individual fuel and consequently the liquid yields were higher. The results indicated that there exists a synergetic effect in the co-pyrolysis of biomass and coal and might explained by that biomass in blends offers plenty of hydrogen donors and plays a hydrogenation role on coal pyrolysis.

Kumabe et al. ^[15] carried out a study on the co-gasification of woody biomass and coal in an oxygen-containing atmosphere in a pressurized fluidized bed reactor and found that the synergy due to the mixture of woody biomass and coal might be observed in the extent of water-gas shift reaction based on the finding that the extent of the shift reaction in the equilibrium did not vary significantly with the biomass ratio, in contrast, the extents of the shift reaction in the experiment varied significantly with the biomass ratio and reached the maximum value at the biomass ratio of 0.5.

Similar findings were reported by Sjostrom et al. ^[16], who studied the reactivity of char in co-gasification of biomass and coal. In their study, a noticeable phenomenon was that the mixtures of the fuels and their char formed in situ demonstrated an unexpected high reaction rate of gasification under studied conditions. The yield of char decreased and consequently the production of gas increased. Further, both the formations of tar and nitrogen compounds also seemed affected synergetically in the co-gasification experiments of the fuels. The yields of tar and of ammonia were lower than expected. Although not very certain, they reported the occurrence of synergetic effects in the co-gasification of birch wood with two different types of coal in experiments performed in the pressurized fluidized-bed reactor. The reactivity of the fuels in the mixtures and the formed chars was seen to have increased, leading to promoted gas production.

In another investigation, Collot et al. ^[17] co-pyrolyzed and co-gasified coal and biomass in bench-scale fixed- and fluidized-bed reactors. They found that, in pyrolysis experiments, neither intimate contact between fuel particles nor their relative segregation led to synergistic effects. They however reported that mineral matter residues from the wood appear to have played a catalytic effect during combustion. Generally, they concluded that there was no evidence of synergy that was found with the fluidized-bed

reactor, thereby demonstrating the lack of contact between coal and biomass particles in the system.

Another recent work is that by Feroso et al.,^[18] who co-gasified coal, biomass and petroleum coke at high pressure. From this work, a synergistic effect was observed for blends of coal with pet-coke and an increase in the production of H₂ and CO was obtained. Furthermore, the addition of a small amount of biomass (up to 10%) led to an increase in H₂ and CO production. Finally, blending biomass with coal/pet-coke blends did not produce any significant change in H₂ production, although slight variations were observed in the production of CO and CO₂.

Yoon et al.^[19] has done preliminary study of gasification of coal and petroleum coke mixtures, thermogravimetric analysis was performed at various temperatures (1100, 1200, 1300 and 1400°C) and the isothermal kinetics were analyzed and compared. The activation energies of coal, petroleum coke and coal/petroleum coke mixture were calculated by using both a shrinking core model and a modified volumetric model. The results showed that the activation energies for the anthracite and petroleum coke used in this study were 9.56 and 11.92 kcal/mol and reaction times were 15.8 and 27.0 min. In the case of mixed fuel, however, the activation energy (6.97 kcal/mol) and reaction time (17.0 min) were lower than the average

value of the individual fuels, confirming that a synergistic effect was observed in the co-processing of coal and petroleum coke.

Alkali metal salts, especially potassium and calcium salts, are considered to be effective catalysts for carbon gasification by steam and CO₂ while too expensive for industry application. Zhua et al. ^[20] used an herbaceous type of biomass, which has a high content of potassium to act as a source of catalyst by co-processing with coal. The co-pyrolysis chars revealed higher gasification reactivity than that of char from coal, especially at high levels of carbon conversion. On the influence of the alkali in the char and the pyrolysis temperature on the reactivity of co-pyrolysis char, experimental results showed that the co-pyrolysis char prepared at 750°C had the highest alkali concentration and reactivity as compared to the char prepared at 850°C.

Vuthaluru ^[21] on his study of thermal behaviour of coal/biomass blends during co-pyrolysis reported no interactions between coal and biomass and the 50:50 coal/biomass blend had the highest reaction rate, ranging from 1×10^9 to $2 \times 10^9 \text{ min}^{-1}$. There are also some investigations by Cai et al. ^[22] who investigated the thermal behaviour of coal blends with plastics during co-pyrolysis and found that the difference of weight loss between experimental and theoretical data was 2.0-2.7% at 550-650°C,

which was the overlapping degradation temperature interval between coal and plastic, assuming that to be the favourable temperature for hydrogen transfer from plastic to coal. Palmer et al., ^[23] while working on the co-conversion of coal/waste plastic mixtures under various pyrolysis and liquefaction conditions, had almost the same findings as those by Cai et al. ^[22]

Most of these studies reviewed above are based on pure coal or coal blends with other fuels. However, not much research has been conducted on the co-pyrolysis of the coke blend with biomass. The purpose of this study is to investigate any synergies resulting from vastly different characters of fuels: coke high in sulphur, biomass high in calcium and potassium and coal high in silica. The differences in the amount and type of volatile matter in different fuels do have impact on the char character and gasification kinetics.

II-E: Co-gasification of biomass and coal

In recent years, some researchers ^[6-8] have reported on the co-gasification of woody biomass with coal and have pointed out a number of advantages that come with it. The addition of woody biomass to coal gasification do not only reduce CO₂ emissions but also reduce the problems caused by sulphur and ash contained in coal; this is because the woody

biomass has almost no sulphur and has low ash content. However, biomass gasification is relatively expensive and produces relatively larger amount of tar. Therefore, co-gasification can not only reduce the cost of the feedstock but also reduce the problems that occur in plant operation due to the reduction of tar. Moreover, the high thermochemical reactivity of biomass and the high content of volatiles in it suggest that some synergetic effects might exist during the simultaneous thermochemical treatment of biomass and coal.

II-E-1 Factors influencing the co-gasification

1. Temperature:

The rise in gasification temperature promotes hydrocarbons further reactions, leading to a decrease in tars and hydrocarbons contents and an increase in H₂ release and total gas yield. For example, as shown in Figure 2.1, increasing temperature, from 750 to 890 °C, during gasification of a mixture with 60% (w/w) of coal, 20% of pine and 20% of Polyethylene (PE) waste ^[24], led to a decrease in methane and other hydrocarbons concentration of about 30 and 63%, respectively, while hydrogen concentration increased around by 70%.

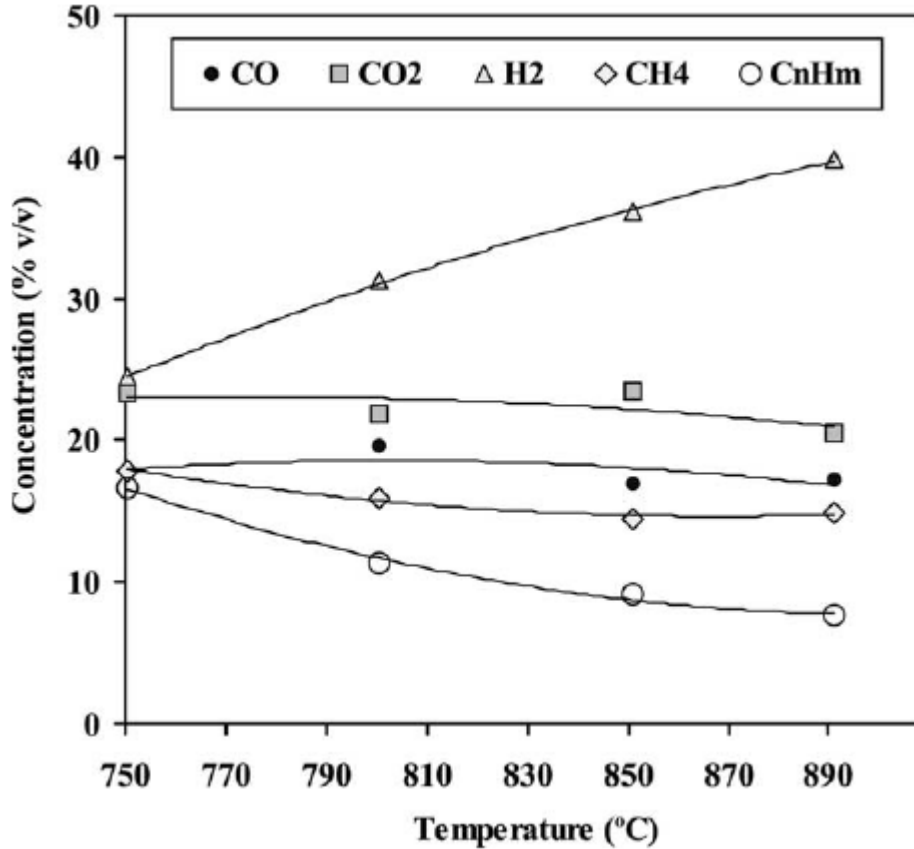


Figure 2.1 Effect of temperature on gas composition for co-gasification ^[24]

Char yield should, in principle, be as little as possible to ensure a high conversion during gasification. The rise of temperature in co-gasification of coal mixed with pine and PE wastes, led to a decrease in char formation of only 9%, which agrees with the results obtained by Gil et al.^[25], which showed that temperature did not influence much char production. However, Herguido et al.^[26] observed a more pronounced decrease of char yield, about 20% (depending on the type of biomass studied), with the rise of temperature, which agreed with the greater increase in gas yield.

2. Gasification gas flow:

Pinto et al. ^[24] studied the influence of reaction flow rate on gasification output parameters for co-gasification of coal with pine and PE waste. They found that a higher O₂/fuel ratio promoted an increase in the quantity of gas produced, as shown in Figure 2.2, due to the increase of combustion reaction rates. It was also noted that there was a clear decrease in HHV (high heat value), which might be due to consumption of hydrocarbons by combustion. These variations led to a reduction in apparent energy conversion with the rise in O₂/fuel ratio. The increase of this ratio also decreased the energy requirements of gasification process due to the energy release in the combustion process.

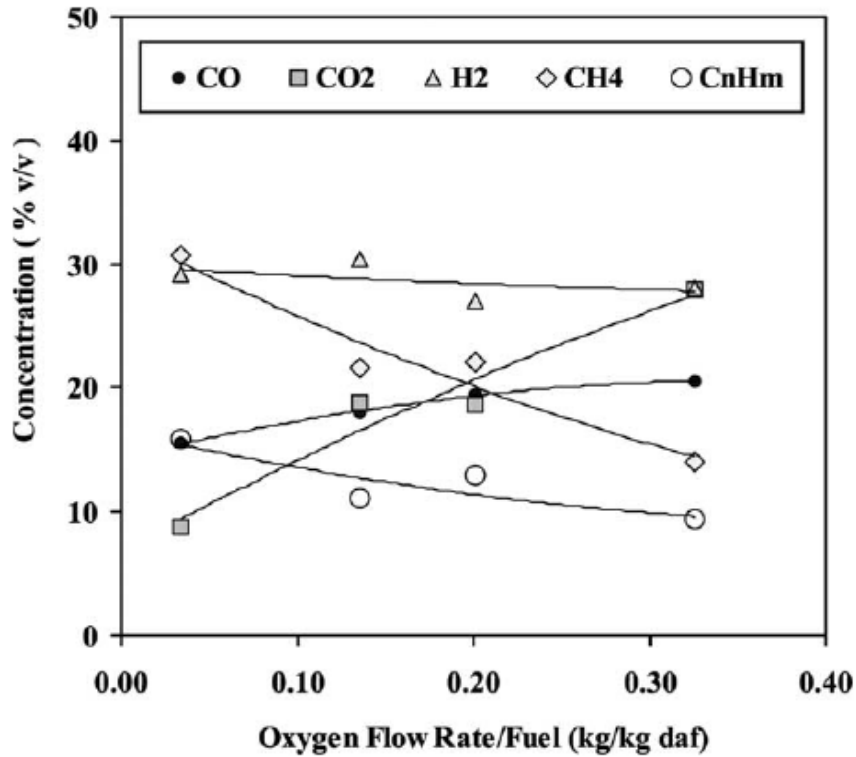


Figure 2.2 Effect of oxygen flow rate/fuel ratio on gas composition for co-gasification ^[33]

However, Pinto et al. ^[24] also pointed that, in principle, any increase in O_2 amount should be determined by the H_2/CO ratio requirement of the end-use application of gas, as shown in Figure 2.3, the conversion rate of H_2 and CO are highly depended on the ratio of O_2 in O_2 and steam mixed gasification medium flow. Higher fractions of oxygen on the gasifying mixture caused some decrease on H_2 , methane and other hydrocarbons, as the combustion and reforming reaction was promoted, meanwhile, both CO and CO_2 concentration increased and the concentration of the latter more than doubled.

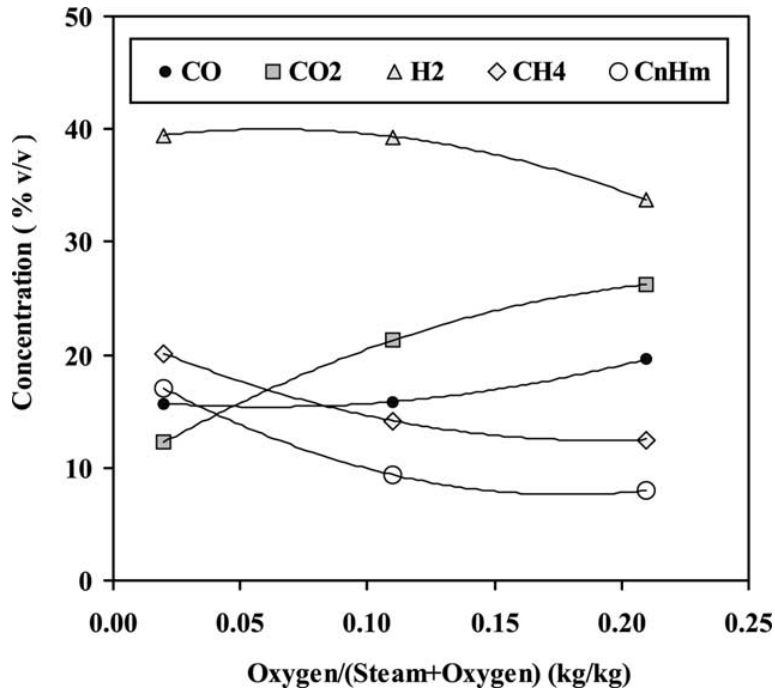


Figure 2.3 Effect of oxygen/steam ratio on gas composition for co-gasification ^[24]

Fairly similar results have been shown by other researchers, no matter what was the nature of the feedstock gasified ^[27-30]. Kim et al. ^[27] studied a sub-bituminous coal (Shenwha) gasification and although using a reactor with different characteristics, they also detected that H₂, C₂H₄, C₂H₆, C₃H₈, C₃H₆ decreased slightly, whilst CO and CO₂ increased with increasing oxygen, thus the HHV of the gas decreased and gas yield increased due to combustion of hydrocarbons. Aznar et al. ^[30] studied biomass gasification with steam and oxygen mixtures in a pilot fluidised bed gasifier. It was reported that the rise of oxygen content led to an increase in gas yield, whose composition showed a decrease in both H₂ and gaseous hydrocarbons.

3. Feedstock composition:

a. Biomass/coal

A research done by Kumabe et al. ^[14] studied the co-gasification behaviour of a woody biomass and coal by varying the biomass content ratio from 0 to 1 in the total feedstock on a carbon basis. The conversion to gas on a carbon basis increased with an increase in the biomass ratio, whereas the conversions to char and tar decreased. With an increase in the biomass ratio, the H₂ composition decreased and the CO₂ composition increased. However, the CO composition was independent of the biomass ratio. A low biomass ratio led to the production of a gas favourable for methanol and hydrocarbon fuel synthesis and a high biomass ratio led to the production of a gas favourable for DME synthesis. The synergy due to the mixture of woody biomass and coal might be observed in the extent of the water–gas shift reaction. The co-gasification conditions in the study provided a cold gas efficiency ranging from 65% to 85%.

Woody biomass has more volatile matter compared to coal. Tar production is an important issue pertaining to biomass gasification. At the higher biomass ratio, the conversion to tar is less because the air–fuel ratio is relatively high ^[14]. In contrast, at the lower biomass ratio, the conversion to char is relatively higher, while that to gas is lower, because the gasification temperature was relatively low as a condition for coal

gasification. The tar derived from pyrolysis can be generally classified into two types: heavy tar, which is difficult to gasify and is finally polymerized to produce char, and light tar, which is easy to gasify and is finally converted to gas. A significantly large amount of heavy tar is produced in coal gasification as compared to that from woody biomass gasification. Consequently, it can be inferred that the lower biomass ratio is responsible for the high conversion to tar and char.

b. Biomass components. (Taking woody biomass for example)

As the feedstock utilized in biomass gasification, inexpensive materials such as forest residue, wood residue and rice straw would be practical. However, the cellulose, hemicelluloses and lignin composition of these materials can differ significantly, as shown in Table 2.4.

Table 2.4 Properties of biomass ^[31]						
	Spent Coffee	Aspen Poplar	Scots Pine	Silver Birch	Rice Straw	Bagasse
Composition wt%, Dry Basis						
Cellulose	49.8	42.3	40.0	41.0	33.0	40.0
Hemi-cellulose	9.5	31.1	28.5	32.4	26.0	29.0
Lignin	22.1	16.2	27.7	22.0	7.0	13.0

Gani ^[32] studied co-combustion and co-gasification technologies of coal with biomass in several practical coal boilers in order to reduce CO₂

emission, fuel cost and so forth. In this study, fundamentals of pyrolysis and combustion characteristics of several types of biomass were studied using a Thermogravimetric Analyzer Drop Tube Furnace. Figure 2.4 shows profiles of the mass decreased fraction of combustible for three types of biomass, cellulose and lignin. From the figure, pyrolysis starts at about 473K for all samples. However, the trend of mass decrease for bark differs from rice husks. Comparing these results with the results for lignin and cellulose, the profile for bark is relatively similar to that for lignin. This is because the bark contains more lignin rather than cellulose. On the contrary, the profile for rice husks comes close to that for cellulose. These results suggest that the volatilization behaviour of biomass depends on the lignin and cellulose content.

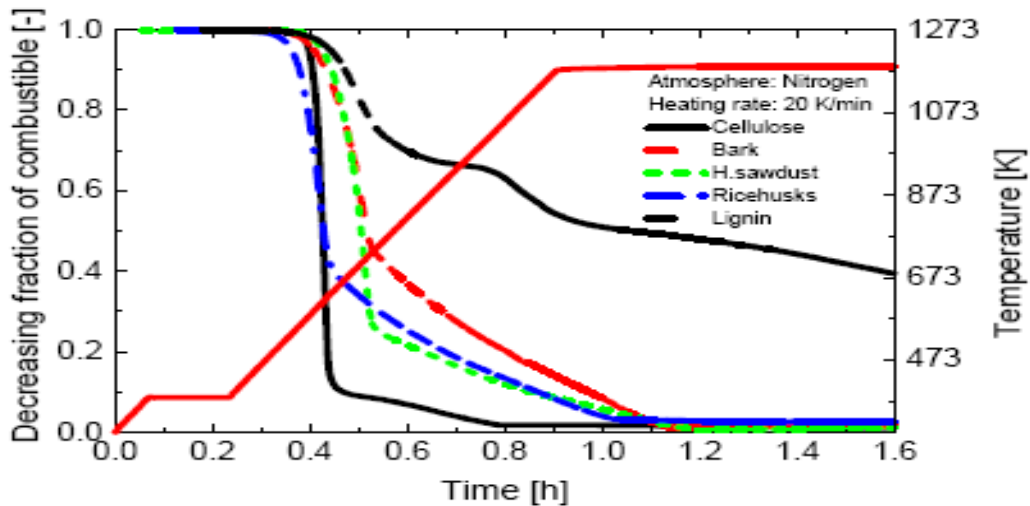


Figure 2.4 Decreasing fraction of combustible for several biomass, lignin and cellulose ^[32]

II-E-2 Catalyst on coal gasification

The catalytic gasification of coal has been studied extensively to develop efficient and economic processes for conversion of coal to clean fuel gas ^[33, 34]. Lee et al. ^[35] undertook some study aimed at increasing the gasification rate and control the composition of the product gas by using various catalysts. The catalytic activities of single salts in steam coal gasification depend considerably on the gasification temperature. The order of activity is $K_2CO_3 > Ni(NO_3)_2 > K_2SO_4 / Ba(NO_3)_2 > FeSO_4$. Of the binary catalysts tested, $K_2SO_4 + Ni(NO_3)_2$ exhibited the greatest cooperative effect. The activity ranking of binary catalyst salts is $K_2SO_4 + Ni(NO_3)_2 > K_2SO_4 + Ba(NO_3)_2 / K_2SO_4 + FeSO_4$.

Brown et al. ^[6] investigated catalytic gasification of coal char using biomass-derived potassium salts. Alkali metal salts, especially those containing potassium, are excellent promoters of gasification reactions but are generally considered too expensive for commercial use. Fast-growing biomass, which contains large quantities of potassium, may prove to be an excellent source of inexpensive gasification catalyst. A series of CO_2 -char gasification tests were performed in a thermogravimetric analyzer (TGA) to evaluate the catalytic activity of alkali-rich biomass-derived materials. Both switchgrass char and switchgrass ash displayed catalytic activity in mixtures with coal char produced from Illinois No. 6 coal. The results

obtained with switchgrass ash were especially impressive, with an almost eight-fold increase in coal char gasification rate at 895°C in a 10:90 mixture of coal char and switchgrass ash. These results give encouragement that biomass could be the source of inexpensive, coal gasification catalysts.

II-E-3 Interaction effect in co-gasification of biomass/coal/pet-coke mixture

Interaction effect (aka: catalytic effect, synergetic effect) is very important in co-gasification, which means the percentage of increasing or decreasing of the experimental yield (yield of co-pyrolysis / co-gasification of the mixture) with respect to the calculated yield (obtained by the linear combination of the pyrolysis/gasification yields of coal, pet-coke and biomass), which evaluate the interactions between blended feedstock.

The high thermochemical reactivity of biomass and the high content of volatiles in it suggest that some synergetic effects might be expected in simultaneous thermochemical treatment of wood and coal, which is demonstrated by some of the experimental ^[17] results on advantageous synergies obtained in co-gasification of birch wood with Daw Mill coal as well as with Polish coal using oxygen-enriched nitrogen in a pressurized fluidized bed gasifier.

Phenomenon of synergy in co-gasification of wood with coal has been reported. Madsen et al. ^[36] reported on a series of air-blown fluidized

bed and entrained bed co-gasification tests with coal and straw. Pressures in the larger unit were up to 14.2 bar and feed rate of the feedstock was a maximum of 720 kg/h. Feeding presented problems, but some synergies were noted. Sjostrom et al. ^[37, 16] also found synergies in fluidized bed co-gasification of wood and coal mixtures at small particle sizes. Reinoso et al. ^[38] reported on a comprehensive experimental program including a series of tests in larger pilot scale air-blown circulating fluidized bed gasifier at near atmospheric pressures. Waste coal, lignite and pine chips were used. Modeling comparisons indicated synergies existed between coal and biomass. Jong et al. ^[39] and Pan et al. ^[40] also noted analogous synergy phenomena in their research.

However, the study of the synergetic effects in co-gasification is still in its early phase, therefore sufficient data are not available for explaining the observations. Based on previous research, the following proposed scheme might be valid for the co-gasification of biomass and coal ^[16]:

1. Gasification is initiated by thermal or oxidative cleavage of the weakest covalent bonds in the organic matter in wood resulting in the formation of abundant volatiles which readily decompose and form plenty of free radicals.

2. The free radicals produced from wood decomposition or oxidation react not only with the organic matter in wood but may also react with the organic matter of coal, and thus initiate and increase the decomposition and oxidation reactions in coal.

3. The hydrogen-rich light molecules obtained in the devolatilization products of wood, as well as the hydrogen obtained in their cracking may react with the free radicals obtained from coal in the moment of their formation, thus preventing the recombination reactions and the formation of less reactive secondary char.

4. In addition, the alkali metals, known as effective catalysts for coal gasification, present in wood biomass might also promote the gasification reaction of coal with oxygen catalytically.

II-F: Gasification power plant: IGCC;

Recently Integrated Coal Gasification Combined Cycle (IGCC) is being considered as a next generation fossil power plant type in the aspects of higher overall cycle efficiency and superior environmental performances compared with conventional coal-fired power plants. IGCC is a combination of two leading technologies. The first technology is called gasification, which use carbonaceous feedstock to create syngas. The

second technology is called combined-cycle, which is the most efficient method of producing electricity commercially available today. Gasification process has been explained in the first chapter, so no need to do it again. The combined cycle consists of a combustion/gas turbine, a heat recovery steam generator and a steam turbine. The exhaust heat from the gas turbine is recovered in the heat recovery steam generator to produce steam which passes through steam turbine to produce more electricity. IGCC is more efficient than conventional power generating systems because it re-uses waste heat. On the other hand, the carbon dioxide produced during gasification is present at much higher concentrations and at higher pressures than in streams produced from conventional combustion, making them easier to capture. The vision is to convert synthesis gas into pure hydrogen using the water-gas shift reaction and use the hydrogen as an ultra-clean fuel with an exhaust gas of nothing but water.

However, because IGCC shows typically very complicated combination of gasification, gas clean-up, gas turbine, steam cycle and air separation unit (ASU) systems with various energy and mass integration schemes affecting the overall performances and the emission characteristics of IGCC^[41], it is very difficult for the engineers in power industry to determine the optimum integration condition of the subsystems.

As shown in Figure 2.5, the fuel of gas turbine combustor of IGCC is derived from coal or even heavy residue oil in refinery process [42]. In general, the heating value of the syngas fuel is about 20-30% of the natural gas. For this reason, the IGCC gas turbine combustor requires 4-5 times fuel consumption of the syngas compared with the natural gas combustor at the same turbine inlet temperature (TIT) condition. Another different feature of IGCC from conventional coal and natural gas power plants can be found in ASU-gas turbine integration scheme. Air is extracted from gas turbine compressor and then is fed to the ASU, which separates oxygen from air for the oxidizer of coal gasification and the nitrogen for the dilution agent of NO_x control in gas turbine combustor.

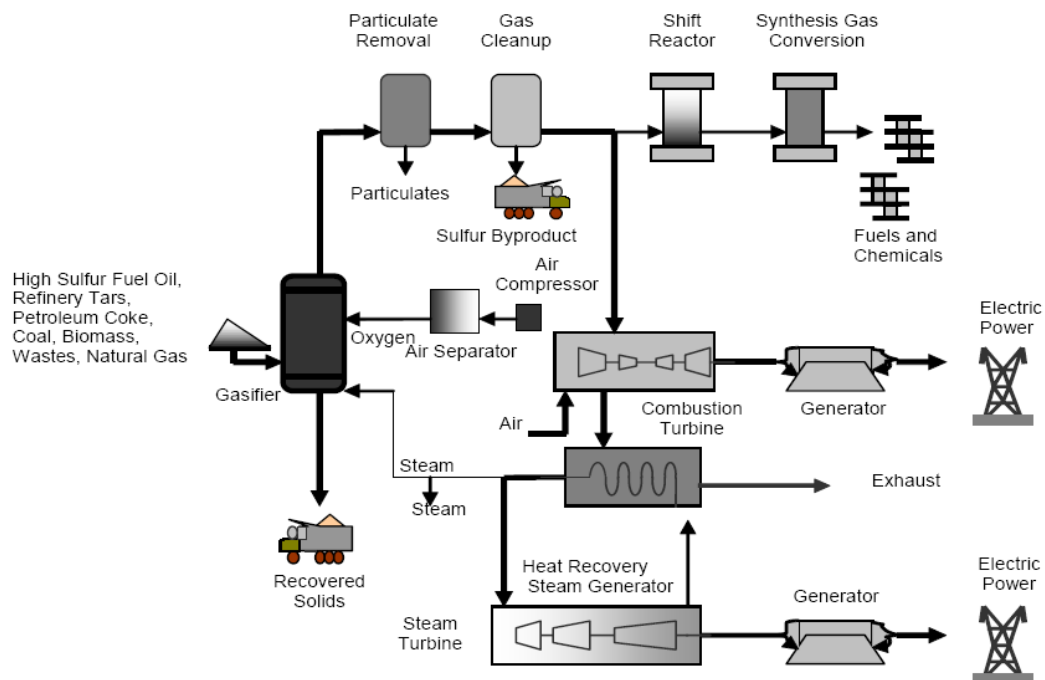


Figure 2.5 IGCC integration scheme [43]

II-G: Review of experimental procedures;

II-G-1: Drop tube furnace (DTF)

In order to determine the optimum integration condition of the subsystems in IGCC power plant, an air-blown two-stage entrained flow gasification technology has been employed in the demonstration plant. Because these plants are operated at high temperature and high pressure, a pressurized drop tube furnace facility (PDTF), as shown in Figure 2.6, is used to investigate coal reactivity under the same conditions as inside a gasifier.

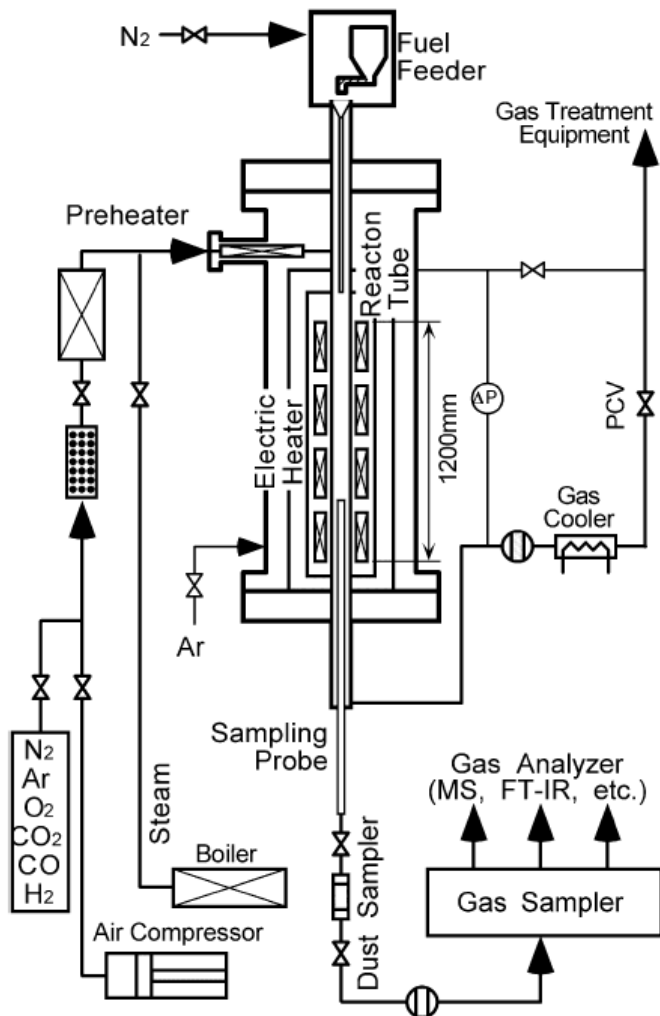


Figure 2.6 Schematic of the PDTF facility ^[44]

Reaction kinetic studies of coal and carbonaceous materials are usually carried out in one of the following types of apparatus: electrically heated wire grid, thermal gravimetric/derivative thermal gravimetric analyzers, pyroprobe, fluidized bed, shock tube, flat flame burner, plug flow reactor and drop-tube furnace. Among the above mentioned techniques, the drop-tube furnace, with its high heating rates (10^4 – 10^5 K/s),

high temperatures and dynamic conditions, may better reflect the pulverized fuel combustion/gasification environment.

Zhang et al. ^[45] studied tar destruction and coke formation of biomass in three different conversion processes: pyrolysis, steam gasification and partial oxidation. An entrained drop-tube furnace (DTF) was applied to all experimental tests. It was found that raising the temperature remarkably decreases tar evolution. Steam and oxygen also have a positive effect on tar destruction. Benzene and toluene are the most difficult condensable tar species to destroy.

In the report from Jiyi Luan et al. ^[46], a one-dimensional temperature-controlled drop tube furnace (DTF) was employed to study re-burning characteristics of corn straw, rice husk, and bituminous coal for the sake of reducing NO_x emission.

In another investigation ^[47], combustion behaviour of blends of two Indian coals of same rank with wide variation in mineral matter content were studied using Thermogravimetric Analyzer (TGA) and Drop Tube Furnace (DTF). DTF studies on coals and their blends and the role of macerals on the morphology of chars were well-documented. Miura ^[48] on his study of gasification reaction of coke, a pressurized drop tube furnace at

high pressure and high temperature was used. Matsuoka et al. ^[49] obtained useful and reliable pyrolysis data under high pressures, continuous pyrolysis experiments via a drop tube furnace. Similarly, pressurized drop tube furnace (PDTF) was used to understand the effect of coal type on coal gasification process, and then a numerical study was conducted ^[50]. DTF was also adopted in characterization of the properties of size fraction from coal and their char. ^[51]

II-G-2: Thermogravimetric analyzer (TGA)

Thermogravimetric Analysis or TGA is a testing procedure that is performed on samples to determine changes in weight in relation to change in temperature. Such analysis relies on a high degree of precision in three measurements: weight, temperature and temperature change. As many weight loss curves look similar, the weight loss curve may require transformation before results may be interpreted. A derivative weight loss curve can be used to tell the point at which weight loss is most apparent. Again, interpretation is limited without further modifications and deconvolution of the overlapping peaks may be required.

The TGA usually consists of a high-precision balance with a pan (generally platinum) loaded with the sample. The pan is placed in a small electrically heated oven with a thermocouple to accurately measure the

temperature. The atmosphere may be purged with an inert gas to prevent oxidation or other undesired reactions. A computer is used to control the instrument.

TGA is commonly employed in research and testing to determine characteristics of materials such as polymers, to determine degradation temperatures, absorbed moisture content of materials, the level of inorganic and organic components in materials, decomposition points of explosives and solvent residues. It is also often used to estimate the corrosion kinetics in high temperature oxidation.

Simultaneous TGA-DTA/DSC measures both heat flow and weight changes (TGA) in a material as a function of temperature or time in a controlled atmosphere. Simultaneous measurement of these two material properties not only improves productivity but also simplifies interpretation of the results. The complimentary information obtained allows differentiation between endothermic and exothermic events which have no associated weight loss (e.g., melting and crystallization) and those which involve a weight loss (e.g., degradation).

The temperature in many testing methods routinely reaches 1000°C or greater, but the oven is so greatly insulated that an operator would not be

aware of any change in temperature even if standing directly in front of the device. After the data is obtained, curve smoothing and other operations may be done such as to find the exact points of inflection.

This device can be used to generate continuous decomposition data of a sample as a function of either time (isothermal TGA) or temperature (dynamic TGA). It is one of the most common techniques used to investigate thermal events and reaction kinetics. TGA has been widely used in understanding pyrolysis and gasification rate of fuels and their chars. Brown et al. ^[52] performed a series of CO₂-char gasification tests in a thermogravimetric analyzer (TGA) to evaluate the catalytic activity of alkali-rich biomass-derived materials. Vuthaluru ^[53] investigated into the thermal behaviour during co-pyrolysis of coal, biomass materials and coal/biomass blends prepared at different ratios (10:90, 20:80, 30:70 and 50:50) using a TGA apparatus. Li et al. ^[54] performed thermogravimetric studies on biomass showed that the DTG peaks of devolatilisation move to a higher temperature range and the peak becomes wider with the increase of the heating rate and expected that the pyrolysis processes with different devolatilisation temperatures could happen simultaneously under very fast heating rate pyrolysis condition as is in the case of free fall reactor. Similarly, Sadhukhan et al. ^[55] carried out pyrolysis experiments in Helium

atmosphere with blends of biomass and high volatile coal in TGA – FTIR to help to set up pyrolysis model.

Recently, Naredi et al. ^[56] pyrolyzed a high volatile bituminous coal in a DTR at different furnace temperatures and in a TGA to observed the char reactivity profile. Zhang et al. ^[57] determined the reactivity of the chars (TGA) method in 0.1 MPa air in the same way.

II-G-3: Brunauer-Emmett-Teller measurement (BET)

BET theory is a rule for the physical adsorption of gas molecules on a solid surface and serves as the basis for an important analysis technique for the measurement of the specific surface area of a material. In 1938, Stephen Brunauer, Paul Hugh Emmett and Edward Teller published an article about the BET theory in a journal for the first time; “BET” consists of the first initials of their family names.

The concept of the theory is an extension of the Langmuir theory, which is a theory for monolayer molecular adsorption, to multilayer adsorption with the following hypotheses: (a) gas molecules physically adsorb on a solid in layers infinitely; (b) there is no interaction between each adsorption layer; and (c) the Langmuir theory can be applied to each layer. The resulting BET equation is expressed by Eqn 2.1 and Eqn 2.2 ^[58]:

$$\frac{1}{v[(P_0/P)-1]} = \frac{c-1}{v_m c} \left(\frac{P}{P_0} \right) + \frac{1}{v_m c} \quad \text{Eqn 2.1}$$

$$c = \exp\left(\frac{E_1 - E_L}{RT}\right) \quad \text{Eqn 2.2}$$

P and P_0 are the equilibrium and the saturation pressure of adsorbate at the temperature of adsorption, v is the adsorbed gas quantity (for example, in volume units), and v_m is the monolayer adsorbed gas quantity. BET constant is c .

E_1 is the heat of adsorption for the first layer, and E_L is that for the second and higher layers and is equal to the heat of liquefaction. Equation (1) is an adsorption isotherm and can be plotted as a straight line with $1 / v[(P_0 / P) - 1]$ on the y-axis and $\phi = P / P_0$ on the x-axis according to experimental results. This plot is called a BET plot. The linear relationship of this equation is maintained only in the range of $0.05 < P / P_0 < 0.35$. The value of the slope A and the y-intercept I of the line are used to calculate the monolayer adsorbed gas quantity v_m and the BET constant c . The following equation can be used:

$$c = 1 + \frac{A}{I} \quad \text{Eqn 2.3}$$

$$v_m = \frac{1}{A + I} \quad \text{Eqn 2.4}$$

The BET method is widely used in surface science for the calculation of surface areas of solids by physical adsorption of gas molecules. A total surface area S_{total} and a specific surface area S are evaluated by the Eqn 2.5 and Eqn 2.6:

$$S_{BET} = \frac{S_{total}}{a} \quad \text{Eqn 2.5}$$

$$S_{BET, total} = \frac{(v_m N_s)}{V} \quad \text{Eqn 2.6}$$

N: Avogadro's number; s: adsorption cross section; V: molar volume of adsorbent gas; a: molar weight of adsorbed species.

Liu et al. ^[59] determined the specific surface of coal or chars with BET method during gasification to help investigate the gasification reactivity of those chars. Ismadji et al. ^[60] determined that the surface area and pore volume of activated carbon prepared from vacuum pyrolysis char were 1150 m²/g and 0.43 cm³/g, respectively, by the method of BET analyzer. By studying the pore size distribution using BET analysis, Chiang et al. ^[61] believed that the mesopore had the greatest effect on the bio-sludge pyrolysis. Yu et al. ^[62] studied pore size distribution, surface area together with particle size distribution, swelling behaviour to help understand char characteristics and particle matter formation during coal combustion process.

II-G-4: Laser diffraction mastersizer

Before discussing methods for particle sizing, it is worth understanding how particle size distributions are defined. Particles are three-dimensional objects for which three parameters (the length, breadth and height) are required in order to provide a complete description. As such, it is not possible to describe a particle using a single number that equates to the particle size. Most sizing techniques therefore assume that the material being measured is spherical, as a sphere is the only shape that can be described by a single number (its diameter). This equivalent sphere approximation is useful in that it simplifies the way particle size distributions are represented. However, it does mean that different sizing techniques can produce different results when measuring non-spherical particles.

Laser diffraction based particle size analysis relies on the fact that particles passing through a laser beam will scatter light at an angle that is directly related to their size. As particle size decreases, the observed scattering angle increases logarithmically. Scattering intensity is also dependent on particle size, diminishing with particle volume. Large particles therefore scatter light at narrow angles with high intensity whereas small particles scatter at wider angles but with low intensity.

It is this behaviour that instruments based on the technique of laser diffraction exploit in order to determine particle size. A typical system consists of a laser, to provide a source of coherent, intense light of fixed wavelength; a series of detectors to measure the light pattern produced over a wide range of angles; and some kind of sample presentation system to ensure that material under test passes through the laser beam as a homogeneous stream of particles in a known, reproducible state of dispersion. The dynamic range of the measurement is directly related to the angular range of the scattering measurement, with modern instruments making measurements from around 0.02 degrees through to beyond 140 degrees. The wavelength of light used for the measurements is also important, with smaller wavelengths (e.g. blue light sources) providing improved sensitivity to sub-micron particles ^[63].

Leuschner et al. ^[64] studied particle size distributions of Bacillus spores. Laser diffracting with a Malvern Mastersizer and scanning transmission electron microscopy (STEM) were used to record images of 50–100 individual spores. Good agreement between the average individual spore dimensions determined by electron microscopy and those obtained by laser diffracting was evident.

Laser diffraction has been questioned because of potential evaporative losses of the small particles at the edge of the plume, causing an apparent shift in the particle size distribution and thus a larger mass median diameter (MMD). Kwong et al. ^[65] compared particle size of nebulized aerosols measured directly using laser diffraction or by evaluating aerodynamic properties by cascade impaction and got good match result between each other.

On the contrary, Choi et al. ^[66] used six analyzers, such as Mastersizer Microplus (Malvern Instruments Ltd., UK), LS230 (Coulter Electronics Ltd., USA) LMS30 (Seishin, Japan), Analysette22 (Fritsch, Germany), HELOS (Sympatec, Germany) based on a laser diffraction and scattering method, and the SKC-2000S (Seishin Co., Ltd., Japan) based on the centrifugal sedimentation method to study the particle size distribution of poly component particulate systems. It was reported that they failed to find reasonably good agreement between the different analyzer.

II-G-5: Scanning electron microscope (SEM)

The scanning electron microscope (SEM) is a type of electron microscope that images the sample surface by scanning it with a high-energy beam of electrons in a raster scan pattern. The electrons interact with the atoms that make up the sample producing signals that contain

information about the sample's surface topography, composition and other properties such as electrical conductivity.

The types of signals produced by an SEM include secondary electrons, back-scattered electrons (BSE), characteristic X-rays, light cathodoluminescence, specimen current and transmitted electrons. Secondary electron detectors are common in all SEMs, but it is rare that a single machine would have detectors for all possible signals. The signals result from interactions of the electron beam with atoms at or near the surface of the sample. In the most common or standard detection mode, secondary electron imaging or SEI, the SEM can produce very high-resolution images of a sample surface, revealing details about less than 1 to 5 nm in size. Due to the very narrow electron beam, SEM micrographs have a large depth of field yielding a characteristic three-dimensional appearance useful for understanding the surface structure of a sample. This is exemplified by the micrograph of pollen shown to the right. A wide range of magnifications is possible, from about 10 times (about equivalent to that of a powerful hand-lens) to more than 500,000 times, about 250 times the magnification limit of the best light microscopes.

Back-scattered electrons (BSE) are beam electrons that are reflected from the sample by elastic scattering. BSE are often used in analytical SEM

along with the spectra made from the characteristic X-rays. Because the intensity of the BSE signal is strongly related to the atomic number (Z) of the specimen, BSE images can provide information about the distribution of different elements in the sample. For the same reason, BSE imaging can image colloidal gold immunolabels of 5 or 10 nm diameters which would otherwise be difficult or impossible to detect in secondary electron images in biological specimens. Characteristic X-rays are emitted when the electron beam removes an inner shell electron from the sample, causing a higher energy electron to fill the shell and release energy. These characteristic X-rays are used to identify the composition and measure the abundance of elements in the sample ^[67].

SEM technology has been widely used in fuels studies. A lot works are reported for a qualitative analysis of the morphology of fuels chars. For instance, Jindarom et al. ^[68] employed scanning electron microscopy (SEM) technique to observe the surface morphology of the as received sewage sludge and char, which help to support the increase in the BET surface area as a function of temperature. SEM image was performed to show no traces of soot in the char samples and incomplete meltage of the wood sample during pyrolysis. ^[69]. Alonso et al. ^[70] indicated the difference of 300°C between the low and high temperature runs seems to have been enough to

provoke a significant improvement in inertinite devolatilisation based on the morphologies of the char sample given by SEM micrographs.

SEM observation plays an indispensable role in particle size, porosity and morphology studies. SEM images are very definite, can be magnified to obtain accurate details or, vice versa, enlarged to give a global vision of a pulverized sample with minor loss in precision. It helps to differ a certain component from others, to evaluate the structural variations in particles after different thermal treatments, to observe superficial pores and qualitatively relate porosity, surface area and adsorption capacity and so on

[71-80]

References

- [1]. Khosrow Nikkhah. Hydropyrolysis of various biomass materials and coals with catalysts. A thesis for the degree of Doctor of Philosophy in University of Saskatchewan, 1992
- [2]. Fengel D. and Wenqer G., Wood: Chemistry, Ultrastructure, Reactions. Walter de Gruyter, Berlin, 1984
- [3]. Sungga Lee, James G. Speight, Sudarshan K. Handbook of alternative fuel technologies. CRC Press, 2007
- [4]. Antonio Valero, Sergio Uson. Oxy-co-gasification of coal and biomass in an integrated gasification combined cycle (IGCC) power plant. Energy, Vol. 31, pp. 1643-1655, 2006
- [5]. Alice Kristiansen, Understanding coal gasification, 1996
- [6]. Brown CR, Liu Q, Norton G. Catalytic effects observed during the co-gasification of coal and switchgrass. Biomass Bioenerg, Vol. 18, pp. 499-506, 2000
- [7]. Chmielniak T, Sciazko M. Co-gasification of biomass and coal for methanol synthesis. Appl Energ, Vol. 74, pp. 393-403, 2003
- [8]. McLendon TR, Lui AP, Pineault RL, Beer SK, Richardson SW. High-pressure co-gasification of coal and biomass in a fluidized bed. Biomass and Bioenerg, Vol. 26, pp. 377-388, 2004

- [9]. Demirbas. A mechanisms of liquefaction and pyrolysis reactions of biomass. *Energy Convers. Manage.*, Vol. 41, pp. 633–646, 2000
- [10]. Prins M. J., Ptasinski K. J., Janssen F. J. J. G. From coal to biomass gasification: comparison of thermodynamic efficiency. *Energy*, Vol. 32, pp. 1248–1259, 2007
- [11]. Salo K., Mojtahedi W. Fate of alkali and trace metals in biomass gasification. *Biomass and Bioenergy*, Vol. 15, No. 3, pp. 263–267, 1998
- [12]. Li K., Zhang R., Bi J. Experimental study on syngas production by co-gasification of coal and biomass in a fluidized bed. *Int. J. Hydrogen Energy* 2009, in press
- [13]. Pinto F., Franco C., Andre R. N., Tavares C., Dias M., Gulyurtlu I., Cabrita I. Effect of experimental conditions on co-gasification of coal, biomass and plastics wastes with air/steam mixtures in a fluidized bed system. *Fuel*, Vol. 82, pp. 1967–1976, 2003
- [14]. Zhang L., Xu S., Zhao W., Liu S. Co-pyrolysis of biomass and coal in a free fall reactor. *Fuel*, Vol. 86, pp. 353–359, 2007
- [15]. Kumabe K., Hanaoka T., Fujimoto S., Minowa T., Sakanishi, K. Co-gasification of woody biomass and coal with air and steam. *Fuel*, Vol. 86, pp. 684–689, 2007
- [16]. Sjostrom K.,; Chen G, Yu Q., Brage C., Rosen C. Promoted reactivity of char in co-gasification of biomass and coal: Synergies in the thermo-chemical process. *Fuel*, Vol. 78, pp. 1189–1194, 1999

- [17]. Collot A.G., Zhuo Y., Dugwell D. R., Kandiyoti R. Co-pyrolysis and co-gasification of coal and biomass in bench-scale fixed bed and fluidised bed reactors. *Fuel*, Vol. 78, pp. 667–679, 1999
- [18]. Feroso J., Arias B., Plaza M. G, Pevida C., Rubiera F., Pis J. J., Garcí'a-Pe~na F., Casero P. High-pressure co-gasification of coal with biomass and petroleum coke. *Fuel Process. Technol.*, Vol. 90, pp. 926–932, 2009
- [19]. Sang Jun Yoon, Young-Chan Choi, See-Hoon Lee, Jae-Goo Lee. Thermogravimetric study of coal and petroleum coke for co-gasification. *Korean J. Chem. Eng.*, Vol. 24, No. 3, pp. 512-517, 2007
- [20]. Zhua W., Song W., Lin W. Catalytic gasification of char from co-pyrolysis of coal and biomass. *Fuel Process. Technol.*, Vol. 89, pp. 890–896, 2008
- [21]. Vuthaluru H. B. Thermal behaviour of coal/biomass blends during co-pyrolysis. *Fuel Process. Technol.*, Vol. 85, pp. 141–155, 2003
- [22]. Cai J., Zhou L., Huang Q. Thermogravimetric analysis and kinetics of coal/plastic blends during co-pyrolysis in nitrogen atmosphere. *Fuel Process. Technol.*, Vol. 89, pp. 21–27, 2008
- [23]. Palmer S. R., Hippo E. L., Tandan D. Co-conversion of coal/waste plastic mixtures under various pyrolysis and liquefaction conditions. *Prepr. Symp.-Am. Chem. Soc., Div. Fuel Chem.*, Vol. 40, pp. 29–33, 1995

- [24]. Filomena Pinto, Carlos Franco, Rui Neto Andre, C. Tavares, M.Dias, I.Gulyurtlu, I. Cabrita. Effect of experimental conditions on co-gasification of coal, biomass and plastics wastes with air/steam mixtures in a fluidized bed system. *Fuel*, Vol. 82, pp. 1967-1976, 2003
- [25]. Gil J, Aznar MP, Caballero MA, Frances E, Corella J. Biomass gasification in fluidized bed at pilot scale with steam-oxygen mixtures. *Energy Fuels.*, Vol. 11, No. 6, pp. 1109-1118, 1997
- [26]. Herguido J, Corella J, Gonzalez-saiz. Steam gasification of lignocellulosic residues in a fluidized bed at a small pilot scale. *Ind Eng Chem Res.*, Vol. 31, No. 5, pp. 1274-1282, 1992
- [27]. Kim YJ, Lee SH, Kim SD. coal gasification characteristics in a downer reactor. *Fuel*, Vol. 80, No. 13, pp. 1915-1922, 2001
- [28]. Zhuo Y, Messenbock R, Collot A-G, Megaritis A, Paterson N, Dugwell DR, Kandiyoti R. Conversion of coal particles in pyrolysis and gasification: comparison of conversions in a pilot-scale gasifier and bench-scale test equipment. *Fuel*, Vol. 79, No. 7, pp. 793-802, 2000
- [29]. Ocampo A, Arenas E, Chejne F, Aguirre J, Perez JD. An experimental study on gasification of Colombian coal in fluidised bed. *Fuel*, Vol. 82, No. 2, pp. 161-164, 2003
- [30]. Aznar MP, Corella J, Gil J, Martin JA, Caballero MA, Olivares A, Perez P, Frances E. Developments in thermochemical biomass conversion. Vol.2. Blackie Academic and Profesional, pp. 1194-1208, 1997

- [31]. Food and agriculture organization of the united nation (FAO). Improved solid biomass burning cookstoves: A development manual, Bangkok, September 1993
- [32]. Asri Gani. Fundamentals on Co-combustion and co-gasification of Low-grade coal with biomass. International Conference on Fluid and Thermal Energy Conversion, 2003
- [33]. Haga T., Nogi K., Amaya M. and Nishiyama Y. Composite catalysts for carbon gasification. Applied catalysis. A. General, Vol. 67, No. 2, pp. 189-202, 1991
- [34]. Mckee D. W., Spiro C. L., Kosky P. G. and Lamby E. Eutectic salt catalysts for graphite and coal char gasification. Fuel, Vol. 64, pp. 805, 1985
- [35]. Woon Jae Lee, Sang Done Kim. Catalytic activity of alkali and transition metal salt mixtures for steam-char gasification. Fuel, Vol. 74, No. 9, pp. 1387-1393, 1995
- [36] Madsen M, Christensen E. Combined gasification of coal and straw. In: APAS Clean Coal Technology Programme, Vol. 3, pp. 1992–1994
- [37] Sjostrom K, Bjornbom E, Chen G, Brage C, Rosen C, Yu Q. Synergetic effects in co-gasification of coal and biomass. In: APAS Clean Coal Technology Programme, Vol. 3, pp. 1992–1994. p. C3
- [38] Reinoso C, Cuevas A, Janssen K, Morris M, Lassing K, Nilsson T, Grimm HP, Puigjaner L, Ying Gang P, Velo E, Zaplana M, McMullan JT,

Williams BC, Sloan EP, McIlveen-Wright D. Fluidized bed combustion and gasification of low-grade coals and biomass in different mixtures in pilot plants aiming to high efficiency and low emission processes. In: APAS Clean Coal Technology Programme, Vol. 3, pp. 1992–1994. p. C5

[39] De Jong W, Andries J, Hein KRG. Coal-biomass gasification in a pressurized fluidized bed gasifier. In: ASME International GT and Aerospace Congress, Stockholm, SE, June 2–5, pp. 1–7, 1998

[40] Pan YG, Velo E, Roca X, Manya JJ, Puigjaner L. Fluidized bed co-gasification of residual biomass/poor coal blends for fuel gas production. Fuel, Vol. 79, pp. 1317 –1326, 2000

[41]. Smith A.R., Klosek J., Woodward W. Next generation integration concepts for air separation units and gas turbines. ASME Journal of Gas Turbines and Power, Vol. 119, pp. 298-304, 1997

[42]. Kwon S.H., Shin J.W., Oh J.K., Heaven D.L., Condorelli P. Hydrogen production alternatives in an IGCC Plant. Hydrocarbon Processing, pp. 73-76, 1999

[43]. Chan Lee, Seung Jong Lee. Evaluation on the performance and the NO_x emission of IGCC power plant integrated with air separations unit. International Energy Journal, Vol. 8, pp. 37-44, 2007

[44]. S.Kajitani, S.Hara, H.Matsuda. Gasification rate analysis of coal char with a pressurized drop tube furnace. Fuel, Vol. 81, pp. 539-546, 2002

- [45]. Yan Zhang, Shiro Kajitani, Masami Ashizawa, Yuso Oki. Tar destruction and coke formation during rapid pyrolysis and gasification of biomass in a drop-tube furnace. *Fuel*, Vol. 89, pp. 302–309, 2010
- [46]. Jiye Luan, Rui Sun, Shaohua Wu, Junfeng Lu, Na Yao. Experimental studies on reburning of biomasses for reducing NO_x in a drop tube furnace. *Energy & Fuels*, Vol. 23, pp. 1412–1421, 2009
- [47]. Biswas S., Choudhury N., Sarkar P., Mukherjee A., Sahu S.G. Studies on the combustion behaviour of blends of Indian coals by TGA and Drop Tube Furnace. *Fuel Processing Technology*, Vol. 87, pp. 191 – 199, 2006
- [48]. Kouichi Miuraa, Hiroyuki Nakagawaa, Shin-ichi Nakaia, Shiro Kajitani. Analysis of gasification reaction of coke formed using a miniature tubing-bomb reactor and a pressurized drop tube furnace at high pressure and high temperature. *Chemical Engineering Science*, Vol. 59, pp. 5261 – 5268, 2004
- [49]. Koichi Matsuoka, Zhi-xin Ma, Hiroyuki Akiho, Zhan-guo Zhang, Akira Tomita. High-pressure coal pyrolysis in a drop tube furnace. *Energy & Fuels*, Vol. 17, pp. 984-990, 2003
- [50]. Han Chang Cho, Kil Won Cho, Yong Kuk Lee, Hyun Dong Shin, Dal Hong Ahn. Effect of coal type on gasification in pressurized drop tube furnace. *Int. J. Energy Res.*, Vol. 25, pp. 427-438, 2001

- [51]. Cloke M, Lester E, Belghazi A. Characterisation of the properties of size fractions from ten world coals and their chars produced in a drop-tube furnace. *Fuel*, Vol. 81, No. 5, pp. 699-708, 2002
- [52]. Robert C. Brown^a, Qin Li^a, Glenn Norton^b. Catalytic effects observed during the co-gasification of coal and switchgrass. *Biomass and Bioenergy*, Vol. 18, pp. 499-506, 2000
- [53]. Vuthaluru H.B. Thermal behaviour of coal/biomass blends during co-pyrolysis. *Fuel Processing Technology*, Vol. 85, pp. 141– 155, 2003
- [54]. Shiguang Li, Shaoping Xu, Shuqin Liu, Chen Yang, Qinghua Lu. Fast pyrolysis of biomass in free-fall reactor for hydrogen-rich gas. *Fuel Processing Technology*, Vol. 85, pp. 1201– 1211, 2004
- [55]. Anup Kumar Sadhukhan^a, Parthapratim Gupta, Tripurari Goyal, Ranajit Kumar Saha. Modelling of pyrolysis of coal–biomass blends using thermogravimetric analysis. *Bioresource Technology*, Vol. 99, pp. 8022– 8026, 2008
- [56]. Prabhat Naredi, Sarma V. Pisupati. Interpretation of Char Reactivity Profiles Obtained Using a Thermogravimetric Analyzer. *Energy and Fuels*, Vol. 22, pp. 317–320, 2008
- [57]. Shou-Yu Zhang, Jun-Fu Lu, Jian-Sheng Zhang, Guang-Xi Yue. Effect of pyrolysis intensity on the reactivity of coal char. *Energy and Fuels*, Vol. 22, pp. 3213–3221, 2008

- [58]. Holmberg, Krister. Handbook of applied surface and colloid chemistry. 2002
- [59]. Tie feng Liu, Yi tian Fang, Yang Wang. An experimental investigation into the gasification reactivity of chars prepared at high temperatures. Fuel, 2007
- [60]. Ismadji S., Sudaryanto Y. Activated carbon from char obtained from vacuum pyrolysis of teak sawdust: pore structure development and characterization. Bioresource Technology, Vol. 96, pp. 1364-1369, 2005
- [61]. Huang lung Chiang, Ching guan Chao, C.Y.Chang, C.F.Wang, P.C.Chiang. Residue characteristics and pore development of petrochemical industry sludge pyrolysis. Wat. Res., Vol. 18, pp. 4331-4338, 2001
- [62]. Yun Yu, Minghou Xu, Hong Yao, Dunxi Yu, Yu Qiao, Jiancai Sui, Xiaowei Liu, Qian Gao. Char characteristics and particulate matter formation during Chinese bituminous coal combustion. Proceedings of the Combustion Institute, Vol. 31, pp. 1947-1954, 2007
- [63]. Malvern laser diffraction Mastersizer 2000 optical system manual.
- [64]. Renata G.K. Leuschner, Antony C. Weaver, Peter J. Lillford. Rapid particle size distribution analysis of Bacillus spore suspensions. Colloids and Surfaces B: Biointerfaces, Vol. 13, pp. 47-57, 1999
- [65]. Jenny Kwong W.T., Sharon L. HO, Allan L. Coates. Comparison of nebulized particle size distribution with malvern laser diffraction analyzer

- versus Andersen Cascade impactor and low-flow Marple Personal Cascade Impactor. *Journal of aerosol medicine*, Vol. 13, No. 4, pp. 303-314, 2000
- [66]. Heekyu Choi, Woong Lee, Dong-Uk Kim, Shalendra Kumar, Jonghak Ha, Seongsoo Kim, Jungeun Lee. A comparative study of particle size analysis in fine powder: The effect of a poly component particulate system. *Korean J. Chem. Eng.*, Vol. 26, No. 1, pp. 300-305, 2009
- [67]. Buschow K.H, Rober W. *Encyclopedia of materials-science and technology*, 2001
- [68]. Charothon Jindarom, Vissanu Meeyoo, Boonyarach Kitiyanan, Thirasak Rirksomboon, Pramoch Rangsunvigit. Surface characterization and dye adsorptive capacities of char obtained from pyrolysis /gasification of sewage sludge. *Chemical Engineering Journal*, Vol. 133, pp. 239–246, 2007
- [69]. Michelangelo Dall’Ora, Peter Arendt Jensen, Anker Degn Jensen. Suspension Combustion of Wood: Influence of pyrolysis conditions on char yield, morphology, and reactivity. *Energy & Fuels*
- [70]. Alonso M.J.G., Borrego A.G., Alvarez D., Parra J.B. Influence of pyrolysis temperature on char optical texture and reactivity. *Journal of Analytical and Applied Pyrolysis*, Vol. 58-59, pp. 887-909, 2001
- [71]. Shenqi Xu, Zhijie Zhou, Xuxia Gao, Guangsu Yu, Xin Gong. The gasification reactivity of unburned carbon present in gasification slag from

entrained-flow gasifier. *Fuel Processing Technology*, Vol. 90, pp. 1062–1070, 2009

[72]. Biagini E., Narducci P., Tognotti L. Size and structural characterization of lignin-cellulosic fuels after the rapid devolatilization. *Fuel*, Vol. 87, pp. 177–186, 2008

[73]. Chan ML, Jones JM, Pourkashanian M, Williams A. The oxidative reactivity of coal chars in relation to their structure. *Fuel*, Vol. 78, pp. 1539–1552, 1999

[74]. Liu H, Luo C, Toyota M, Kato S, Uemiya S, Kojima T, et al. Mineral reaction and morphology change during gasification of coal in CO₂ at elevated temperatures. *Fuel*, Vol. 82, pp. 523–530, 2002

[75]. Yu J, Lucas J, Strezov V, Wall T. Swelling and char structures from density fractions of pulverized coal. *Energy Fuel*, Vol. 17, pp. 1160–1174, 2003

[76] Gergova K, Eser S. Effects of activation method on the pore structure of activated carbons from apricot stones. *Carbon*, Vol. 34, pp. 879–888, 1996

[77]. Guo J, Lua A.C. Characterization of chars pyrolyzed from oil palm stones for the preparation of activated carbons. *J Anal Appl Pyrol*, Vol. 46, pp. 113–125, 1998

- [78]. Della Rocca PA, Cerrella EG, Bonelli PR, Cukierman AL. Pyrolysis of hardwoods residues: on kinetics and chars characterization. *Biomass Bioenerg*, Vol. 16, pp. 79–88, 1999
- [79]. Sharma RK, Wooten JB, Baliga VL, Lin X, Chan WG, Hajaligol M.R. Characterization of chars from pyrolysis of lignin. *Fuel*, Vol. 83, pp. 1469–1482, 2004
- [80] Shim H.S., Hajaligol M.R., Baliga V.L. Oxidation behaviour of biomass chars: pectin and *Populus deltoides*. *Fuel*, Vol. 83, pp.1495–1503, 2004

CHAPTER III

EXPERIMENTAL PROCEDURES

The objective of the this present work is to investigate the kinetic properties and morphology of char particles prepared from the co-pyrolysis of coal/biomass/fluid coke at different temperatures and investigate the interaction of these different fuels to elucidate any advantages that may arise from the binary co-gasification.

The experimental procedure involved char samples preparation using a Drop Tube Furnace (DTF) under nitrogen atmosphere and rapid heating conditions. Reactivity of the produced chars was assessed using thermogravimetric analyses (TGA) and CO₂ was supplied as the oxidizing agent. The morphological properties of the char particles were studied using scanning electron (SEM). Particle size distribution was determined using a laser diffraction Mastersizer. Also, surface area and pore structure was studied by Brunauer-Emmett-Teller (BET) analyses.

III – A: Experimental apparatus

A drop tube furnace (DTF), shown in Figure 3.1, was used for the feedstock co-pyrolysis tests, which allows to simulate an entrained flow reactor in conditions similar to those encountered in practical plants.

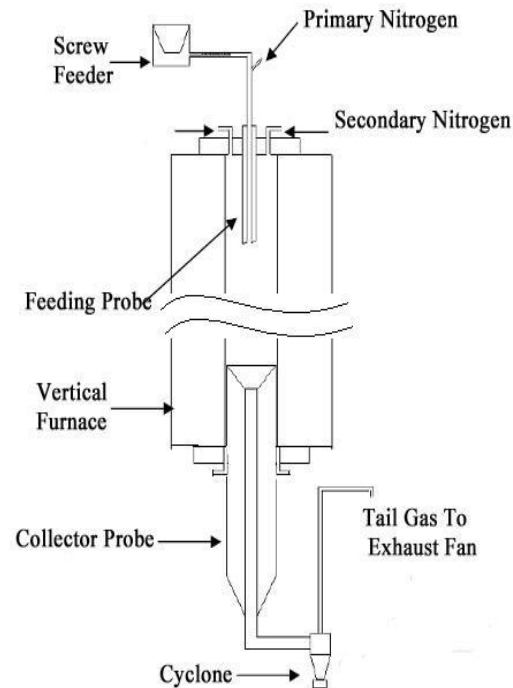


Figure 3.1 Schematic of DTF

The furnace contains an electrically heated vertical core of Mullite tube (inner diameter of 60 mm) of 140 cm long, with an effective heated zone of 120 cm. DTFs have been widely used because of their similarity to the entrained reactor in practical plants.

DTF is made up of three parts: feeding section, reaction furnace tube and collecting part. Let introduce this plant from top to bottom. A screw

feeder attached to a hopper with pulsating walls, which prevents bridging of fine particles, was used to feed particles into the DTF. The nominal capacity of feeder ranged from 8 to 60 g/hr for coal. The water-cooled feeding probe was used to prevent ignition of particles inside the feeder which is crucial in estimating the particle residence time. The feeder probe was shielded from the heat using high-temperature insulation material. When the depth that the feeding probe was inserted into the furnace was adjusted, the residence time could be changed. The pyrolysis products were collected through a water-cooled collection probe, shown in Figure 3.2. To prevent condensation of pyrolysis products on the inner shell of the collector probe, the probe was equipped with a sintered stainless steel inner shell through which gas (nitrogen) was passed. There were two gas inlets on the collector probe: the quench gas inlet, which quenched the combustion products in the top section of the collector and prevented the reactions from progressing further, and the wall gas inlet, which prevented condensation and deposition of particles in the lower section of the probe. The cooled gas and products were then sent to the cyclone.

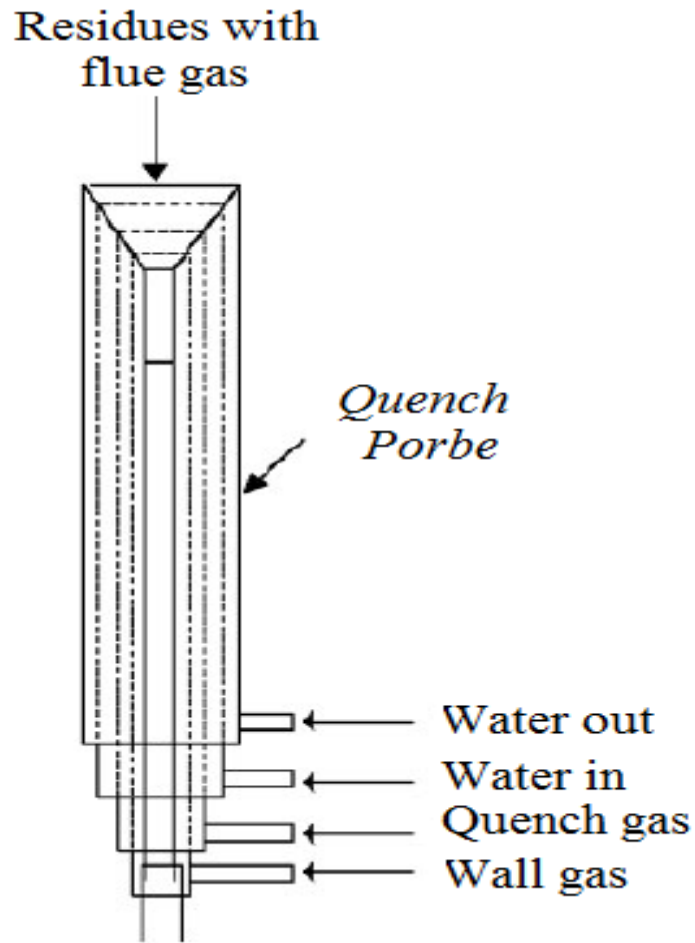


Figure 3.2 Schematic of collector probe

Three proportional-integral-derivative (PID) temperature controllers adjust the temperature of the reactor at constant in three different zones. A K-type thermocouple was used to roughly calibrate the gas temperatures inside the tube while no flow gas was injected into the furnace, as shown in Figure 3.3. The maximum attainable gas temperature in this furnace is 1650 °C.

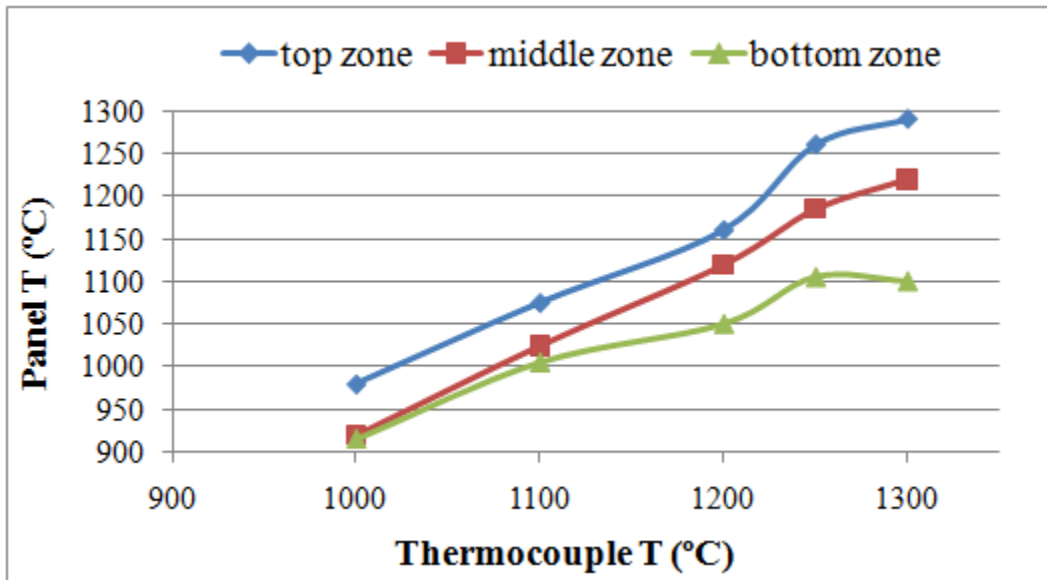


Figure 3.3 Temperature calibration for DTF

III – B: Fuels characterization

Biomass, coal and fluid coke are carriers of accumulated solar energy and have been important solid fuels. However, the different histories of formation of these three fuels make for differences in their natures and availability. Coal and fluid coke have a higher energy content compared to biomass. Biomass, though it carries lower energy content, is more environmentally friendly when utilized for energy production. Besides, the higher thermochemical reactivity of biomass facilitates the conversion and upgrading of the fuel.

Three different raw materials, Genesee coal, fluid coke (Syncrude coke), and woody biomass from a carpentry shop, were used in this study. The fuels were crushed and ground using a Ball mill and a pulveriser, sieved

and classified to obtain a particle size cut of 53-75 μm for both Genesee coal and fluid coke, while a particle size range of 250-300 μm was selected for woody biomass. These particle sizes were chosen because they are the ones normally used for these fuels in practical situations. The samples were oven-dried at 105°C for 2 hours to eliminate the effect of moisture, which could lead to the agglomeration of particles and also to maintain smooth flow rates. The samples were then fed to the DTF. Table 3.1 presents the ultimate and proximate analyses of the fuels used in this study. All these tests on the composition of fuels are based on ASTM standards. (ASTM standard D 3172 Standard Practice for Proximate Analysis of Coal and Coke; E 870 – 82 Standard Test Methods for Analysis of Wood Fuels).

sample	Proximate analysis (%)(w/w,as received)				Ultimate analysis (%)(w/w,daf)			
	fixed carbon	volatile matter	ash	moisture	C	H	N	S
Genesee								
Coal	40.15	23.44	30.62	5.79	76.09	4.51	1.09	0.42
Fluid coke	85.81	6.60	6.22	1.37	86.72	1.76	2.09	6.70
Sawdust	12.38	84.17	0.43	3.02	49.15	6.54	0.27	0.51

III – C: Char preparation

Calibration of feeding speed on different fuels and their mixtures was done first, under some conditions with that for char preparation to ensure all char was collected at the same feeding rate.

Sawdust was blended with coal or coke at different ratios by weight, as shown in Table 3.2. The blending was performed before feeding into the reactor. The pyrolysis of the samples was conducted at four different temperatures: 700°C, 1100°C, 1250°C and 1400 °C.

Table 3.2 Blending fuels ratio and their abbreviation			
Sample	component by weight percent		
	Genesee coal	Sawdust	Fluid coke
GC	100	0	0
FC	0	0	100
S	0	100	0
GCS 2-1	67	33	0
GCS 1-1	50	50	0
GCS 1-2	33	67	0
FCS 2-1	0	33	67
FCS 1-1	0	50	50
FCS 1-2	0	67	33

For every experimental run, the reactor tube was heated to a set pyrolysis temperature. Once the temperature reached the desired point, air was purged from the DTF by passing N₂ for thirty minutes at a flow rate of 10 L/min to make sure the system was air-free. After that, the prepared sample was fed into the reactor. The fast pyrolysis took place when the sample particles passed through the heated zone of the furnace and the char particles were collected in the cyclone. The N₂ flow rate, feeding rate and residence time were fixed for all of the experiments.

III – D: Measurement of Char Gasification Reactivity

The gasification reactivity of the co-pyrolyzed char was measured at isothermal conditions using TGA. The reactivity is defined in terms of the reaction rate constant of K.

Before the tests, the samples were dried at 105°C to remove moisture. In TGA experiments, nitrogen was used as the sweeping gas during the period of heating to the desired temperature (in this case, 800°C) with a heating rate of 10 °C/min. The mass of the sample was approximately 12 mg. When the set temperature is reached, the isothermal gasification reaction of the co-pyrolyzed char sample was initiated by switching on a flow of carbon dioxide. The experiment was stopped when no more mass loss was detected and the rate constant was determined from the weight loss curves.

CHAPTER IV

RESULTS AND DISCUSSION

IV – A: Effect of blending on the char surface area

The BET surface area and pore volume of char were obtained from N₂ adsorption isothermally at 77 K using an Omnisorp 360 analyzer. The specific surface area was calculated by the BET equation. Prior to the analysis, the samples were degassed at 350°C for 4 hours.

Information on the effect of blending was obtained from the determination of the surface area using BET analysis on both pure and blended (GCS 1-1 and FCS 1-1) chars, as shown in Figure 4.1.

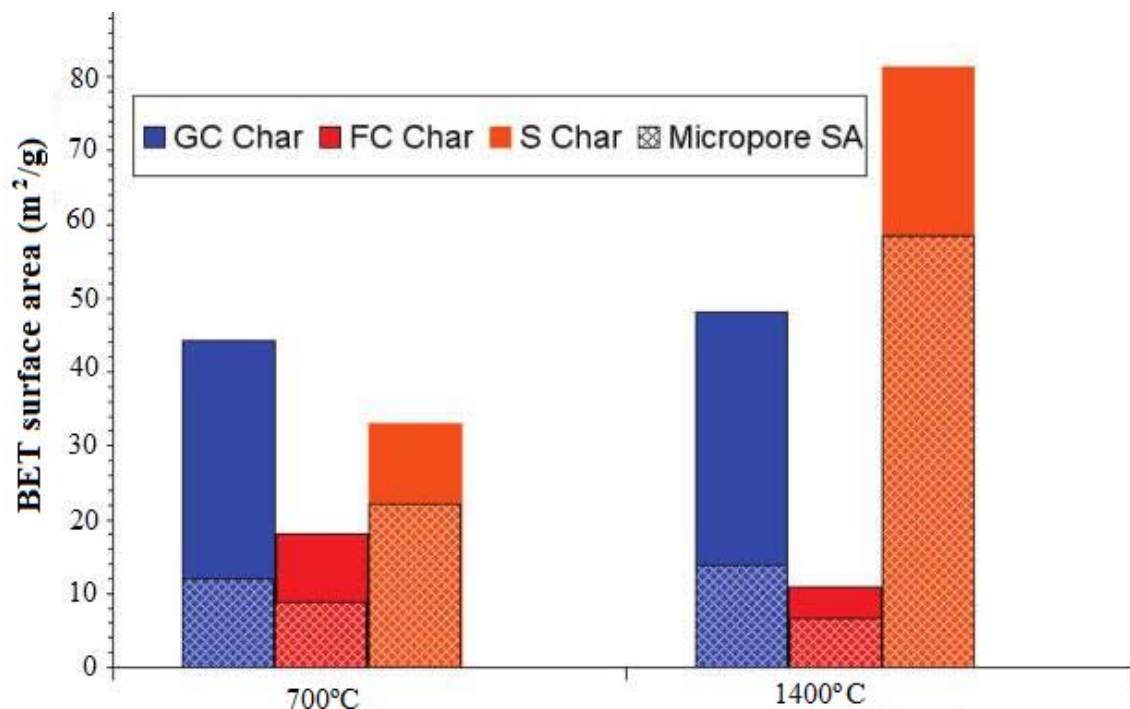


Figure 4.1 Temperature effect on the surface area (SA) for three pure chars, namely, Genesee coal, fluid coke, and sawdust chars.

Results showed that the porosity of the chars increase with an increase in the pyrolysis temperature because of the removal of volatile matters. Given the fact that the residence time in the DTF is fixed and the temperature of 700°C is not high enough to achieve complete devolatilization of fuel, the BET surface area of Genesee coal char slightly increased with increasing the pyrolysis temperature from $44.2 \text{ m}^2 \text{ g}^{-1}$ (at 700 °C) to $48.2 \text{ m}^2 \text{ g}^{-1}$ (at 1400 °C), while that of sawdust char went up from $33.0 \text{ m}^2 \text{ g}^{-1}$ (at 700 °C) to $81.3 \text{ m}^2 \text{ g}^{-1}$ (at 1400 °C). However, results from fluid coke char exhibited an opposite trend, whereby the surface area decreased with the temperature, as shown in Table 4.1.

Table 4.1 Pore structure and BET surface area of Genesee coal/Fluid coke/Biomass pure and blended chars at ratio of 1:1			
Sample	BET SA (m ² /g)	Micropore V (cm ³ /g)	Mesopore V (cm ³ /g)
S,700	33.0	0.00675	0.01112
S,1400	81.3	0.01461	0.01973
GC,700	44.2	0.00452	0.00537
GC,1400	48.2	0.00519	0.00666
FC,700	18.0	0.00575	0.00398
FC,1400	10.8	0.00311	0.00560
GCS 1-1,700	12.8	0	0.00581
GCS 1-1,1400	64.0	0.02282	0.01746
FCS 1-1,700	6.6	0	0.00401
FCS 1-1,1400	12.5	0.00382	0.00838

The pore volume and BET surface area of the three pure chars prepared at 700 and 1400 °C are compared in Table 4.1.

In Table 4.1, there are two points can be summarized. Firstly, char prepared at a higher temperature always has bigger Surface area except for FC char, which gives an opposite trend towards temperature increase. Higher pyrolysis temperature means higher heating rate which will promote devolatilization process to convert more solid phase content into liquid and gas phase. Another possible reason needs to take in account is pore type change. Generally, pores in char

particles are divided into three classes: micropores, mesopores, and macropores. The boundary between micro- and mesopores is 2 nm, while the boundary of meso- and macropores is 50 nm by convention. Results indicate that, the lower the pyrolytic temperature, the larger the macropore contribution to the pore structure. Moisture and other highly volatile molecules were vaporized to generate the macropore during the initial stage of the pyrolytic process. As the pyrolytic temperature increases, the cell wall cracks to generate both meso- and micropore.

Secondly, surface area for GCS/FCS 1-1 prepared at 700°C is smaller than that of pure GC/FC char prepared under same condition. However, at 1400°C, it shows an opposite result, that is blended GCS/FCS char has larger SA compared to their corresponding pure char. This might due to the thermal cracking of volatiles in gas and liquid phases at 1400°C. Sawdust contains more volatiles, so when it is blended with coal/pet-coke, the blended fuel will release more volatiles compared with pure coal/pet-coke. At high temperature, such as 1400 °C, those liquefied and gasified volatiles will process thermal cracking, during which larger molecule will be broken down to smaller one. In the downstream in DTF, those larger molecules will condense to the particle surface whilst smaller volatiles particle will still stay in gas phase. Thermal cracking reaction can not happen at 700 °C. More volatiles in the blended fuel will cause more small broken molecules to escape and fewer molecules to condense. Those condensed molecules might

block pores and form a smoother layer on char particle surface, which will result in a decrease in surface area.

IV – B: Char Reactivity

The reaction of char with oxygen or carbon dioxide has generally been described as being governed by the following controlling stages: (i) mass transfer (by diffusion) of oxygen to reaction sites; (ii) chemisorptions of oxygen on the carbon surface, reaction of chemisorbed oxygen or carbon dioxide with carbon to form products, and desorption of products; and (iii) mass transport of the gaseous products from the reaction sites. Theoretically, in the absence of external diffusion limitations, the reaction rate, R , of the porous solid can be written in the general form

$$-dw/dt = R = K_i C_g \quad \text{Eqn 4.1}$$

where, $K_i = k_i(T) A_g \eta w C_s$.

This rate form can be rewritten as

$$-dx/dt = k(1-x) \quad \text{or} \quad -\ln(1-x) = kt \quad \text{Eqn 4.2}$$

where $k = k_i(T) A_g \eta C_s C_g$.

$x = 1 - w/w_0$ is the solid conversion

w is the weight (daf) of the sample at any time

k expresses the dependence of the reaction rate on the concentrations of the gaseous species C_g

k_i is the kinetic constants

T is the particle temperature

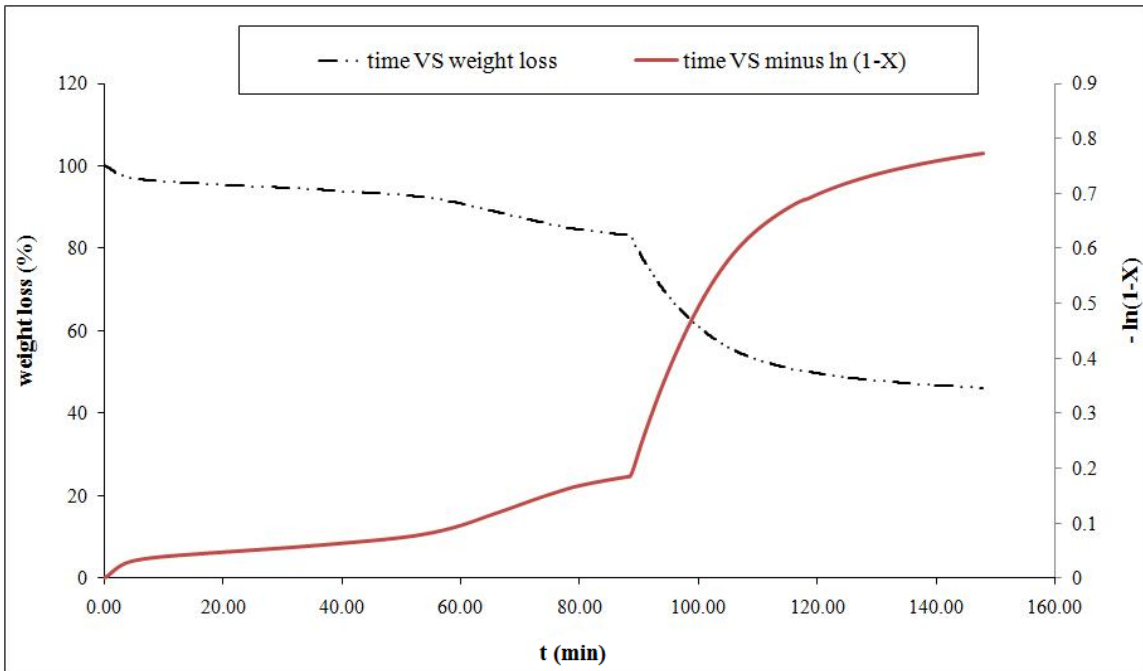
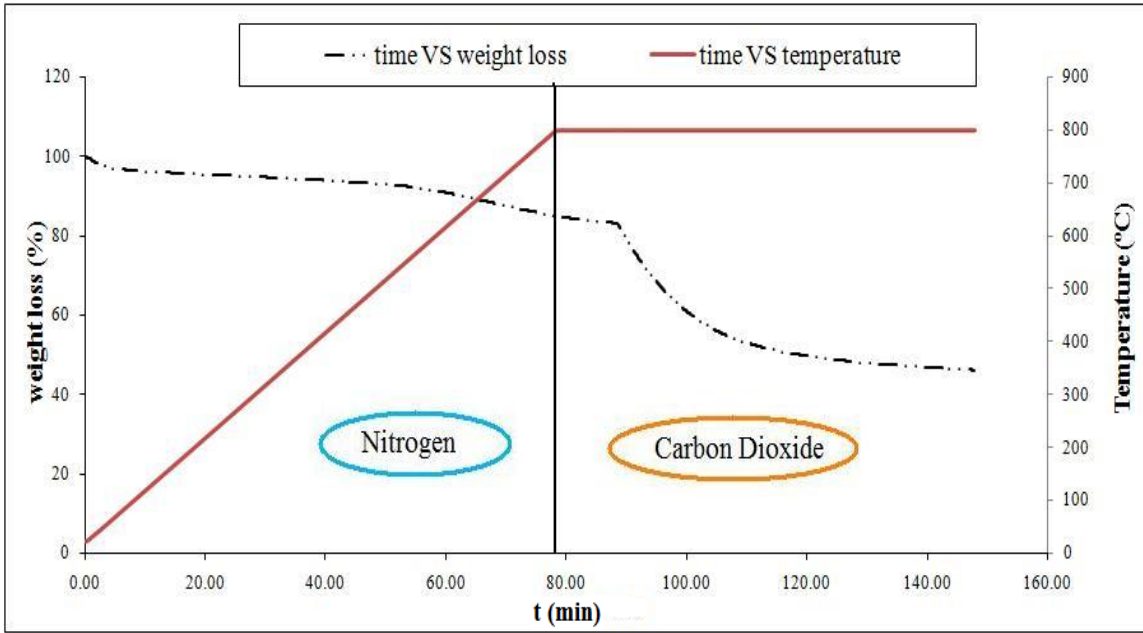
A_g is the surface area

η is fractional availability of the surface area

C_s is the concentration of accessible active sites

Thus, in a kinetic controlled zone, the rate of the reaction should only depend upon the concentration of accessible active sites C_s .

As mentioned above, one of the objectives of this work is to examine if co-pyrolysis and/or co-gasification of different fuels have any effect on the reaction kinetics of the fuels. In this work, reactivity of different co-pyrolyzed samples was compared on the basis of their reaction rate constants, k . The reaction rate constant quantifies the speed of a chemical reaction, and thus, it is a good indicator when it comes to the comparison of reactivity. Here is an example about how to calculate reaction rate constant k based on TGA result as shown in Figure 4.2. As mentioned, in TGA experiments, isothermal gasification reaction of the co-pyrolyzed char sample was initiated by switching on a flow of carbon dioxide at 1200 or 800°C. Sample weight, time and temperature were recorded continuously during the experiment as the first plot shown in Figure 4.2. Based on Eqn 2, reaction rate constant k can be calculated as the slope in the relationship plot between $-\ln(1-x)$ and time.



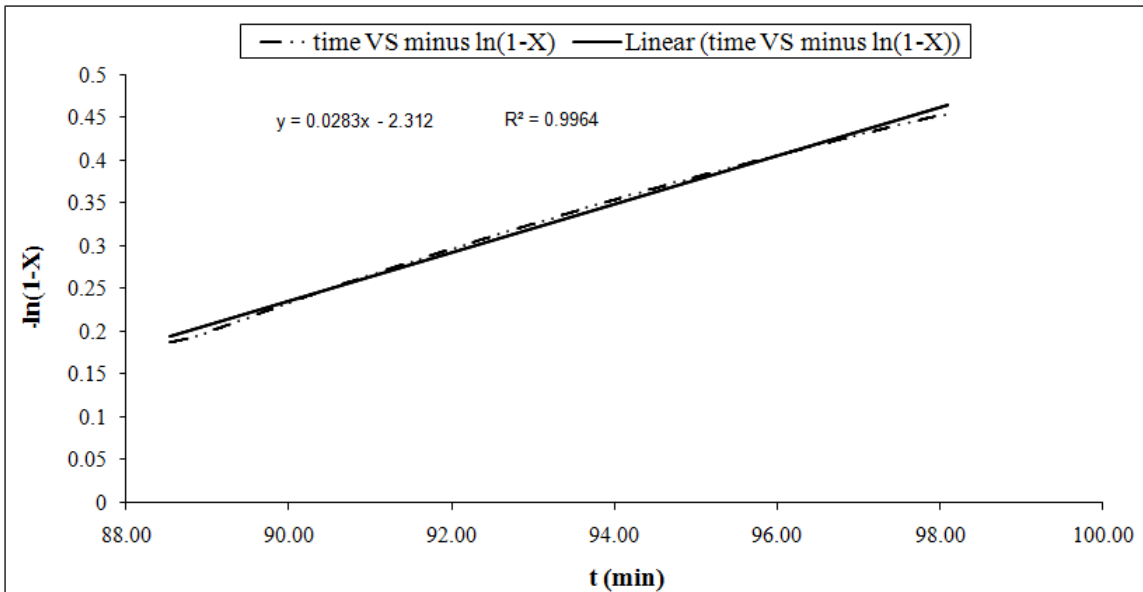


Figure 4.2 Scheme of how to calculate k based on TGA result

IV-B-1 Char reactivity rate with CO₂ at 1180°C

All these chars from DTF were gasified with carbon dioxide isothermally at 1180°C in a thermogravimetric analyzer. TG results for the group of GCS chars, prepared at 700°C, 1100 °C, 1250 °C, 1400 °C, respectively, are as shown in Figure 4.3.

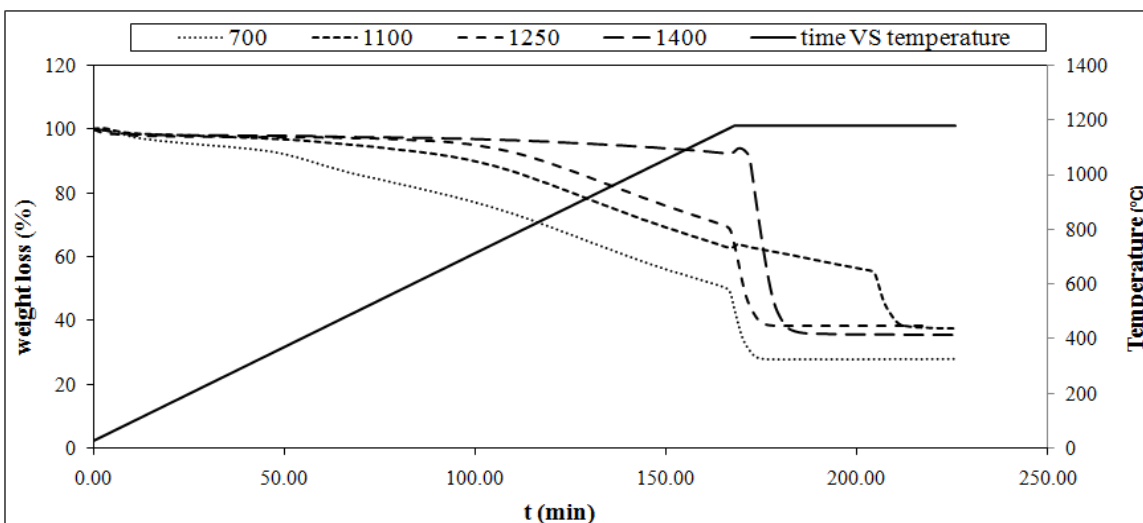


Figure 4.3 TG results for GCS 1-1 chars, gasified isothermally at 1180°C with carbon dioxide.

From the figure above, it is above to find the temperature effects at which chars were prepared in DTF, on the gasification reactivity. The higher the prepared temperature is, the less reactive the chars are. This can be explained by the fact that the higher co-pyrolysis temperature leads to more volatiles being driven out of the particles, hence, rendering the remaining char less reactive. The increase in heat treatment temperature in DTF results in a substantial reactivity reduction, associated with major changes of the turbostatic carbon structure, and thus with a variation in the amount and/or accessibility of active sites ^[1-2]. Massive loss of active sites with increasing temperature has been reported for explaining this phenomenon ^[3-4]. In this work, it might indicate the abundant remainder of the relatively active compositions at the lower temperature (at 700°C) because of incomplete pyrolysis of fuels.

And due to the setting gasification reaction temperature was much higher than two chars conducted temperature, chars produced at 700 °C and 1100 °C had a greatly mass loss before reaction happened in TGA equipment. For instance, for GCS 1-1 char produced at 700°C, the remaining weight percent was also 52.37% when the temperature reached the setting point. Based on this fact, another group of TGA tests have been done, and the setting temperature was lowered to 800 °C. Such temperature can not only ensure the gasification reaction happens not too slow, but also let the char reserve most of its weight before reaction starts.

IV-B-2 Char reactivity rate with carbon dioxide at 800°C

All these chars from DTF were gasified with carbon dioxide isothermally at 800°C in a thermogravimetric analyzer. These experiments conducted at a lower temperature to assure the assumption of negligible diffusion resistance.

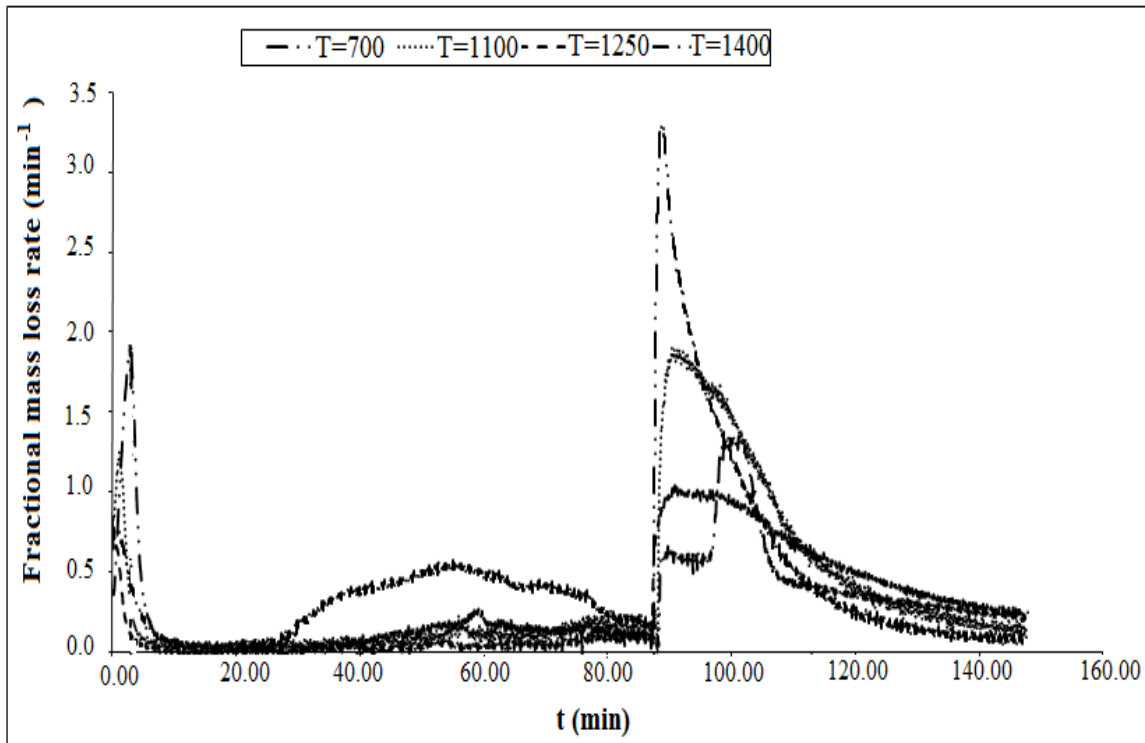


Figure 4.4 DTG curves for rate of gasification vs. Time for GCS 1-1 blended chars, formed at 700,1100,1250,1400°C, respectively.

All these chars from DTF were gasified with carbon dioxide isothermally at 800°C in a thermogravimetric analyzer. The DTG curves for Genesee coal, sawdust 50:50 blends produced at four different temperatures in DTF are presented in Figure 4.4. It is evident that for all four samples the degradation started at the very beginning then the rate decreased to zero due to the release of

initial moisture remaining in the samples. And after the loss of moisture, under nitrogen environment, all four samples had different extent of degradation, which can be explained by the escape of the remaining volatile matters in the sample. For the blended sample produced at 700 °C the rate of degradation was the largest with the rate increasing sharply as soon as the carbon dioxide gas was injected into the TGA apparatus. As the co-pyrolysis temperature increased, the gasification peak in the Figure 4.4 became much lower and indicated less reactive of the char samples. Moreover, for the blended char prepared at 1400 °C, the gasification peak was shown as two parts which suggest that more complicated reactions took place.

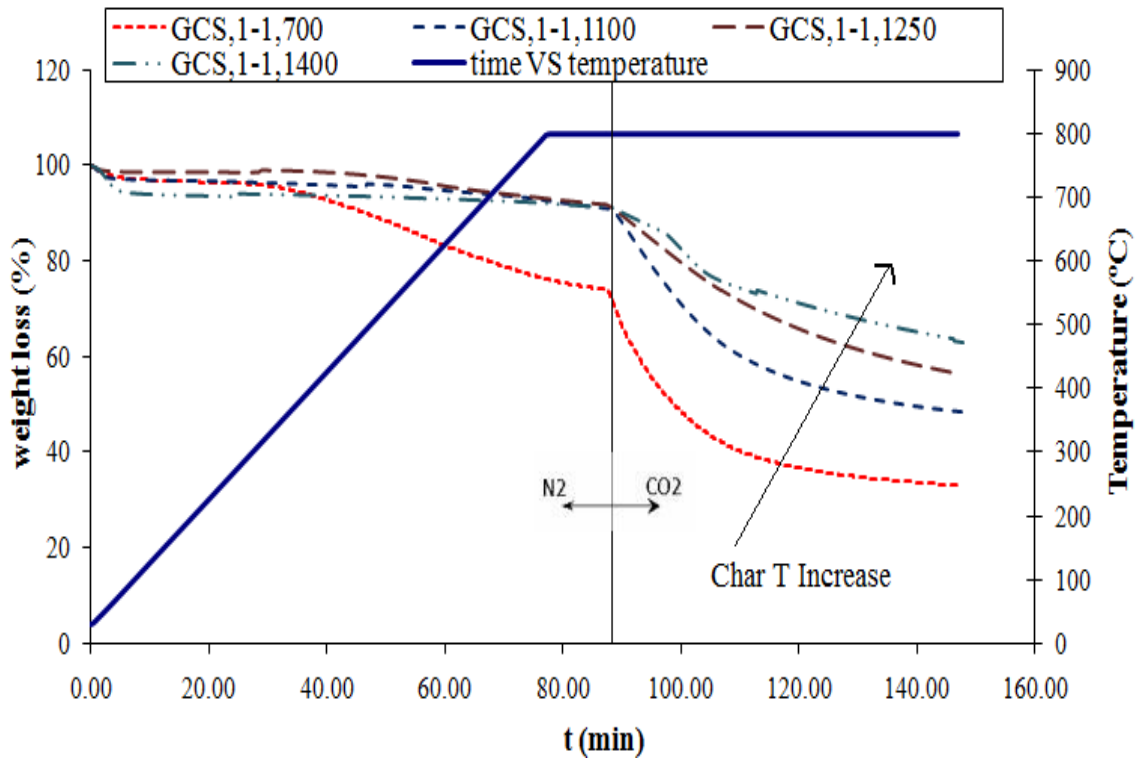


Figure 4.5 TGA results for Genesee coal and sawdust (GCS 1-1) blended char pyrolyzed at 700, 1100, 1250 and 1400°C

Figure 4.5 shows the weight loss curves for the pyrolyzed Genesee coal and sawdust 1:1 blend chars produced at all four temperatures, namely, 700, 1100, 1250, and 1400°C. The curves distinctively show the difference between these chars, with the char produced at 700°C being the most reactive, while that produced at 1400°C being the least reactive. For the char produced at 700°C, it can be seen that the weight loss starts much earlier at a temperature of about 450 °C and this is before the CO₂ reaction even starts, something which is not supposed to happen. This could be due to the fact that 700°C is the lowest temperature used in char preparation and, because the height of the drop tube is fixed, the residence in the furnace may not have been long enough to drive all of the volatiles out of the particle. Upon reheating during gasification with CO₂, the remaining volatiles will start to be released at the shown lower temperatures, hence, leading to the observed particle weight loss.

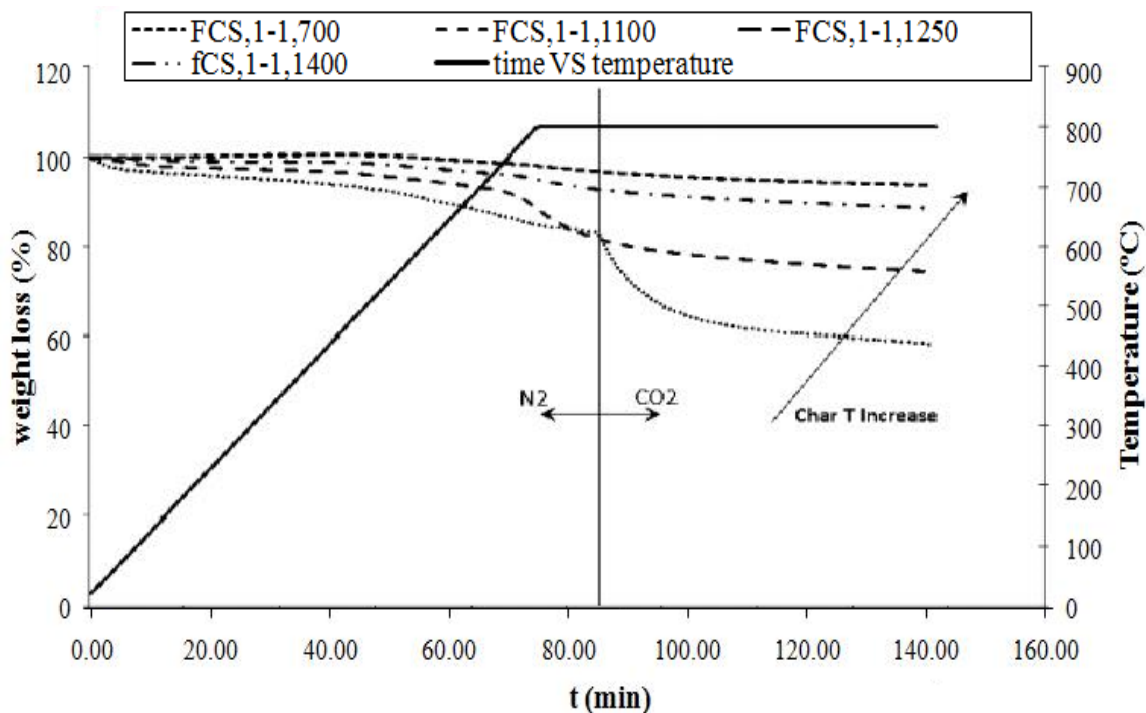


Figure 4.6 TGA results for fluid coke and sawdust (FCS 1-1) blended char pyrolyzed at 700, 1100, 1250, and 1400°C

The trend observed for the Genesee coal-sawdust blend was also observed in the 1:1 fluid coke/sawdust blend, as shown in Figure 4.6 above. Again, the char produced at 700°C had the most weight loss, indicating its high reactivity, while the char produced at 1400°C had the lowest weight loss, thus being the least reactive. The early weight loss for the 700°C char was again observed here and an almost similar trend was observed for the char produced at 1100°C, although the onset of the weight loss was at a much higher temperature. The same explanation as the one given for the coal-sawdust blend above is valid in this case as well. A simple comparison between these two figures shows that the coal-sawdust blend is more reactive than the fluid coke-sawdust blend.

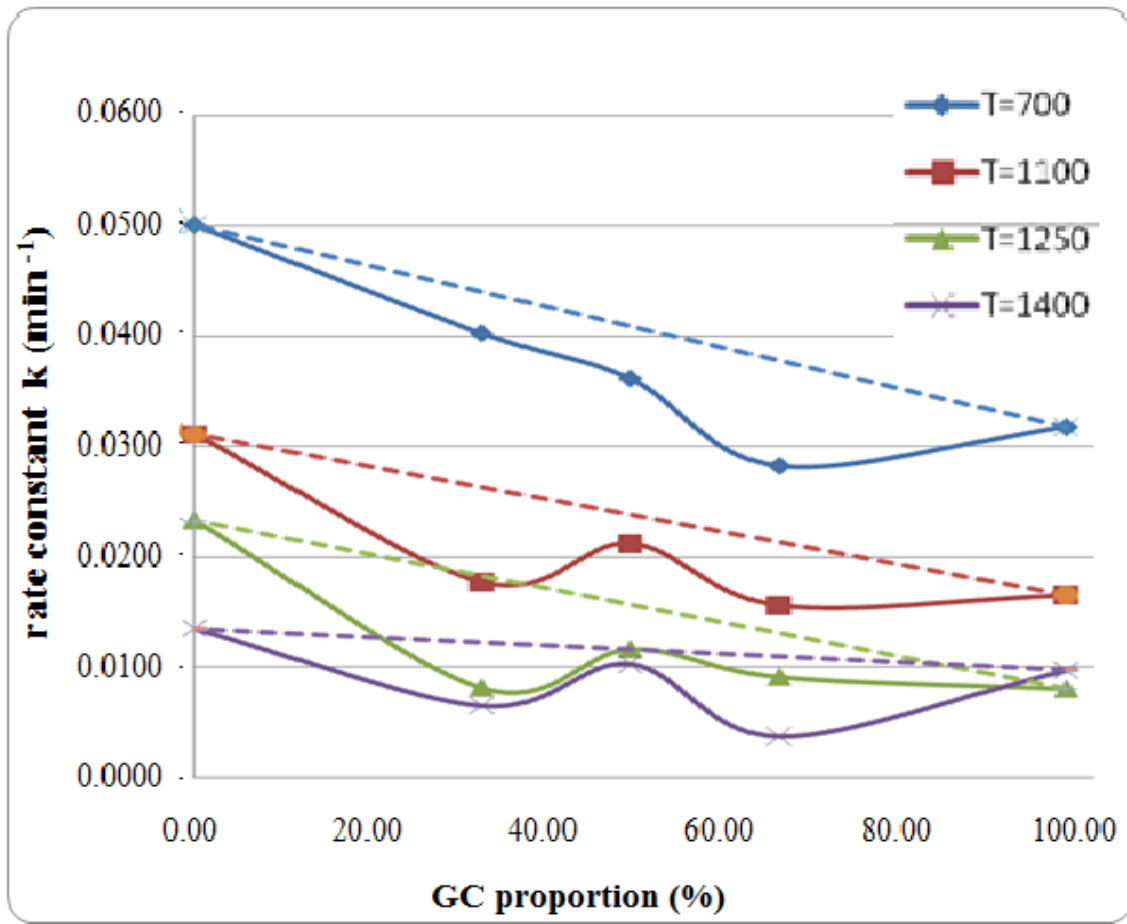


Figure 4.7 Effect of the blending ratio and pyrolysis temperature on reactivity of Genesee coal and sawdust blended char (the units of k are min^{-1}).

Figure 4.7 gives a comparison of the reactivity in terms of the reaction rate constant k . X-axis is the Genesee coal weight proportion in the blended fuel. Four solid lines give the actual rate constant calculated from TGA analyses for char prepared at different pyrolysis temperature. Consistent to what has been reported above, for a given blend ratio, the reactivity of lower temperature produced char is higher than the reactivity of those prepared at higher temperatures. Moreover, assuming that there is no catalytic interaction by the sawdust on the coal char,

reactivity of chars prepared from the mixture of Genesee Coal and Sawdust should display a simply weighted average of the individual rates for the blending chars, in another word, be additive on the rate constant k based on the weight proportion (see dashed line in Figure 4.7). From Figure 4.7, there is no hesitation to say that all solid lines (experimental lines) do not coincide with dashed lines. To be more specific, the char prepared from the mixture shows consistently lowered gasification reactivity compared to the averaged reactivity, which means by blending sawdust with coal/pet-coke, there is an interaction between different fuel particles and gives an overall negative effect on the blended char gasification reactivity.

Figure 4.7 further presents the effect of the blending ratio on the reactivity of the chars. Sawdust char is more reactive than coal char. So the blended char has higher reactivity compared with pure coal char. There are at least two possible interaction factors happened during pyrolysis process, and one plays a positive role on reactivity and the other plays an opposite role. Firstly, as stated in Chapter II, there might exist the synergetic effect during co-pyrolysis process due to the Alkali salt in sawdust working as a catalyst on coal/pet-coke char, which will have a positive effect on gasification rate constant k of the blended char.

However, on the other hand, decreased surface area (active sites) of blended char will decrease gasification reactivity of char. Agglomeration phenomenon among char particles is expected to decrease the surface area and active sites. This phenomenon can be seen directly in the SEM images, as shown in Figure 4.10 and Figure 4.11 in the next section. Furthermore, volatile molecule in the gas phase, which released from feedstock particle at earlier stage in DTF may condense on the surface area of char particles when it passes through water-cooled collector probe, forming a surface layer modifying the char particle surface by blocking small pores on the surface of coal char to reduce the surface area as well as availability of active sites on char particles. This surface modification hypothesis is consistent with the one in BET analyses section to explain surface area change with blending ratio. At 700°C pyrolysis temperature, surface area of sawdust char, GC char and GCS 1-1 char are 33.0, 44.2 and 12.8 m²/g, respectively. Blended char has the smallest surface area compared with pure chars under same pyrolysis condition. The decrease on surface area might due to the condensed volatile matter blocking pores on coal char particles.

There are some other interesting findings based on Figure 4.7. Considering the much higher volatile matter contents in sawdust, it is easy to conclude that the majority of the blending char would be composed by coal/fluid coke char. Consequently, the reactivity of the chars from co-pyrolysis at the lower blending ratio (around 33.3 wt %) should be close to that of coal char alone. And the

reactivity of the chars from co-pyrolysis under the higher blending ratio conditions (around 66.7 wt %) should be averagely higher than that of coal char alone. However, it is quite interesting that, in my study, only for low pyrolysis temperature, to be specific, reactivity of chars produced at 700 °C are in line with the above. And those chars prepared at 1100, 1250, 1400 °C, except for coal or fluid coke blending with sawdust at half and half, seem like the sawdust blending ratio has little influence on the reactivity of the blending chars.

From the Figure 4.7 it can be seen that, for the case of the char pyrolyzed at 700°C, the reactivity of the chars is higher when the biomass (sawdust) proportion increases. As the proportion of sawdust decreases (increasing coal proportion), the reactivity is also seen to decrease. Apart from the char prepared at 700°C, it is difficult to conclude the same for the chars prepared at the remaining three temperatures, i.e., 1100, 1250, and 1400°C, where the variation of the rate constant k does not give any particular pattern. It is tempting to conclude that by increasing the proportion of raw sawdust in the feeding materials, reactivity of blended char will be increase when the materials are pyrolyzed at a lower temperature but the same conclusion does not hold when chars are prepared above 1100°C. The increased reactivity at a higher biomass blending ratio could be due to the interaction between two fuels. These findings are in agreement with the work of Zhang et al. ^[5], who pyrolyzed biomass and coal at temperatures between 500 and 700°C but found that the synergetic effect was more pronounced on the char

produced at 600°C than the one produced at 700°C. Another work with similar findings is that of Zhua et al. ^[6], who produced char at 850°C, with lower reactivity than the one produced at 750°C.

One possible explanation for this is the melting of the potassium silicate normally found in biomass and is a big contributor to the enhancement of the reactivity in co-gasification processes, as reported by Fryda et al. ^[7] and Velez et al. ^[8]. Fryda et al. ^[7], when investigating the fluidized bed gasification of biomass, pointed out that the high potassium content of some biomass causes the formation of melt responsible for total defluidization. The main defluidization mechanism is the total melting of the silicate ash forming a highly viscous liquid. Melts consist mainly of alkali silicates and, to a lesser extent, other oxides or alkali salts. In this case, bed particle grains were either adhered to the sticky melt or joined together by a molten layer on their surfaces. This is characteristic for silica systems and is described as viscous flow sintering. According to the sintering and coating mechanisms described, collisions with the reacting fuel particles may dominate the transfer of K-rich compounds to the bed particle surfaces. No obvious chemical interaction between the bed material and the fuel ash in the gasifier was observed with the SEM/energy-dispersive spectrometry (EDS) analyses.

A similar mechanism can be used to explain results from DTF, in which the interaction between the two fuel particles occurs during pyrolysis. Once the

melting of the silicates occur (MP for potassium silicate is 740°C), the transfer of K-rich compounds from biomass to coal or fluid coke is hindered, hence leading to less reactive chars. This can explain why the effect of the blending ratio on reactivity (k) is not so significant when the chars produced at higher temperatures (>700°C) are gasified with CO₂ in the TGA.

The effect of the blending ratio on char reactivity for the fluid coke-sawdust blend, as shown in Figure 4.8, was almost the same as the one depicted in Figure 4.7, and the same reasons can explain the results.

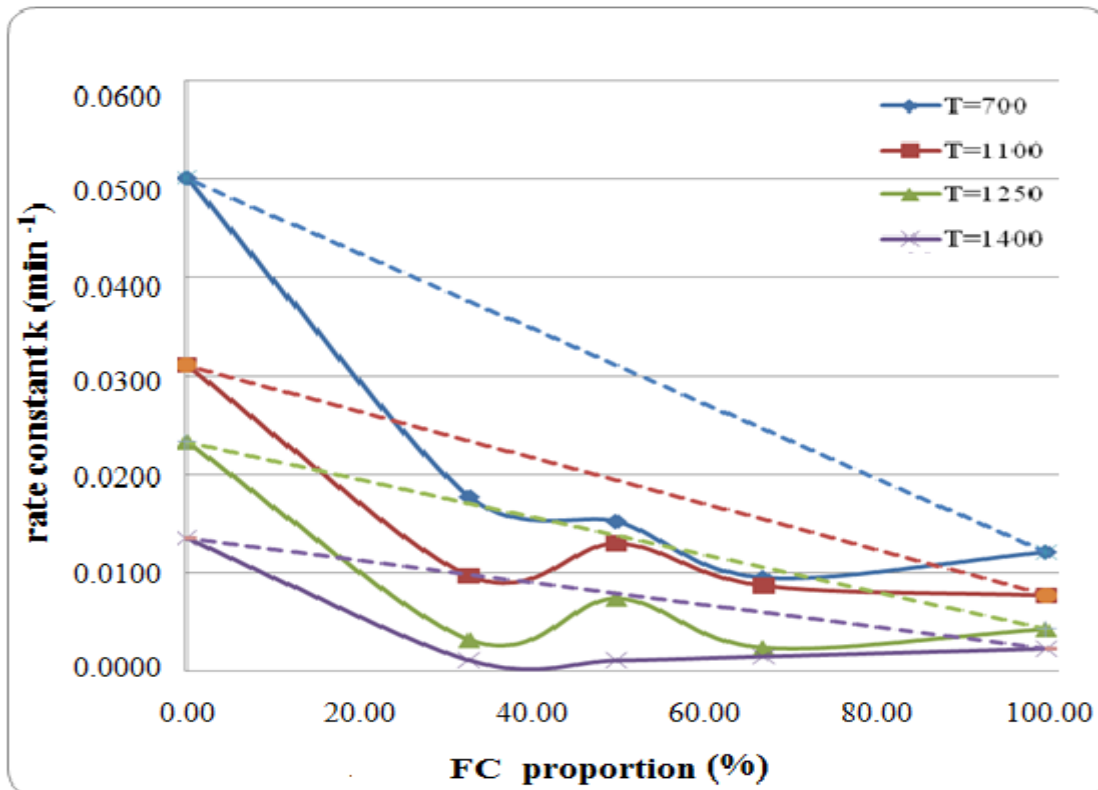


Figure 4.8 Effect of the blending ratio and pyrolysis temperature on reactivity of fluid coke and sawdust blended char (the units of k are min⁻¹).

Furthermore, as expected, biomass char particles showed the highest reactivity, followed by Genesee coal, and fluid coke char particles had the least reactivity. For instance, the rate constant k for char produced at 1400°C in DTF for sawdust, Genesee coal and fluid coke, and then gasified in carbon dioxide atmosphere isothermally at 800° C in TGA, are 0.0135, 0.0097, 0.0023 s⁻¹, respectively.

As stated in the proximate analysis, volatile matter (VM) percentage as received in feedstock is 23.44%, 6.60%, 84.7% for GC, FC and S respectively. So, for biomass, volatiles represent a significant portion of the carbonaceous fuel. It is obvious that sawdust should contribute much less proportion in blended char produced from DTF than its proportion in the raw blended feedstock. If it is assumed that devolatilization in DTF is complete and all volatile matter based on proximate analysis result is released. Then the proportion of GCS or FCS blended char that came from GC or FC can be calculated. For instance, VM in GC and S is 23.44% and 84.7% and moisture in GC and S is 5.79% and 3.02%. So for GCS 2-1 char, the proportion of GC char should be equal to:

$$\begin{aligned} \text{Assumed GC char \%} = & 100\% * (2/3) * (1 - 23.44\% - 5.79\%) / ((2/3) * (1 - 23.44\% - 5.79\%) \\ & + (1/3) * (1 - 84.17\% - 3.02\%)) \end{aligned}$$

Using same method, GC or FC char percentage in the blended char under this assumption can be calculated, shown as table 4.2.

Table 4.2 Assumed GC or FC proportion in blended char				
Fuel	VM%	GC&FC% in raw	assumed GC char %	assumed FC char %
GC	23.44%	100.00	100.00	100.00
FC	6.60%	66.67	91.70	93.51
S	84.17%	50.00	84.67	87.80
		33.33	73.42	78.25
		0.00	0.00	0.00

In this case, by replacing X axis in Figure 4.7 and Figure 4.8 with corresponding assumed GC or FC char %, these two figures will become Figure 4.9 and Figure 4.10 as below.

Compared Figure 4.9, 4.10 with Figure 4.7, 4.8, it is not hard to find that most of the point has been squeezed down to the right bottom corner by a different expression of feedstock proportion.

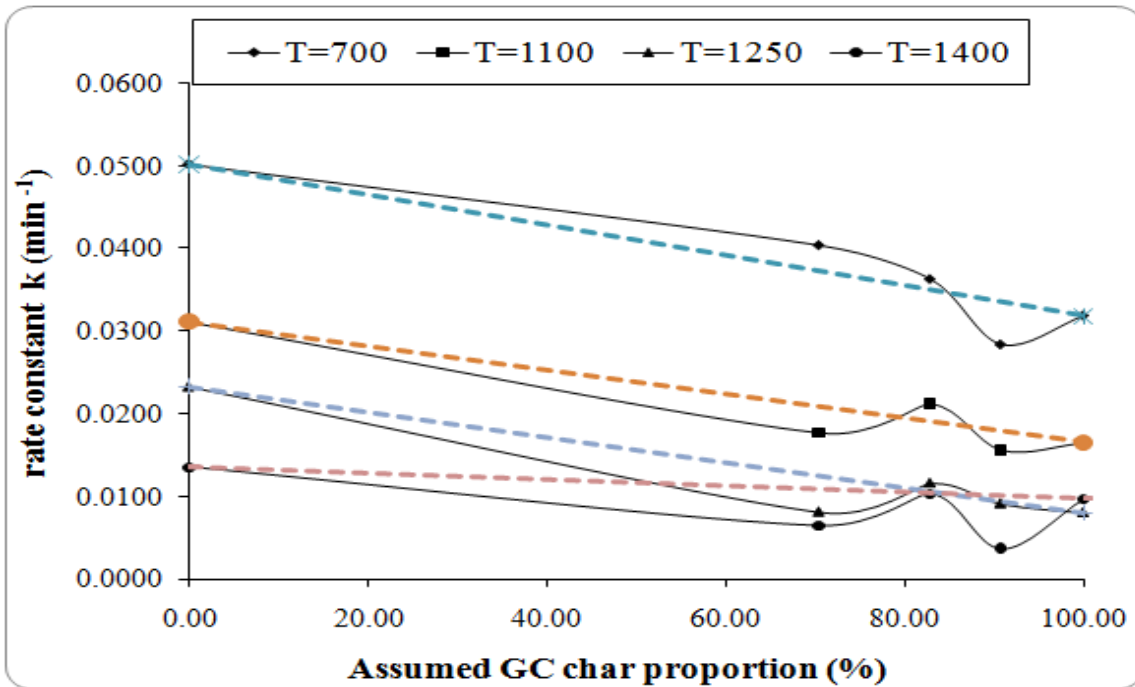


Figure 4.9 Effect of the assumed blending ratio and pyrolysis temperature on reactivity of coal and sawdust blended char (the units of k are min^{-1}).

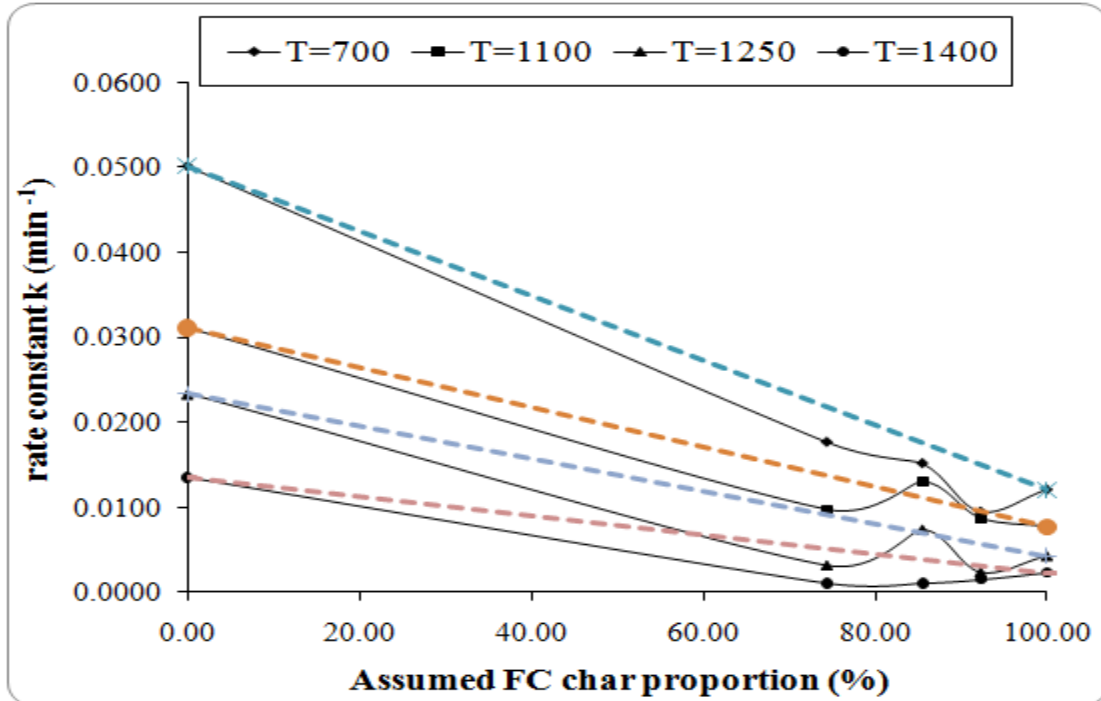


Figure 4.10 Effect of the assumed blending ratio and pyrolysis temperature on reactivity of coke and sawdust blended char (the units of k are min^{-1}).

But it should be noticed that, residence time in DTF is less than 2.5 second and heating rate is around 10-15k K/s ^[9]. And devolatilization or pyrolysis depends on a large amount of factors, the more important factors are: composition and structure of the original carbonaceous; heating rate imposed upon the carbonaceous particles; temperature, pressure, and composition of the atmosphere involving the particles. Proximate analysis was conducted in Muffle Furnace which has a constant temperature during reaction. VM content using to convert GC proportion to Assumed GC char proportion is based on proximate analysis. However, VM percentage will be changed on different heating rate. So the assumed GC or FC Char proportion is not a accurate number. It can only be used to get a rough idea on source of blended char.

IV – C: Morphological Analysis of Pyrolysis Char

The surface morphology of the char samples was examined using SEM. Figure 4.11 shows SEM images for biomass-coal blends pyrolyzed at the four temperatures mentioned before (i.e., 750, 1100, 1250, and 1400°C). The first image a, which is a co-pyrolyzed char produced at 700°C shows needle-like particles. The needle-like particles are mostly biomass particles that are composed of lodgepole and jack pines, both belonging to the softwood group. The next image b, which is for char produced at 1100°C, still exhibits needle-shaped particles, but they are much shorter as compared to those in image a. As the co-

pyrolysis temperature is increased to 1400°C, particles are seen to have become more porous and spherical. This is in agreement with the findings by Cetin et al. [11], who had reported that softwoods show a shape transition from needle-like to spherical with increasing temperature.

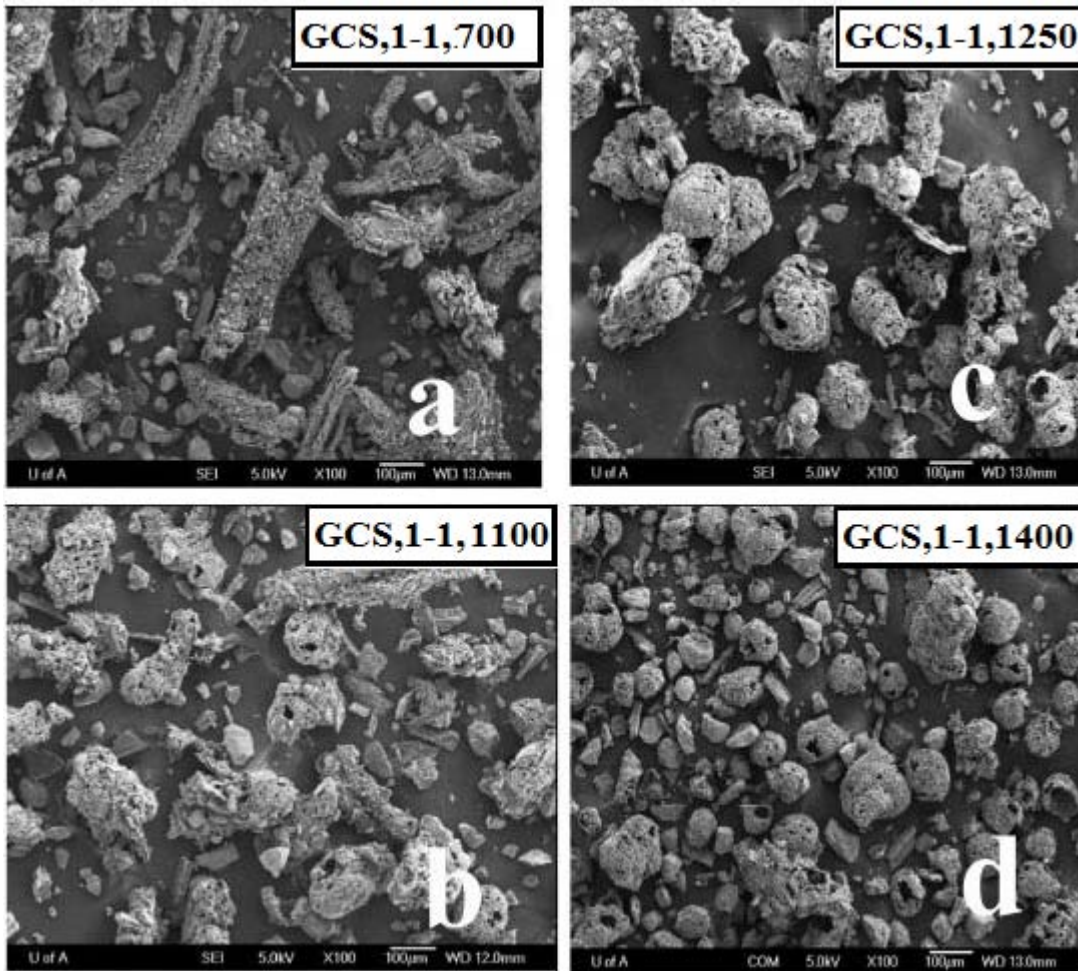


Figure 4.11 SEMs of chars at 100× magnification, showing effect of pyrolysis temperature on morphology of Genesee coal and sawdust at 1:1 blending ratio. Pyrolysis temperatures are (a) 700°C, (b) 1100°C, (c) 1250°C, and (d) 1400°C.

Further investigation revealed that, as the pyrolysis temperature was increased beyond 1250°C, agglomeration seemed to start occurring. Close

observation showed coal particles either covered by the sawdust pieces or attached to the sawdust and becoming a part of the sawdust surface. The reason for the agglomeration could be the same as the one given in the preceding section, where the melting of silicates was pointed out to be the cause of this. The molten layer on the surface enables coal particles to attach themselves to sawdust particles, leading to the observed agglomeration.

The seemingly higher porosity of the particles at higher temperature (as compared to lower temperature) could be due to the enhanced release of volatile matter during the pyrolysis process and also coalescence of smaller pores to form bigger pores, not only as shown in the figure above, which is more obvious in Fig 4.12. When reaction happened at higher temperature, sawdust particles was with bigger openings compared with char prepared at lower temperature, which should be the gas release path during pyrolysis reaction. And the smaller holes are connected with each other to form a chamber-the biggest holes for gas to escape. Those hollow woody char particles become more and more evident as char reaction temperature climbing. FC-S blends is accordant in this point with GC-S, that is the higher the temperature is, the bigger the holes are in sawdust particles.

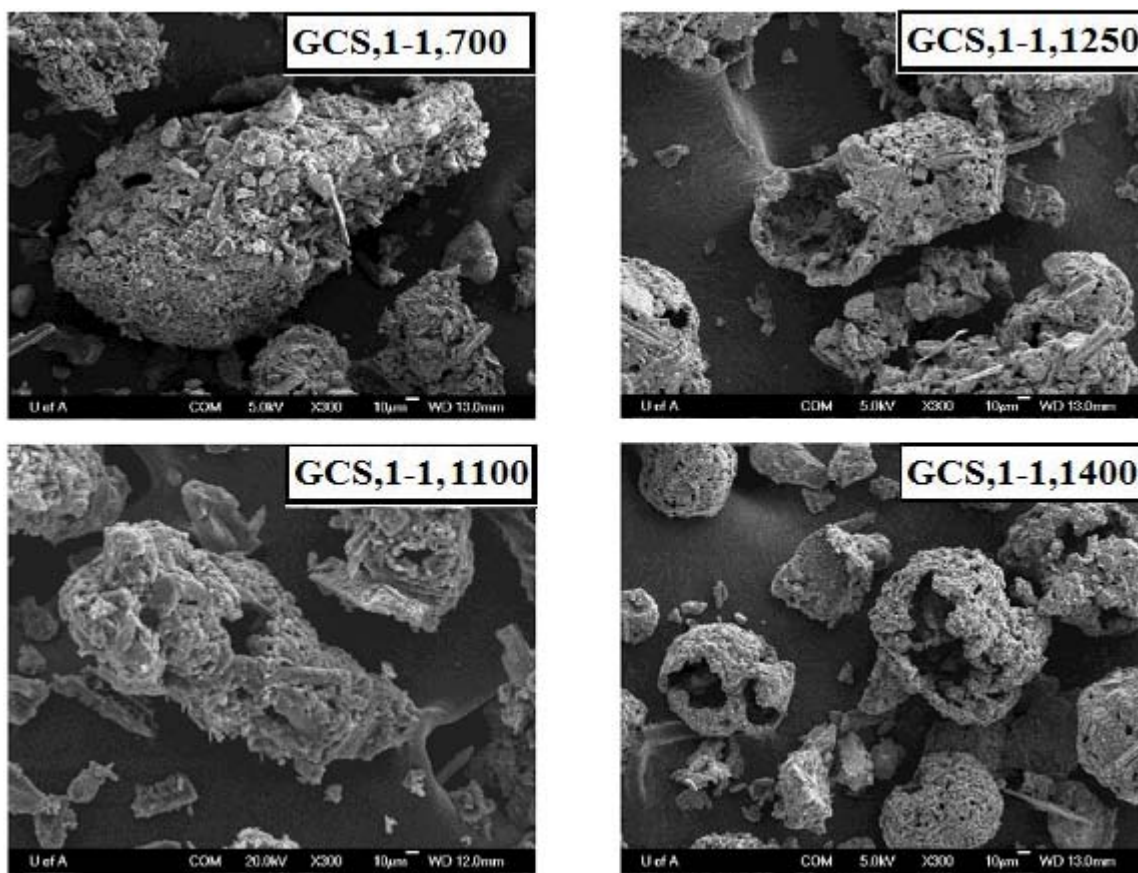


Figure 4.12 SEMs of chars at 300× magnification, showing effect of pyrolysis temperature on porosity of char particles. Pyrolysis temperatures are (a) 700°C, (b) 1100°C, (c) 1250°C, and (d) 1400°C.

Figure 4.13 shows an example of agglomerated particles, where coal particles are seen to have attached themselves onto biomass particles. Similar shape changes were observed for the fluid coke-biomass blend. The morphological analysis of fluid coke revealed a significant growth of pores in coke chars at high temperatures when compared to the chars at low temperatures, as depicted in Figure 4.14. The char prepared at 1400°C appears to be more spongy than the one prepared at 700°C. Generally, results from the morphological study of pyrolysis

chars complement the findings from TGA on why the effect of fuel blending is less pronounced when the pyrolysis temperature is increased.

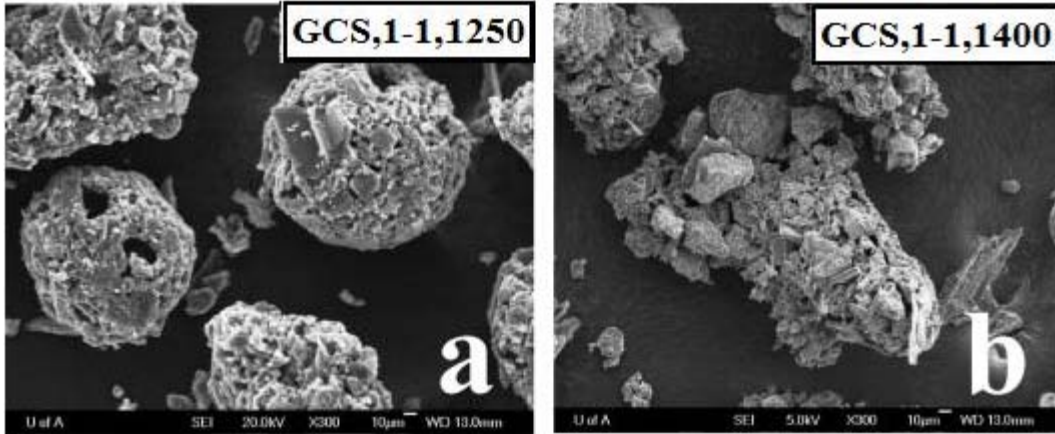


Figure 4.13 Agglomeration between coal and biomass particles at higher temperature. Image (a) is char produced at 1250°C, and image b is char produced at 1400 °C. Magnification was 300×.

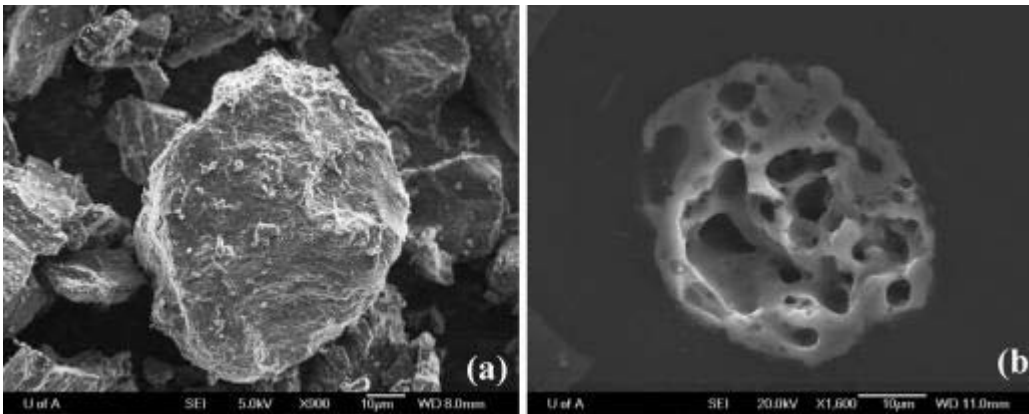


Figure 4.14 Pores development in fluid coke chars at (a) 700°C and (b) 1400°C.

IV – D: Particle size distribution.

To investigate further the effect of the co-pyrolysis temperature on particle sizes, the particle size distribution of the collected char from DTF was analyzed

using a laser diffraction Mastersizer 2000 instrument. For this particular analysis, 1:1 blends of both coal and fluid coke were used.

Figure 4.15 shows the variation of the particle size with the char pyrolysis temperature. In this particular case, the particle size variation is explained using $d(0.1)$, which means 10% of the particles were smaller than this size, and $d(0.9)$, at which 90% of the particles were smaller.

For the coal biomass blend, the effect of pyrolysis is shown in the top panel of Figure 4.15, starting with a blend that was not pyrolyzed at all, shown at 25°C. It can clearly be seen that $d(0.9)$ particle sizes initially decrease with an increase in the pyrolysis temperature up to 1250°C. Thereafter, an increase in the particle size is observed when the temperature increases to 1400°C. For the case of $d(0.1)$, it looks like there are a lot of fine particles at 25°C. As the temperature increases, the proportion of fines decrease as the $d(0.1)$ is seen to increase. A similar trend is observed for the fluid coke-biomass blend, as shown in the bottom panel of Figure 4.15. The initial decrease in the $d(0.9)$ particle size can be caused by shrinking of the particles because of devolatilization, as explained previously. The higher the temperature, the more volatiles will be released and the more structural deformation of the now void particles will occur, thus leading to smaller particle sizes. As the pyrolysis temperature is increased further, agglomeration, as described above, starts to take place and leads to a number of particles sticking

together forming larger particles, as exhibited in Figure 4.13. The shrinking and agglomeration phenomena are consistent with SEM results discussed in the previous section and support further reactivity results presented in the section of char reactivity. On the other hand, the increase in the $d(0.1)$ particle size signifies the decrease of the proportion of fines in the blend. While it may be difficult to explain this completely, one of the possibilities is the early onset of agglomeration. Additionally, some fines could likely be lost during pyrolysis, hence, raising the $d(0.1)$.

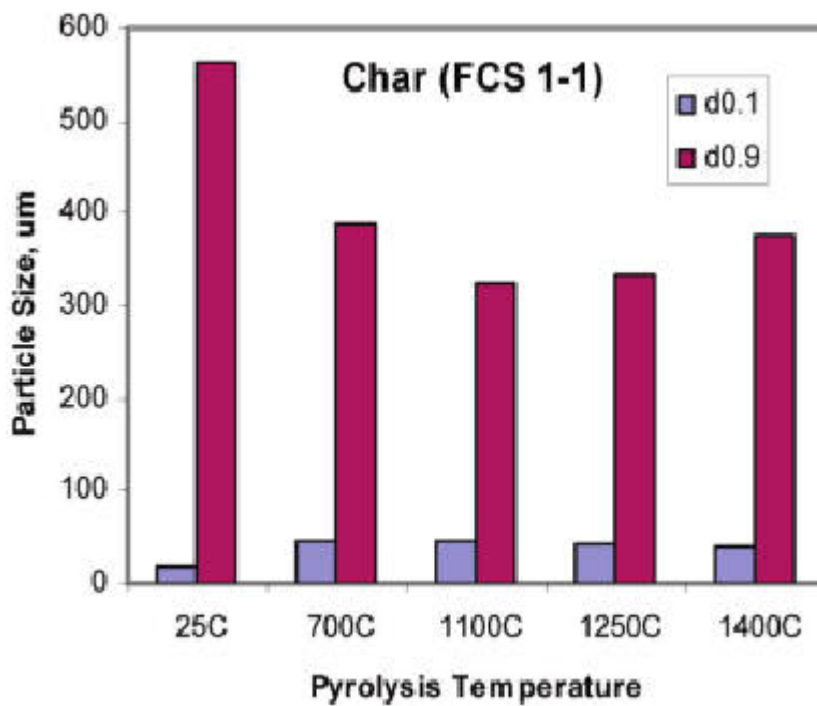
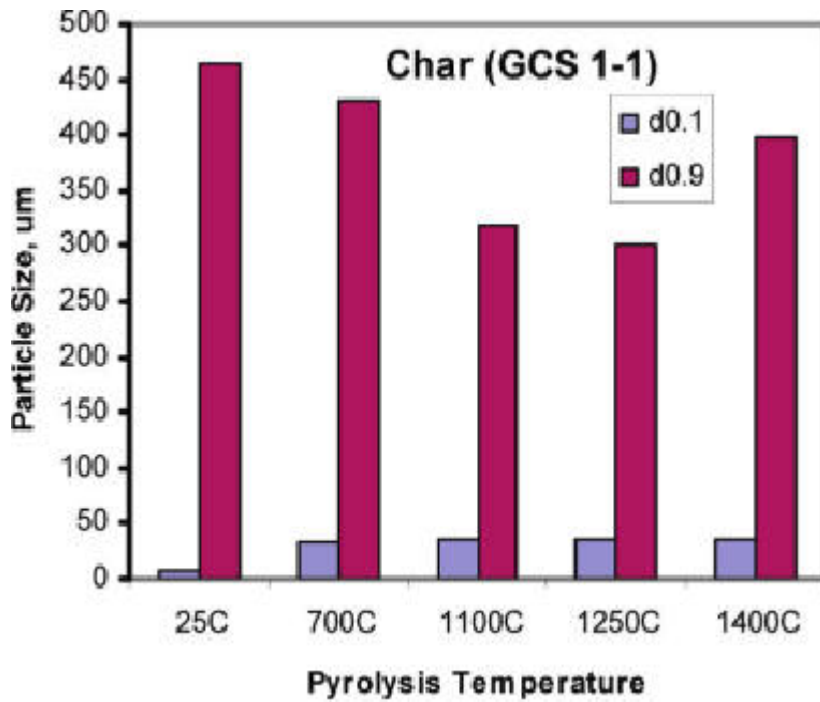


Figure 4.15 Effect of pyrolysis temperature on the particle size distribution of char from Genesee coal & sawdust blend (top) and fluid coke & sawdust blend (bottom).

A closer look on Figure 4.15 shows particle sizes of over 450 μm , while in experiment, the particle sizes used for coal and fluid coke were 53-75 μm and, for biomass, the particles were 250-300 μm . The reason for this is that particle size fractions used were initially determined by sieve analysis, and that was when the size cuts of 53-75 μm and 250-300 μm were established. In sieve analysis, however, pin shaped particles could vertically go through a sieve. Later, the blend particle sizes were measured by the Mastersizer, in which case the longest dimension of the pin-shaped particles is measured and recorded. The difference between the two measuring techniques could be the reason for the discrepancy.

The Mastersizer measurements however are purely for comparison purpose, therefore posing no threat to the final results.

References

- [1]. Lu L.M., Sahajwalla V., Harris D. Characteristics of chars prepared from various pulverized coals at different temperatures using drop tube furnace. *Energy Fuels*, Vol. 14, No. 4, pp. 869-876, 2000
- [2]. Senneca O., Russo P., Salatino P., Masi S. The relevance of thermal annealing to the evolution of coal char gasification reactivity. *Carbon*, Vol. 35, No. 1, pp. 141-151, 1997
- [3]. Cai H.Y., Guell A.J., Chatzakis I.N., Lim J.Y., Dugwell D.R., Kandiyoti R. Combustion reactivity and morphological change in coal chars: effect of pyrolysis temperature, heating rate and pressure. *Fuel*, Vol. 75, pp. 15-24, 1996
- [4]. Khan M.R. Significance of char active surface area for appraising the reactivity of low- and high- temperature chars. *Fuel*, Vol. 66, pp. 1626-1634, 1987
- [5]. Zhang L., Xu S., Zhao W., Liu S. Co-pyrolysis of biomass and coal in a free fall reactor. *Fuel*, Vol. 86, pp. 353–359, 2007
- [6]. Zhua W., Song W., Lin W. Catalytic gasification of char from co-pyrolysis of coal and biomass. *Fuel Process. Technol.*, Vol. 89, pp. 890–896, 2008
- [7]. Fryda L. E., Panopoulos K. D., Kakaras E. Agglomeration in fluidised bed gasification of biomass. *Powder Technol.*, Vol. 181, pp. 307–320, 2008
- [8]. Velez J. F., Chejne F., Valdes C. F., Emery E. J., Londono C. A. Co-gasification of Colombian coal and biomass in fluidized bed: An experimental study. *Fuel*, Vol. 88, pp. 424–430, 2009

- [9]. Hong Zhang, Wen-Xiu Pu, Si Ha, Ying Li, Ming Sun. The influence of included minerals on the intrinsic reactivity of chars prepared at 900 °C in a drop tube furnace and a muffle furnace. *Fuel*, Vol. 88, pp. 2303-2310, 2009
- [10]. Smoot, L.D., Pratt, D.T., eds. *Pulverized-Coal Combustion and Gasification*. New York: Plenum Press, 133–147
- [11]. Cetin E., Moghtaderi B., Gupta, R., Wall T. F. Influence of pyrolysis conditions on the structure and gasification reactivity of biomass chars. *Fuel*, Vol. 83, pp. 2139–2150, 2004

CHAPTER V

CONCLUSION

Co-pyrolysis of sawdust with Genesee coal/ Fluid coke was performed in a Drop Tube Furnace working at atmospheric pressure and Nitrogen environment and the effects of blending ratio as well as temperature on synergy were investigated. Char was gasified with carbon dioxide in a TGA apparatus to record the char mass change over an isothermal temperature course. The surface morphology was characterized by SEM and the particle size of char samples was measured by a Mastersizer. BET surface area determination of the DTF char samples was carried out.

From TGA studies, sawdust char has the highest gasification rate with Carbon Dioxide, while pet-coke char has the lowest. Reactivity decreases with increased pyrolysis temperature for both pure char and blended char. It is speculated that char obtained from co-pyrolysis of sawdust with coal/pet-coke would increase gasification reactivity of char particles due to catalytic effect of alkali species, which transfer from sawdust to coal/pet-coke char particles and work as a gasification catalyst on coal/pet-coke char. The interactions between biomass particles with coal/pet-coal particles are more complicated than we thought. Alkali salts improve the reactivity while particle surface area decrease

due to agglomeration and condensation decrease the observed reactivity. But overall, based on the TGA result, reactivity of blended char shows lower reaction rate than that of blends with no synergistic effect. It can be concluded that the effect of the biomass to other fuels blending ratio on the reactivity of the co-pyrolyzed chars is more pronounced on chars prepared at low temperatures and the effect becomes less significant for the chars prepared at higher pyrolysis temperature.

The morphological study using SEM showed a particle size decrease and shape change from needle to spherical shape as the pyrolysis temperature was increased. Further investigation revealed that, as the pyrolysis temperature was increased beyond 1250 °C, agglomeration seemed to start occurring. The reason for the agglomeration could be due to the melting of silicates from the biomass. The molten layer on the surface enables coal particles to attach themselves to sawdust particles, leading to the observed agglomeration. The shrinking and agglomeration phenomena were also verified by the particle size distribution analysis.

From the surface area analysis, it can be pointed out that, even though the surface area of both pure and blended char increases with an increasing pyrolytic temperature, the increase surface area in blended chars is much more pronounced when compared to that of the corresponding pure chars. This might be due to the

strong physical or chemical agglomeration that occurs at high pyrolytic temperatures between biomass and other fuel.

APPENDIX A

PUBLISHED PAPER AND CONFERENCE PRESENTATION

Research results have been presented at CSCHE-Ottawa-2008 conference and will be a part of the presentation given by group member at the upcoming CSCHE-Saskatoon-2010 [submitted]. A paper has been published on Energy & Fuel, entitled “Co-gasification of Biomass with Coal and Oil Sand Coke in a Drop Tube Furnace”. Refer to next pages to view this paper.

Co-gasification of Biomass with Coal and Oil Sand Coke in a Drop Tube Furnace[†]

Chen Gao, Farshid Vejahati, Hasan Katalambula, and Rajender Gupta*

Department of Chemical and Materials Engineering, University of Alberta, 536 CME Building, Edmonton, Alberta T6G 2G6, Canada

Received June 5, 2009. Revised Manuscript Received September 25, 2009

The present paper is aimed at investigating the co-gasification of biomass with coal and oil sand fluid coke. Chars were obtained from individual fuels and blends with different blend ratios of coal, oil sand coke, and biomass in a drop tube furnace at different temperatures. The chars were then gasified in a thermogravimetric analyzer (TGA) under CO₂ atmosphere to determine their reactivity. Results showed that the effect of the blending ratio of biomass to other fuels on the reactivity of the co-pyrolyzed chars is more pronounced on chars prepared at low temperatures and the effect becomes less significant as the pyrolysis temperature increases. The increased reactivity at a higher biomass blending ratio is due to the presence of synergetic effects originating from the interaction of the two fuels. Scanning electron microscopy images showed differences in shapes and particle size distribution of char particles from biomass and coal/coke. These also showed the agglomeration of coal and coke chars with biomass char particles at high temperatures. The agglomeration may be the reason for the non-additive behavior of the blends. The chars were also analyzed for the particle size distribution using a laser diffraction Mastersizer instrument and surface area with the Brunauer–Emmett–Teller (BET) technique. BET analysis showed an increase in the surface area with an increasing temperature from 700 to 1400 °C for biomass and coal, but the trend for coke was inversely related to the temperature.

1. Introduction

In recent years, global warming and its immense effects on our ecosystems because of the emission of greenhouse gases, of particular importance, carbon dioxide, have been the center of attention worldwide. Coal-fired power plants have been held responsible as the main anthropogenic source of carbon emission to the environment. In response to this issue, recently, the acceptance of an integrated gasification combined cycle (IGCC) has increased internationally, which is a more efficient and cleaner way of electricity production. The heart of the IGCC technology is the gasification process, which its cost and reliability are largely influenced by feed quality and operating conditions. Gasification products generally burn hotter and cleaner than conventional coal and, thus, can spin a more efficient gas turbine rather than a steam turbine. Gasification also helps to achieve zero carbon dioxide emissions to the environment, even though the energy comes from the conversion of carbon to carbon dioxide. This is because gasification produces a much higher concentration of carbon dioxide than direct combustion of coal in air, and this helps to make carbon capture and storage more economical than it would be otherwise.¹ Another major factor that leads to the interest in gasification is the volatility and high prices of oil and natural gas. However, adoption of this new technology is

largely related to the full appreciation of the gasification behavior of different fuels and their blends.

Gasification of solid fuel can be divided into two stages: pyrolysis or devolatilization and subsequent gasification of the remaining char, with the second stage being the controlling step of the overall process. Knowledge about the reactivity of chars and their structure variation as reaction progresses is fundamental for the design of gasification reactors because char gasification determines the final conversion achieved in the process.²

The steady increase of synthetic crude production from oil sand in western Canada has resulted in massive production and accumulation of oil sand coke (> 6000 tons/day). Oil sand coke is a byproduct derived from oil sand refinery cracking processes, and two types of coke exist depending upon the production process: fluid and delayed coke. The cokes have high carbon content (above 80%) with nongraphitic structure. Oil sand coke is a free (zero-cost) solid waste, and because of its low reactivity, use of this fuel in its pure form is not well-developed.

Biomass, on the other hand, is one of the environmentally friendly fuels. However, biomass alone cannot be used as a fuel because its heating value is relatively low. Therefore, co-gasification of biomass and coal or coke can be considered as a potential fuel base for gasification, further synthesis gas (syngas: CO + H₂) production, and methanol/dimethyl ether (DME) synthesis.

Previous investigations on the co-gasification of biomass/coal blends have mostly concentrated on the mechanism of

[†] Presented at the 2009 Sino–Australian Symposium on Advanced Coal and Biomass Utilisation Technologies.

*To whom correspondence should be addressed: Chemical and Materials Engineering, Faculty of Engineering, University of Alberta, Edmonton, Alberta T6G 2V4, Canada. Telephone: (780) 492-6861. Fax: (780) 492-2881. E-mail: rajender.gupta@ualberta.ca.

(1) Fitzer, E.; Kochling, K.-H.; Boehm, H. P.; Marsh, H. Recommended terminology for the description of carbon as a solid. *Pure Appl. Chem.* 1995, 67 (3), 473–506.

(2) Everson, R. C.; Neomagus, H. W. J. P.; Kasaini, H.; Njapha, D. Reaction kinetics of pulverized coal-chars derived from inertinite-rich coal discards: Gasification with carbon dioxide and steam. *Fuel* 2006, 85, 1076–1082.

production of gas- and liquid-phase species.^{3–7} Additionally, there are also few studies that have focused on the interaction effect (also known as the catalytic or synergetic effect) between coal, biomass, and other fuels, such as petroleum coke and plastics.^{8–14} Kumabe et al.⁸ studied co-pyrolysis of biomass and coal in a free-fall reactor under atmospheric pressure with nitrogen as the balance gas and reported that, with an increase in the biomass ratio, the H₂ composition decreased and the CO₂ compositions increased. Zhang et al.⁹ carried out a study on the co-gasification of woody biomass and coal in an oxygen-containing atmosphere in a pressurized fluidized-bed reactor and found that the char and liquid yields from the blended samples were higher and lower, respectively, than the theoretical values calculated on the pyrolysis of each individual fuel. Similar findings were reported by Sjoström et al.,¹⁰ who studied the reactivity of char in co-gasification of biomass and coal. Although not very certain, they reported the occurrence of synergetic effects in the co-gasification of birch wood with two different types of coal in experiments performed in the pressurized fluidized-bed reactor. The reactivities of the fuels in the mixtures and the formed chars were seen to have increased, leading to promoted gas production.

In another investigation, Collot et al.¹¹ co-pyrolyzed and co-gasified coal and biomass in bench-scale fixed- and fluidized-bed reactors. They found that, in pyrolysis experiments, neither intimate contact between fuel particles nor their relative segregation led to synergistic effects. They however reported that mineral matter residues from the wood appear to have played a catalytic effect during combustion. Generally, they concluded that there was no evidence of synergy that was found with the fluidized-bed reactor, thereby demonstrating the lack of contact between coal and biomass particles in the system. Another recent work is that by Feroso et al.,¹² who co-gasified coal, biomass, and petroleum coke at high pressure. From this work, a synergistic effect was observed for blends of coal with petcoke and an increase in the production of H₂ and CO was obtained. Furthermore, the addition of a

small amount of biomass (up to 10%) led to an increase in H₂ and CO production. Finally, blending biomass with coal–petcoke blends did not produce any significant change in H₂ production, although slight variations were observed in the production of CO and CO₂.

Alkali metal salts, especially potassium salts, are considered to be effective catalysts for carbon gasification by steam and CO₂ while too expensive for industry application. Zhu et al.¹³ used a herbaceous type of biomass, which has a high content of potassium to act as a source of catalyst by co-processing with coal. The co-pyrolysis chars revealed higher gasification reactivity than that of char from coal, especially at high levels of carbon conversion. On the influence of the alkali in the char and the pyrolysis temperature on the reactivity of co-pyrolysis char, experimental results showed that the co-pyrolysis char prepared at 750 °C had the highest alkali concentration and reactivity as compared to the char prepared at 850 °C.

Vuthaluru¹⁴ on his study of thermal behavior of coal/biomass blends during co-pyrolysis reported to have found no interactions between coal and biomass during co-pyrolysis, and apart from the pyrolysis of coal alone, the 50:50 coal/biomass blend had the highest reaction rate, ranging from 1×10^9 to 2×10^9 min⁻¹. There are also some investigations by Cai et al.¹⁵ who investigated the thermal behavior of coal blends with plastics during co-pyrolysis and found that the difference of weight loss between experimental and theoretical data was 2.0–2.7% at 550–650 °C, which was the overlapping degradation temperature interval between coal and plastic, assuming that to be the favorable temperature for hydrogen transfer from plastic to coal. Palmer et al.,¹⁶ while working on the co-conversion of coal/waste plastic mixtures under various pyrolysis and liquefaction conditions, had almost the same findings as those by Cai et al.¹⁵

Most of these studies reviewed above are based on pure coal or coal blends with other fuels. However, not much research has been conducted on the co-pyrolysis of the coke blend with biomass. The purpose of this study is to investigate any synergies resulting from vastly different characters of fuels: coke high in sulfur, biomass high in potassium, and coal high in silica. The differences in the amount and type of volatile matter in different fuels do have impact on the char character and gasification kinetics.

The underlying objective of the present work is to investigate char particles prepared from the co-pyrolysis of biomass–coal and biomass–fluid coke blends for their kinetic properties and morphology at different temperatures to provide some fundamental understanding of the interaction of the different fuels and elucidate any advantages that may arise from the binary and/or ternary co-gasification of coal/biomass/coke. For the sake of clarity, the oil sand coke used in this study is fluid coke, a term that will be used in the text as well.

In this respect, reactivity of produced chars is assessed using thermogravimetric analysis (TGA) and CO₂ as the oxidizing agent. The morphological properties of the char particles were studied using scanning electron microscopy (SEM). Particle size distribution was determined using a laser diffraction

(3) Demirbas, A. Mechanisms of liquefaction and pyrolysis reactions of biomass. *Energy Convers. Manage.* **2000**, *41*, 633–646.

(4) Prins, M. J.; Ptasiński, K. J.; Janssen, F. J. J. G. From coal to biomass gasification: Comparison of thermodynamic efficiency. *Energy* **2007**, *32*, 1248–1259.

(5) Salo, K.; Mojtahedi, W. Fate of alkali and trace metals in biomass gasification. *Biomass Bioenergy* **1998**, *15* (3), 263–267.

(6) Li, K.; Zhang, R.; Bi, J. Experimental study on syngas production by co-gasification of coal and biomass in a fluidized bed. *Int. J. Hydrogen Energy* **2009**, in press.

(7) Pinto, F.; Franco, C.; Andre, R. N.; Tavares, C.; Dias, M.; Gulyuriltu, I.; Cabrita, I. Effect of experimental conditions on co-gasification of coal, biomass and plastics wastes with air/steam mixtures in a fluidized bed system. *Fuel* **2003**, *82*, 1967–1976.

(8) Kumabe, K.; Hanaoka, T.; Fujimoto, S.; Minowa, T.; Sakanishi, K. Co-gasification of woody biomass and coal with air and steam. *Fuel* **2007**, *86*, 684–689.

(9) Zhang, L.; Xu, S.; Zhao, W.; Liu, S. Co-pyrolysis of biomass and coal in a free fall reactor. *Fuel* **2007**, *86*, 353–359.

(10) Sjoström, K.; Chen, G.; Yu, Q.; Brage, C.; Rosen, C. Promoted reactivity of char in co-gasification of biomass and coal: Synergies in the thermochemical process. *Fuel* **1999**, *78*, 1189–1194.

(11) Collot, A.-G.; Zhuo, Y.; Dugwell, D. R.; Kandiyoti, R. Co-pyrolysis and co-gasification of coal and biomass in bench-scale fixed bed and fluidised bed reactors. *Fuel* **1999**, *78*, 667–679.

(12) Feroso, J.; Arias, B.; Plaza, M. G.; Pevida, C.; Rubiera, F.; Pis, J. J.; García-Peña, F.; Casero, P. High-pressure co-gasification of coal with biomass and petroleum coke. *Fuel Process. Technol.* **2009**, *90*, 926–932.

(13) Zhua, W.; Song, W.; Lin, W. Catalytic gasification of char from co-pyrolysis of coal and biomass. *Fuel Process. Technol.* **2008**, *89*, 890–896.

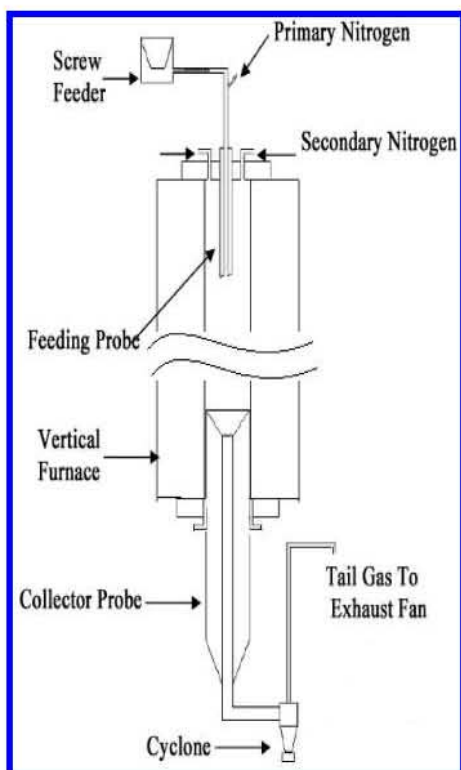
(14) Vuthaluru, H. B. Thermal behaviour of coal/biomass blends during co-pyrolysis. *Fuel Process. Technol.* **2003**, *85*, 141–155.

(15) Cai, J.; Zhou, L.; Huang, Q. Thermogravimetric analysis and kinetics of coal/plastic blends during co-pyrolysis in nitrogen atmosphere. *Fuel Process. Technol.* **2008**, *89*, 21–27.

(16) Palmer, S. R.; Hippo, E. L.; Tandan, D. Co-conversion of coal/waste plastic mixtures under various pyrolysis and liquefaction conditions. *Prepr. Symp.—Am. Chem. Soc., Div. Fuel Chem.* **1995**, *40*, 29–33.

Table 1. Proximate and Ultimate Analyses of Fuels

sample	proximate analysis (%) (w/w, as received)				ultimate analysis (%) (w/w, daf)				
	fixed carbon	volatile matter	ash	moisture	C	H	N	O	S
Genesee coal	40.15	23.44	30.62	5.79	76.09	4.51	1.09	17.89	0.42
fluid coke	85.81	6.60	6.22	1.37	86.72	1.76	2.09	2.73	6.7
sawdust	12.38	84.17	0.43	3.02	49.15	6.54	0.27	43.53	0.51

**Figure 1.** Schematic diagram of the DTF.

technique. Also, the pore structure was studied by Brunauer–Emmett–Teller (BET) analysis.

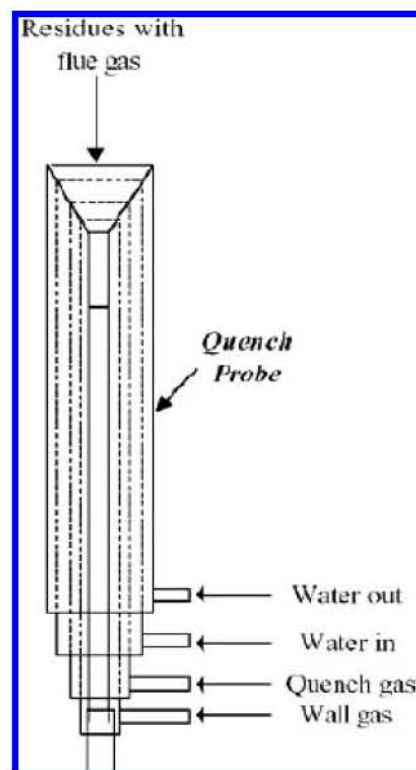
2. Experimental Section

The experimental procedure involved char samples preparation using a drop tube furnace (DTF) under rapid heating conditions and then further analyzing them by TGA, BET, laser diffraction Mastersizer and SEM.

2.1. Raw Materials. Three different raw materials, Genesee coal, fluid coke (syncrude coke), and woody biomass from a carpentry shop, were used in this study. The fuels were crushed and ground using a ball mill and a pulverizer, sieved, and classified to obtain a particle size cut of 53–75 μm for both Genesee coal and fluid coke, while a particle size range of 250–300 μm was selected for woody biomass. These particle sizes were chosen because they are the ones normally used for these fuels in practical situations. The samples were oven-dried at 105 $^{\circ}\text{C}$ for 2 hours to eliminate the effect of moisture, which could lead to the agglomeration of particles, and also to maintain smooth flow rates. The samples were then fed to the DTF. Table 1 presents the ultimate and proximate analyses of the fuels used in this study.

2.2. Equipment. The experimental setup is shown schematically in Figure 1. The furnace contains an electrically heated vertical core of Mullite tube (inner diameter of 60 mm) of 140 cm long, with an effective heated zone of 120 cm. DTFs have been widely used because of their similarity to the pulverized reactor in practical plants.

Three proportional–integral–derivative (PID) temperature controllers adjust the temperature of the reactor at constant

**Figure 2.** Schematic diagram of the collector probe.

temperature in three different zones. A thermocouple is used to calibrate the gas temperature inside the tube. The maximum attainable gas temperature in this furnace is 1650 $^{\circ}\text{C}$. A screw feeder attached to a hopper with vibrating walls, which prevents bridging of fine particles, is used to feed particles into the feeder probe. The nominal capacity of the feeder ranges from 8 to 60 g/h for coal. A water-cooled feeding probe is used to prevent ignition of particles inside the feeder, which is crucial in estimating the true particle residence time. The feeder probe is shielded from the heat using high-temperature insulation material. When the depth that the feeding probe is inserted into the furnace is adjusted, the residence time can be changed. Combustion products are collected through a water-cooled collection probe, shown in Figure 2. To prevent condensation of combustion or gasification products on the inner shell of the collector probe, the probe is equipped with a sintered stainless-steel inner shell through which gas (nitrogen) is passed. There are two gas inlets on the collector probe: the quench gas inlet, which quenches the combustion products in the top section of the collector and prevents the reactions from progressing further, and the wall gas inlet, which prevents condensation and deposition of particles in the lower section of the probe. The cooled gas and products are then sent to the cyclone.

2.3. Char Preparation. Sawdust was blended with coal or coke at different ratios by weight, as shown in Table 2. The blending was performed before feeding into the reactor. The pyrolysis of the samples was conducted at four different temperatures: 700, 1100, 1250, and 1400 $^{\circ}\text{C}$. The DTF was purged for 30 min with nitrogen at a flow rate of 10 L/min to make sure no oxidation occurred in the furnace.

Table 2. Blending Fuels Ratio and Their Abbreviation

samples	component by weight percent		
	Genesee coal	sawdust	fluid coke
GC	100	0	0
FC	0	0	100
S	0	100	0
GCS 2–1	67	33	0
GCS 1–1	50	50	0
GCS 1–2	33	67	0
FCS 2–1	0	33	67
FCS 1–1	0	50	50
FCS 1–2	0	67	33

For every experimental run, the furnace was heated to the set point temperature before the particles were fed into it and the char particles were collected in the cyclone. The N₂ flow rate, feeding rate, and residence time were fixed for all of the experiments.

2.4. Measurement of Char Gasification Reactivity. The gasification reactivity of the co-pyrolyzed char was measured at isothermal conditions using TGA. TGA is one of the most common techniques used to investigate thermal events and reaction kinetics. TGA has also been widely used to study the reactivity of different char particles using an oxidizing agent, such as carbon dioxide.

Before the tests, the samples were dried at 105 °C to remove moisture. In TGA experiments, a flow of nitrogen was used as the sweeping gas during the period of heating to the desired temperature (in this case, 800 °C) with a heating rate of 10 °C/min. The mass of the sample was approximately 12 mg. When the set temperature is reached, the isothermal gasification reaction of the co-pyrolyzed char sample was initiated by switching on a flow of carbon dioxide. The experiment was stopped when no more mass loss was detected and the rate constant was determined from the weight loss curves.

3. Results and Discussion

3.1. Char Reactivity. As mentioned above, the objective of this work is to see if co-pyrolysis and/or co-gasification of different fuels have any effect on the reaction kinetics of the fuels in question. In this work, reactivity of different co-pyrolyzed samples was compared on the basis of their reaction rate constants, k . The reaction rate constant quantifies the speed of a chemical reaction, and thus, it is a good indicator when it comes to the comparison of reactivities.

Figure 3 shows the weight loss curves for the pyrolyzed Genesee coal and sawdust 1:1 blend chars produced at all four temperatures, namely, 700, 1100, 1250, and 1400 °C. The curves distinctively show the difference between these chars, with the char produced at 700 °C being the most reactive, while that produced at 1400 °C being the least reactive. This can be explained by the fact that the higher co-pyrolysis temperature leads to more volatiles being driven out of the particles, hence, rendering the remaining char less reactive. For the char produced at 700 °C, it can be seen that the weight loss starts much earlier at a temperature of about 450 °C and this is before the CO₂ reaction even starts, something which is not supposed to happen. This could be due to the fact that 700 °C is the lowest temperature used in char preparation and, because the height of the drop tube is fixed, the residence in the furnace may not have been long enough to drive all of the volatiles out of the particle. Upon reheating during gasification with CO₂, the remaining volatiles will start to be released at the shown lower temperatures, hence, leading to the observed particle weight loss.

The trend observed for the Genesee coal–sawdust blend was also observed in the 1:1 fluid coke/sawdust blend, as shown in Figure 4. Again, the char produced at 700 °C had the most weight loss, indicating its high reactivity, while the char produced at 1400 °C had the lowest weight loss, thus being the least reactive. The early weight loss for the 700 °C char was again observed here, and an almost similar trend was observed for the char produced at 1100 °C, although the onset of the weight loss was at a much higher temperature. The same explanation as the one given for the coal–sawdust blend above is valid in this case as well. A simple comparison between these two figures shows that the coal–sawdust blend is more reactive than the fluid coke–sawdust blend.

A comparison of the reactivities in terms of the reaction rate constant k is given in Figure 5. Consistent to what has been reported above, for a given blend ratio, the reactivity of lower temperature prepared char is higher than the reactivity of those prepared at higher temperatures. Figure 5 further presents the effect of the blending ratio on the reactivity of the chars, and this is where the presence or absence of the synergetic effect can be established. From the figure, it can be seen that, for the case of the char pyrolyzed at 700 °C, the reactivity of the chars is higher when the biomass (sawdust) proportion is high. As the proportion of sawdust decreases (increasing coal proportion), the reactivity is also seen to decrease. Apart from the char prepared at 700 °C, it is difficult to conclude the same for the chars prepared at the remaining three temperatures, i.e., 1100, 1250, and 1400 °C, where the variation of the rate constant k does not give any particular pattern. It can therefore be concluded that the effect of the blending ratio on the reactivity of the co-pyrolyzed chars is more pronounced on the chars prepared at low temperatures and the effect becomes less significant as the pyrolysis temperature increases. The increased reactivity at a higher biomass blending ratio is due to the presence of synergetic effects originating from the interaction of the two fuels. These findings are in agreement with the work of Zhang et al.,⁹ who pyrolyzed biomass and coal at temperatures between 500 and 700 °C but found that the synergetic effect was more pronounced on the char produced at 600 °C than the one produced at 700 °C. Another work with similar findings is that of Zhu et al.,¹³ whose char, which was produced at 850 °C, had a lower reactivity than the one produced at 750 °C. One possible explanation for this is the melting of the potassium silicate normally found in biomass and is a big contributor to the enhancement of the reactivity in co-gasification processes, as reported by Fryda et al.¹⁷ and Velez et al.¹⁸ Fryda et al.,¹⁷ when investigating the fluidized-bed gasification of biomass, pointed out that the high potassium content of some biomass causes the formation of melt responsible for total defluidization. The main defluidization mechanism is the total melting of the silicate ash forming a highly viscous liquid. Melts consist mainly of alkali silicates and, to a lesser extent, other oxides or alkali salts. In this case, bed particle grains were either adhered to the sticky melt or joined together by a molten layer on their surfaces. This is characteristic for silica systems and is

(17) Fryda, L. E.; Panopoulos, K. D.; Kakaras, E. Agglomeration in fluidised bed gasification of biomass. *Powder Technol.* **2008**, *181*, 307–320.

(18) Vélez, J. F.; Chejne, F.; Valdés, C. F.; Emery, E. J.; Londoño, C. A. Co-gasification of Colombian coal and biomass in fluidized bed: An experimental study. *Fuel* **2009**, *88*, 424–430.

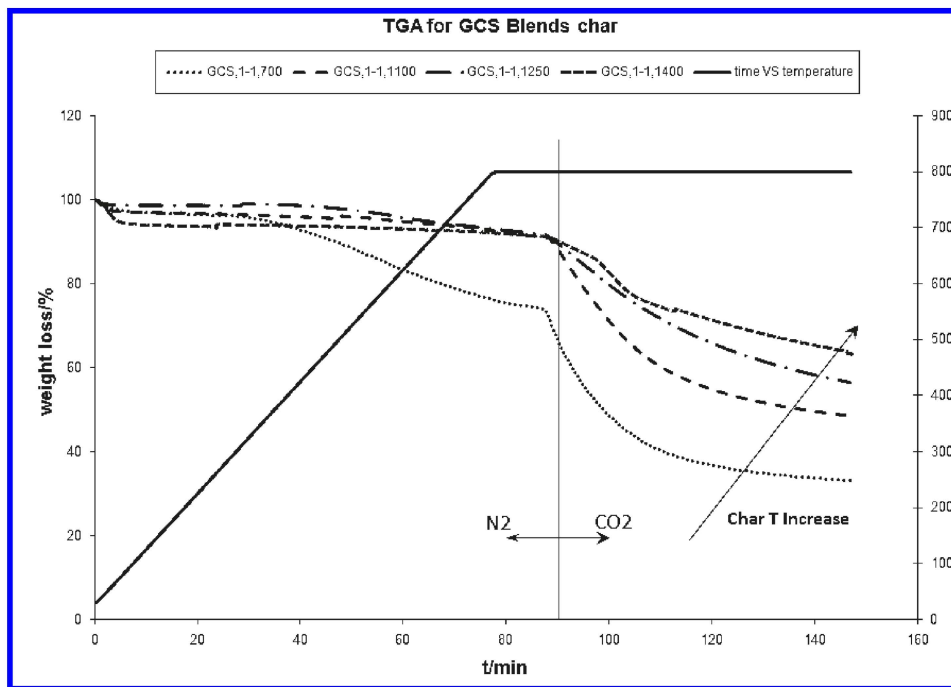


Figure 3. TGA results for Genesee coal and sawdust (GCS 1–1) blended char pyrolyzed at 700, 1100, 1250, and 1400 °C.

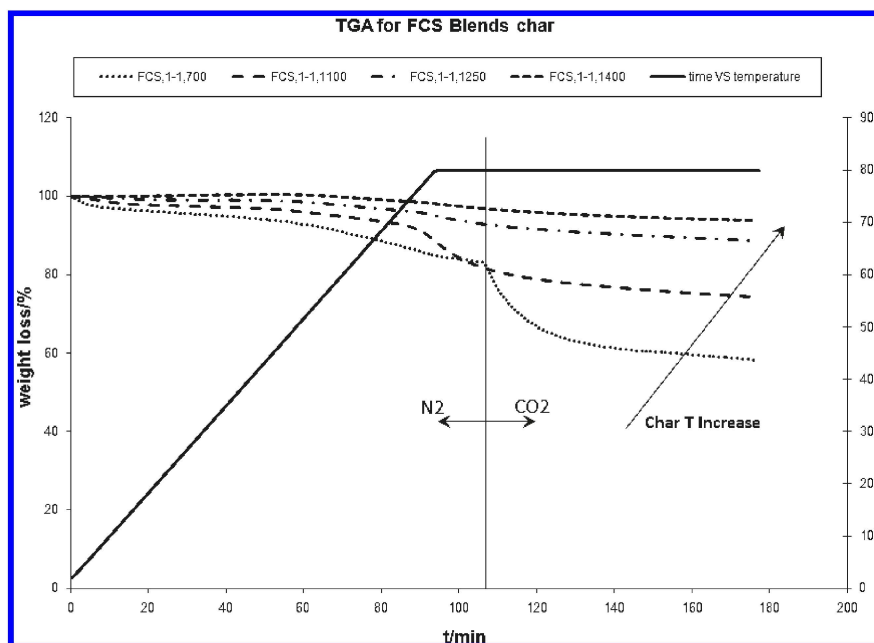


Figure 4. TGA results for fluid coke and sawdust (FCS 1–1) blended char pyrolyzed at 700, 1100, 1250, and 1400 °C.

described as viscous flow sintering. According to the sintering and coating mechanisms described, collisions with the reacting fuel particles may dominate the transfer of K-rich compounds to the bed particle surfaces. No obvious chemical interaction between the bed material and the fuel ash in the gasifier was observed with the SEM/energy-dispersive spectrometry (EDS) analyses. A similar mechanism can be used to explain results from DTF, in which the interaction between the two fuel particles occurs only during the pyrolysis. Once the melting of the silicates occur (MP for potassium silicate is 740 °C), the transfer of K-rich compounds from biomass to coal or fluid coke is hindered, hence leading to less reactive chars. This can explain why the effect of the blending ratio on reactivity (k) is not so significant

when the chars produced at higher temperatures (> 700 °C) are gasified with CO_2 in the TGA.

The effect of the blending ratio on char reactivity for the fluid coke–sawdust blend was almost the same as the one depicted in Figure 5, and the same reasons can explain the results. Furthermore, as expected, biomass char particles showed the highest reactivity, followed by Genesee coal, and fluid coke char particles had the least reactivity.

3.2. Morphological Analysis of Pyrolysis Char. The surface morphology of the char samples was examined using SEM. Figure 6 shows SEM images for biomass–coal blends pyrolyzed at the four temperatures mentioned before (i.e., 750, 110, 1250, and 1400 °C). The first image a, which is a co-pyrolyzed char produced at 700 °C shows needle-like

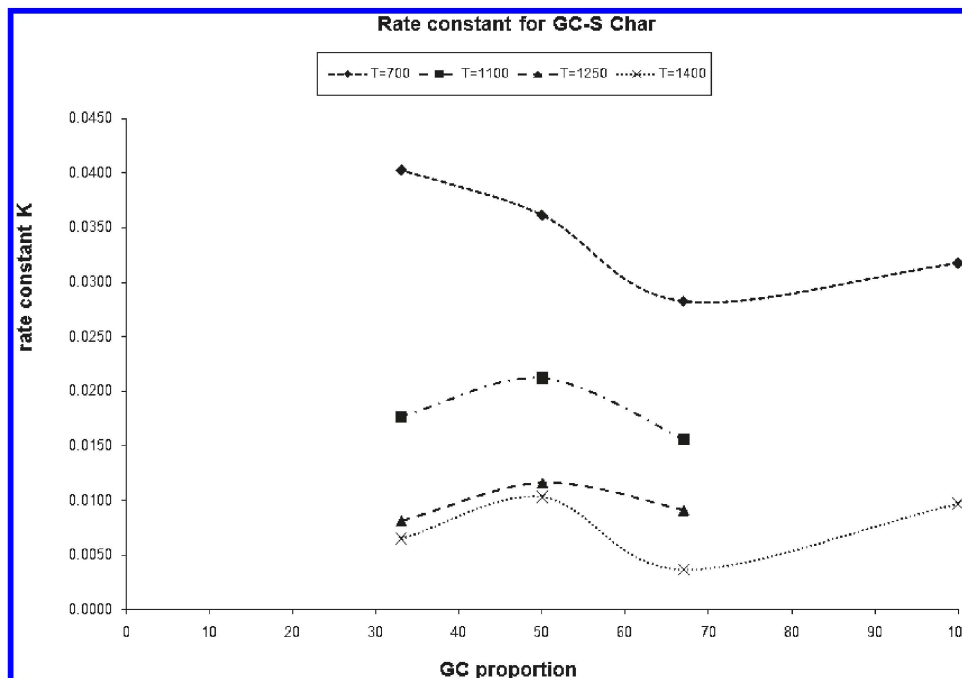


Figure 5. Effect of the blending ratio and pyrolysis temperature on reactivity of Genesee coal and sawdust blended char (the units of k are s^{-1}).

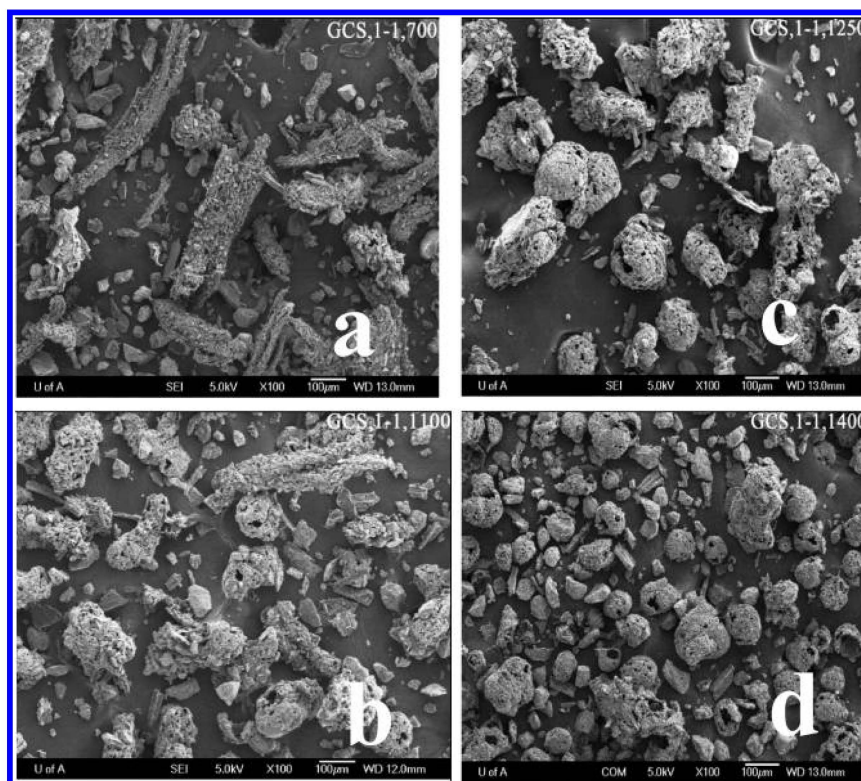


Figure 6. Effect of the pyrolysis temperature on particle morphology of Genesee coal and sawdust 1:1 ratio blend. Pyrolysis temperatures are (a) 700 °C, (b) 1100 °C, (c) 1250 °C, and (d) 1400 °C. SEM magnification was 100 \times .

particles. The needle-like particles are mostly biomass particles that are composed of lodgepole and jack pines, both belonging to the softwood group. The next image b, which is for char produced at 1100 °C, still exhibits needle-shaped particles, but they are much shorter as compared to those in image a. As the co-pyrolysis temperature is increased to 1400 °C, particles are seen to have become more porous and spherical. This is in agreement with the findings by Cetin

et al.,¹⁹ who had reported that softwoods show a shape transition from needle-like to spherical with increasing temperature. On the other hand, the seemingly higher porosity of the particles at higher temperature (as compared to lower

(19) Cetin, E.; Moghtaderi, B.; Gupta, R.; Wall, T. F. Influence of pyrolysis conditions on the structure and gasification reactivity of biomass chars. *Fuel* 2004, 83, 2139–2150.

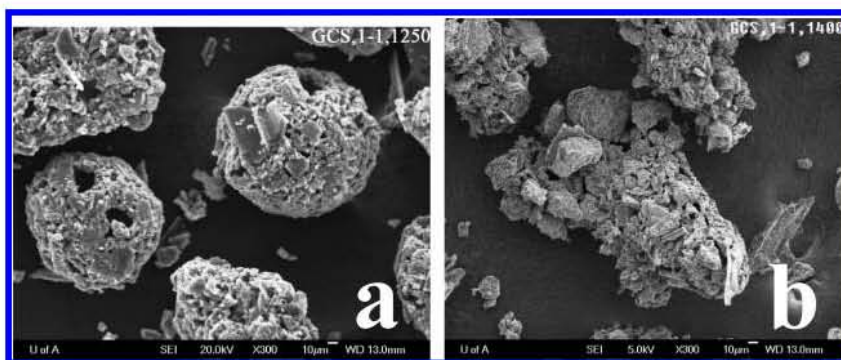


Figure 7. Agglomeration between coal and biomass particles at higher temperature. Image a is char produced at 1250 °C, and image b is char produced at 1400 °C. Magnification was 300×.

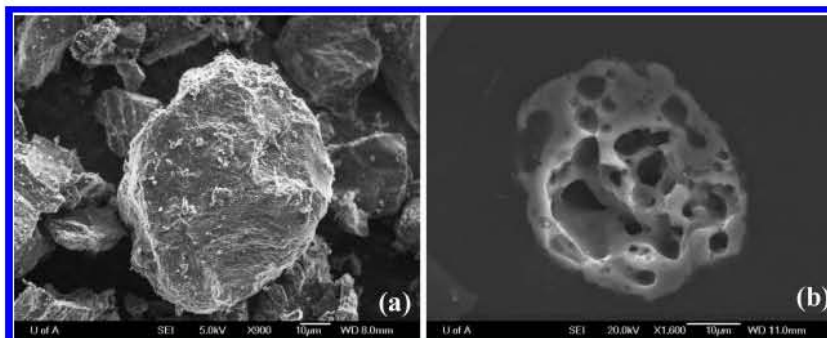


Figure 8. Pores development in fluid coke chars at (a) 700 °C and (b) 1400 °C.

temperature) could be due to the enhanced release of volatile matter during the pyrolysis process and also coalescence of smaller pores to form bigger pores.

Further investigation revealed that, as the pyrolysis temperature was increased beyond 1250 °C, agglomeration seemed to start occurring. Close observation showed coal particles either covered by the sawdust pieces or attached to the sawdust and becoming a part of the sawdust surface. The reason for the agglomeration could be the same as the one given in the preceding section, where the melting of silicates was pointed out to be the cause of this. The molten layer on the surface enables coal particles to attach themselves to sawdust particles, leading to the observed agglomeration. Figure 7 shows an example of agglomerated particles, where coal particles are seen to have attached themselves onto biomass particles. Similar shape changes were observed for the fluid coke–biomass blend. The morphological analysis of fluid coke revealed a significant growth of pores in coke chars at high temperatures when compared to the chars at low temperatures, as depicted in Figure 8. The char prepared at 1400 °C appears to be more spongy than the one prepared at 700 °C. Generally, results from the morphological study of pyrolysis chars complement the findings from TGA on why the effect of fuel blending is less pronounced when the pyrolysis temperature is increased.

3.3. Particle Size Distribution. To investigate further the effect of the co-pyrolysis temperature on particle sizes, the particle size distribution of the collected char from DTF was analyzed using a laser diffraction Mastersizer 2000 instrument. For this particular analysis, 1:1 blends of both coal and fluid coke were used.

Figure 9 shows the variation of the particle size with the char pyrolysis temperature. In this particular case, the particle size variation is explained using $d(0.1)$, which means

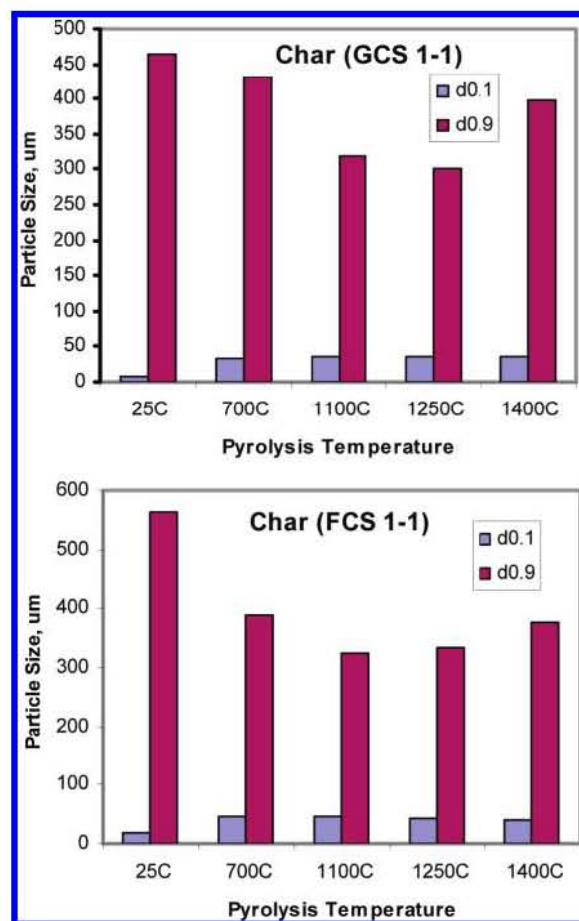


Figure 9. Temperature effect on the particle size distribution of char from Genesee coal + sawdust blend (above) and fluid coke + sawdust blend (below).

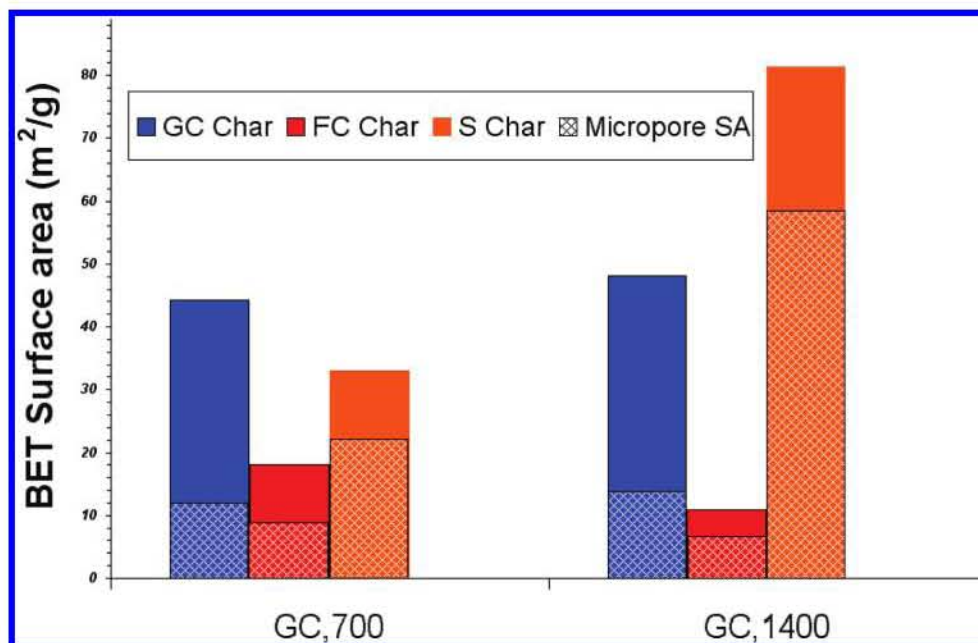


Figure 10. Temperature effect on the surface area (SA) for three pure chars, namely, Genesee coal, fluid coke, and sawdust chars.

10% of the particles were smaller than this size, and $d(0.9)$, at which 90% of the particles were smaller. For the coal–biomass blend, the effect of pyrolysis is shown in the top panel of Figure 9, starting with a blend that was not pyrolyzed at all, shown at 25 °C. It can clearly be seen that $d(0.9)$ particle sizes initially decrease with an increase in the pyrolysis temperature up to 1250 °C. Thereafter, an increase in the particle size is observed when the temperature increases to 1400 °C. For the case of $d(0.1)$, it looks like there is a lot of fine particles at 25 °C. As the temperature increases, the proportion of fines decrease as the $d(0.1)$ is seen to increase. A similar trend is observed for the fluid coke–biomass blend, as shown in the bottom panel of Figure 9. The initial decrease in the $d(0.9)$ particle size can be caused by shrinking of the particles because of devolatilization, as explained previously. The higher the temperature, the more volatiles will be released and the more structural deformation of the now void particles will occur, thus leading to smaller particle sizes. As the pyrolysis temperature is increased further, agglomeration, as described in section 3.2 above, starts to take place and leads to a number of particles sticking together forming larger particles, as exhibited in Figure 7. The shrinking and agglomeration phenomena are consistent with SEM results discussed in the previous section and support further reactivity results presented in section 3.1. On the other hand, the increase in the $d(0.1)$ particle size signifies the decrease of the proportion of fines in the blend. While it may be difficult to explain this completely, one of the possibilities is the early onset of agglomeration. Additionally, some fines could likely be lost during pyrolysis, hence, raising the $d(0.1)$.

A closer look on Figure 9 shows particle sizes of over 450 μm , while in experiments, the particle sizes used for coal and fluid coke were 53–75 μm and, for biomass, the particles were 250–300 μm . The reason for this is that particle size fractions used were initially determined by sieve analysis, and that was when the size cuts of 53–75 μm and 250–300 μm were established. In sieve analysis, however, pin-shaped particles could vertically go through a sieve. Later, the blend particle sizes were measured by the Mastersizer, in which case the longest dimension of the pin-shaped particles is measured and recorded. The difference between the two

measuring techniques could be the reason for the discrepancy. The Mastersizer measurements however are purely for comparison purposes, therefore posing no threat to the final results.

3.4. Effect of Blending on the Char Surface Area. More information on the effect of blending was obtained from the determination of the surface area using BET analysis on both pure and blended (GCS 1–1 and FCS 1–1) chars, as shown in Figure 10. The BET surface area and pore volume of char were obtained from N_2 adsorption isotherms at 77 K using an Omnisorp 360 analyzer. The specific surface area was calculated by the BET equation. Prior to the analysis, the samples were degassed at 350 °C for 4 hours.

Results showed that the porosity of the chars increase with an increase in the pyrolysis temperature because of the removal of volatile matters. Given the fact that the residence time in the DTF is fixed and the temperature of 700 °C is not high enough to achieve complete devolatilization of fuel, the BET surface area of Genesee coal char slightly increased with increasing the pyrolysis temperature from 44.2 $\text{m}^2 \text{g}^{-1}$ (at 700 °C) to 48.2 $\text{m}^2 \text{g}^{-1}$ (at 1400 °C), while that of sawdust char went up from 33.0 $\text{m}^2 \text{g}^{-1}$ (at 700 °C) to 81.3 $\text{m}^2 \text{g}^{-1}$ (at 1400 °C). However, results from fluid coke char exhibited an opposite trend, whereby the surface area decreased with the temperature, as shown in Table 3. The reason for this is not fully understood, but one possible explanation could be that some micropores are blocked, probably because of the softening or melting of the char matrix. Also, the transformation of micropores to macropores could result in the same trend.

Generally, pores in char particles are divided into three classes: micropores, mesopores, and macropores. The boundary between micro- and mesopores is 2 nm, while the boundary of meso- and macropores is 50 nm by convention. Results indicate that, the lower the pyrolytic temperature, the larger the macropore contribution to the pore structure. Moisture and other highly volatile molecules were vaporized to generate the macropore during the initial stage of the pyrolytic process. As the pyrolytic temperature increases, the cell wall cracks to generate both meso- and micropore. The pore volume and BET surface area of the three pure chars prepared at 700 and 1400 °C are compared in Table 3.

Table 3. Pore Structure and BET Surface Area of Genesee Coal/Fluid Coke/Biomass Pure and Blended Chars at a Ratio of 1:1 (SA and V Represent Surface Area and Volume, Respectively)

sample	BET SA (m ² /g)	micropore V (cm ³ /g)	mesopore V (cm ³ /g)
S, 700	33.0	0.00675	0.01112
S, 1400	81.3	0.01461	0.01973
GC, 700	44.2	0.00452	0.00537
GC, 1400	48.2	0.00519	0.00666
FC, 700	18.0	0.00575	0.00398
FC, 1400	10.8	0.00311	0.0056
GCS 1–1, 700	12.8	0	0.00581
GCS 1–1, 1400	64.	0.02282	0.01746
FCS 1–1, 700	6.6	0	0.00401
FCS 1–1, 1400	12.5	0.00382	0.00838

Another observation that can be pointed out from Table 3 is that, even though the surface area of both pure and blended chars is increasing with an increasing pyrolytic temperature (except for the pure fluid coke char), the increase in blended chars is much greater compared to that of the corresponding pure chars. This might be due to the strong physical or chemical agglomeration that occurs at high pyrolytic temperatures between biomass and other fuel. This finding is supported by the previous SEM analysis and particle size distribution results.

4. Conclusion

The effect of the blending of woody biomass material with fluid coke and coal on the co-pyrolysis process was investigated in a DTF.

From this work, it can be concluded that the effect of the biomass to other fuels blending ratio on the reactivity of the co-pyrolyzed chars is more pronounced on chars prepared at low temperatures and the effect becomes less significant as the pyrolysis temperature increases. The increased reactivity at a higher biomass blending ratio is due to the presence of synergetic effects originating from the interaction of the two fuels.

The morphological study using SEM showed a particle size decrease and shape change from needle to spherical shape as the pyrolysis temperature was increased. Further investigation revealed that, as the pyrolysis temperature was increased beyond 1250 °C, agglomeration seemed to start occurring. The reason for the agglomeration could be due to the melting of silicates from the biomass. The molten layer on the surface enables coal particles to attach themselves to sawdust particles, leading to the observed agglomeration. The shrinking and agglomeration phenomena were also verified by the particle size distribution analysis.

From the surface area analysis, it can be pointed out that, even though the surface area of both pure and blended chars increases with an increasing pyrolytic temperature, the increase in blended chars is much more pronounced when compared to that of the corresponding pure chars. This might be due to the strong physical or chemical agglomeration that occurs at high pyrolytic temperatures between biomass and other fuel.

Acknowledgment. The authors express their gratitude to the Alberta Energy Research Institute and the National Scientific and Engineering Research Council for funding this work through the strategic project grant “Synergies in Co-gasification of Biomass, Coke & Coal”.